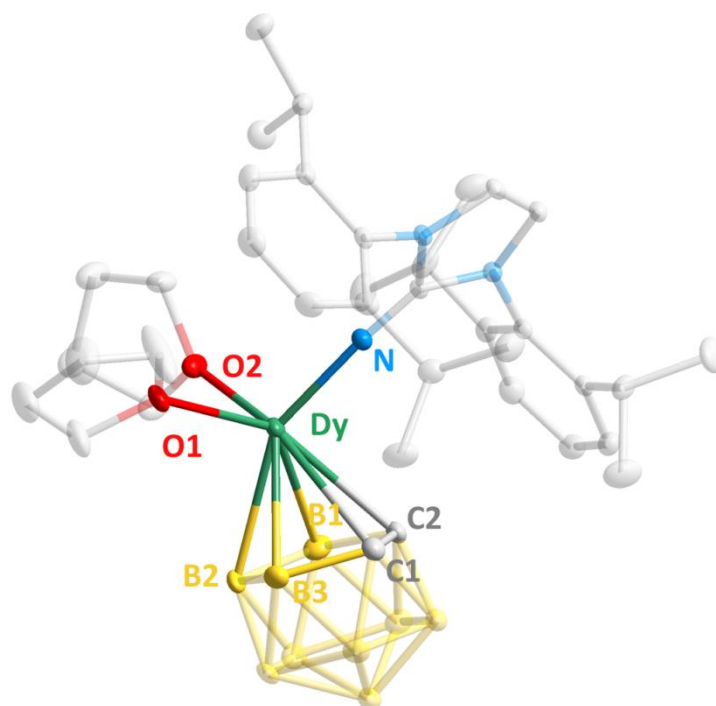**Supplemental information**

A study of cation-dependent inverse

hydrogen bonds and magnetic exchange-couplings

in lanthanacarborane complexes

Peng-Bo Jin, Qian-Cheng Luo, Yuan-Qi Zhai, Yi-Dian Wang, Yan Ma, Lei Tian, Xinliang Zhang, Chao Ke, Xu-Feng Zhang, Yi Lv, and Yan-Zhen Zheng

Table S1 Crystallographic data for complexes 1Dy, 2Dy, 2Y, 3Dy, 4Dy, 5Dy, 5Y, 6Dy and 6Y. Related to Figure 1.

Compound	1Dy	2Dy	2Y	3Dy	4Dy
Formula	$C_{37}H_{63}B_9DyN_3O_2$	$C_{66}H_{110}B_{18}Dy_2N_6O_2$	$C_{66}H_{110}B_{18}N_6O_2Y_2$	$C_{45}H_{69}B_9DyN_3O_2$	$C_{82}H_{122}B_{18}Dy_2N_6O_2$
M, g mol^{-1}	841.69	1539.17	1391.99	943.82	1743.43
Temperature, K	150(2)	150(2)	150(2)	150(2)	150(2)
Space group	$P2_1/c$	$P2_1/n$	$P2_1/n$	$P2_1/c$	P-1
a, Å	10.7984(19)	13.366(5)	13.381(5)	17.668(3)	12.1280(14)
b, Å	17.615(3)	14.274(5)	14.238(5)	10.9187(18)	14.0662(16)
c, Å	22.557(4)	20.527(8)	20.345(7)	24.013(4)	15.8091(18)
α, deg	90	90	90	90	85.535(2)
β, deg	99.741(2)	96.831(5)	97.199(5)	94.488(2)	88.410(2)
γ, deg	90	90	90	90	66.3980(10)
V, Å^3	4228.8(13)	3888(3)	3846(2)	4618.2(13)	2463.8(5)
Z	4	2	2	4	1
d_{cal}, g cm^{-3}	1.322	1.315	1.202	1.357	1.175
2θ range, deg	2.95 to 52.548	3.458 to 53.268	3.454 to 51	3.402 to 55.298	3.168 to 55.5
R_{int}	0.0366	0.0347	0.0644	0.0286	0.0243
Final indices [$I>2\sigma(I)$]	$R_1 = 0.0351$, $wR_2 = 0.0780$	$R_1 = 0.0355$, $wR_2 = 0.0875$	$R_1 = 0.0623$, $wR_2 = 0.1624$	$R_1 = 0.0346$, $wR_2 = 0.0823$	$R_1 = 0.0293$, $wR_2 = 0.0705$
R indices (all data)	$R_1 = 0.0515$, $wR_2 = 0.0877$	$R_1 = 0.0494$, $wR_2 = 0.0951$	$R_1 = 0.0912$, $wR_2 = 0.1803$	$R_1 = 0.0446$, $wR_2 = 0.0874$	$R_1 = 0.0358$, $wR_2 = 0.0736$
Goodness-of-fit on F^2	1.134	1.054	1.032	1.147	1.059
Residual map, e Å^{-3}	1.68/-0.78	1.46/-0.57	1.92/-1.06	1.91/-1.13	2.20/-0.63

Compound	5Dy	5Y	6Dy	6Y
Formula	$C_{59}H_{86}B_9ClDyNaO_6$	$C_{59}H_{86}B_9ClYNaO_6$	$C_{102}H_{140}B_{18}Cl_2Dy_2Na_2O_8$	$C_{102}H_{140}B_{18}Cl_2Na_2O_8Y_2$
M, g mol^{-1}	1209.5	1135.91	2130.59	1983.41
Temperature, K	150(2)	150(2)	150(2)	150(2)
Space group	P-1	P-1	P-1	P-1
a, Å	10.906(8)	10.800(3)	12.028(13)	11.903(4)
b, Å	12.748(10)	12.656(4)	13.414(14)	13.288(5)
c, Å	22.995(17)	22.867(7)	18.360(19)	18.157(6)
α, deg	83.962(9)	84.045(4)	103.382(13)	103.693(4)
β, deg	81.446(9)	81.609(4)	105.519(13)	105.507(4)
γ, deg	83.577(9)	83.531(4)	92.387(13)	92.146(4)
V, Å^3	3129(4)	3060.3(16)	2760(5)	2673.0(16)
Z	1	1	1	1
d_{cal}, g cm^{-3}	1.284	1.233	1.282	1.232
2θ range, deg	3.228 to 55.554	3.252 to 55.208	2.378 to 51.432	3.174 to 47.234
R_{int}	0.0366	0.0341	0.0555	0.0423
Final indices [$I>2\sigma(I)$]	$R_1 = 0.0339$, $wR_2 = 0.0983$	$R_1 = 0.0410$, $wR_2 = 0.0917$	$R_1 = 0.0434$, $wR_2 = 0.1142$	$R_1 = 0.0492$, $wR_2 = 0.1263$
R indices (all data)	$R_1 = 0.0429$, $wR_2 = 0.1069$	$R_1 = 0.0617$, $wR_2 = 0.0995$	$R_1 = 0.0678$, $wR_2 = 0.1318$	$R_1 = 0.0799$, $wR_2 = 0.1414$
Goodness-of-fit on F^2	0.800	1.016	0.833	1.106
Residual map, e Å^{-3}	1.27/-0.64	0.54/-0.34	1.45/-0.86	0.73/-0.52

Figure S1 Thermal ellipsoid (30% probability) representation of the simplified molecular structure of 1Dy. All the hydrogen atoms are omitted for clarity. Related to Figure 1.

Dy-O1	2.362(3)
Dy-O2	2.353(3)
Dy-N	2.095(3)
Dy-B1	2.623(5)
Dy-B2	2.641(5)
Dy-B3	2.627(5)
Dy-C1	2.667(4)
Dy-C2	2.666(4)
Dy-C$_2$B$_3$ (centroid)	2.230
N-Dy-C$_2$B$_3$ (centroid)	116.98

Table S2 Selected bond lengths (Å) and angle (°) for 1Dy. Related to Figure 1.
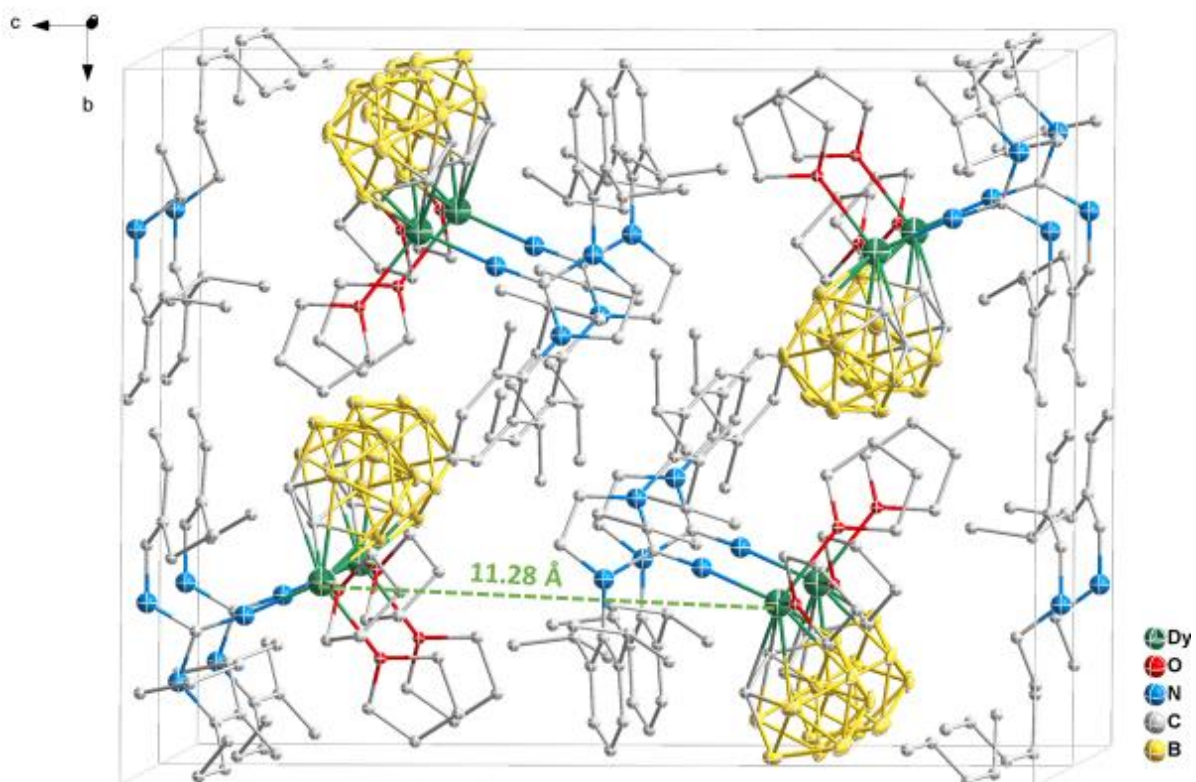
Figure S2 The crystal packing diagram for 1Dy. Related to Figure 1.
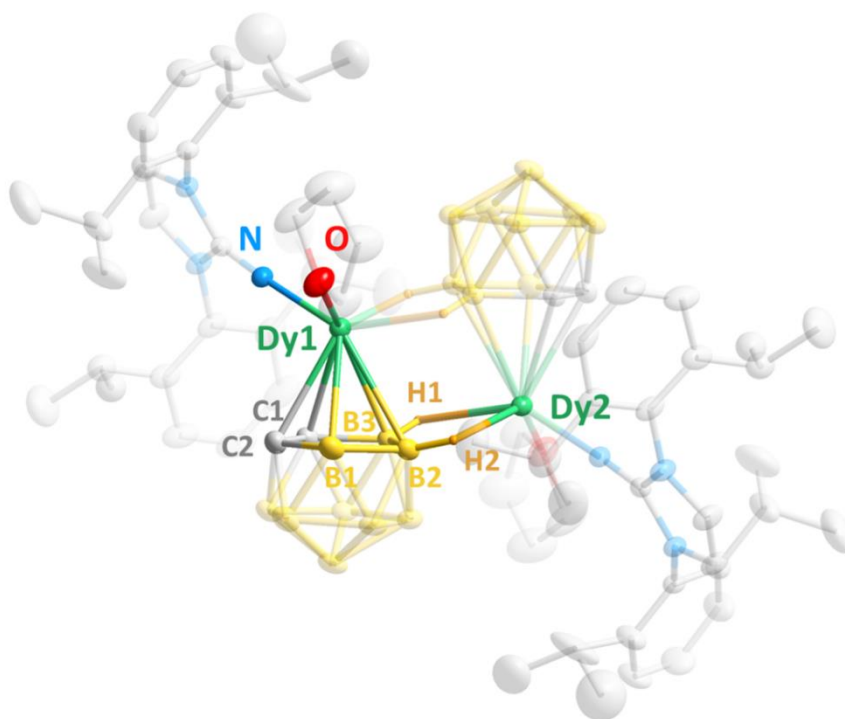
Figure S3 Thermal ellipsoid representation of the simplified molecular structure of 2Dy shown at the 30% probability level. All the hydrogen atoms are omitted for clarity except coordinated ones. Related to Figure 1.

Dy1-O	2.377(3)
Dy1-N	2.107(3)
Dy1-B1	2.717(5)
Dy1-B2	2.835(5)
Dy1-B3	2.787(5)
Dy1-C1	2.701(4)
Dy1-C2	2.653(4)
Dy2-H1	2.461
Dy2-H2	2.251
Dy1-Dy2	4.081
Dy1-C_2B_3 (centroid)	2.343
N-Dy1-C_2B_3 (centroid)	117.27
B3-H1-Dy2	96.43
B2-H2-Dy2	109.44

Table S3 Selected bond lengths (Å) and angles (°) for 2Dy. Related to Figure 1.

Figure S4 The crystal packing diagram for 2Dy. Related to Figure 1.

Figure S5 Thermal ellipsoid representation of the simplified molecular structure of 3Dy shown at the 30% probability level. All the hydrogen atoms are omitted for clarity except coordinated ones. Related to Figure 1.

Dy-O1	2.365(2)
Dy-O2	2.354(2)
Dy-N	2.123(3)
Dy-B1	2.712(4)
Dy-B2	2.641(4)
Dy-B3	2.601(4)
Dy-C1	2.698(3)
Dy-C2	2.788(3)
Dy-C_2B_3 (centroid)	2.275
N-Dy-C_2B_3 (centroid)	131.37

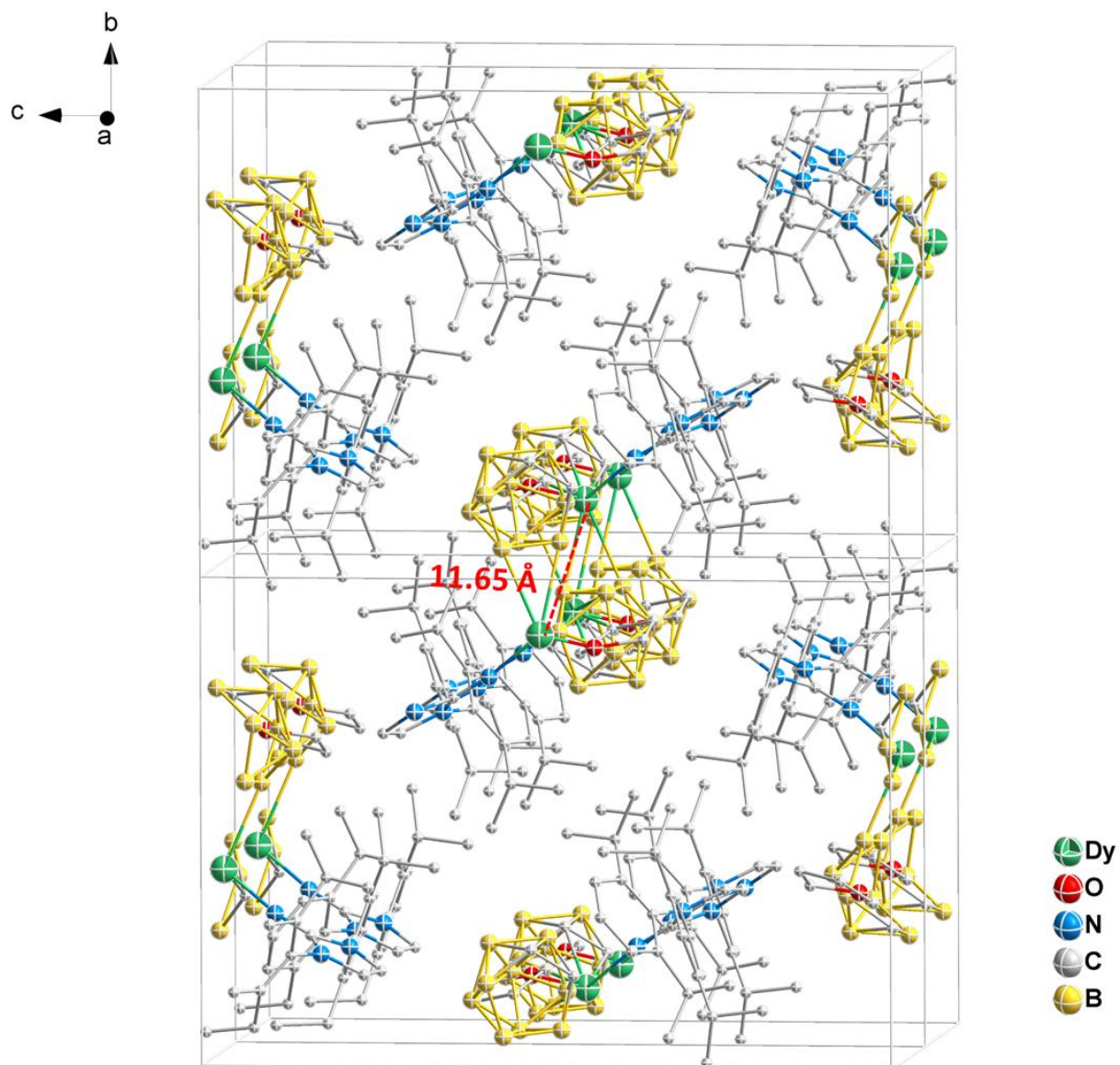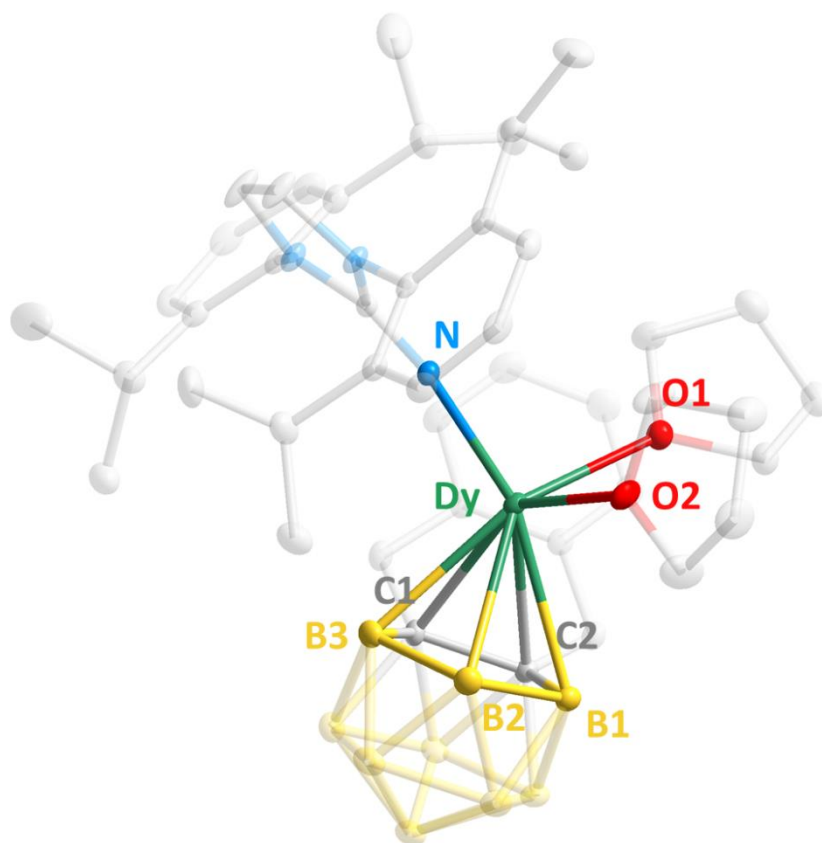**Table S4 Selected bond lengths (Å) and angle (°) for 3Dy.** Related to Figure 1.

Figure S6 The crystal packing diagram for 3Dy. Related to Figure 1.
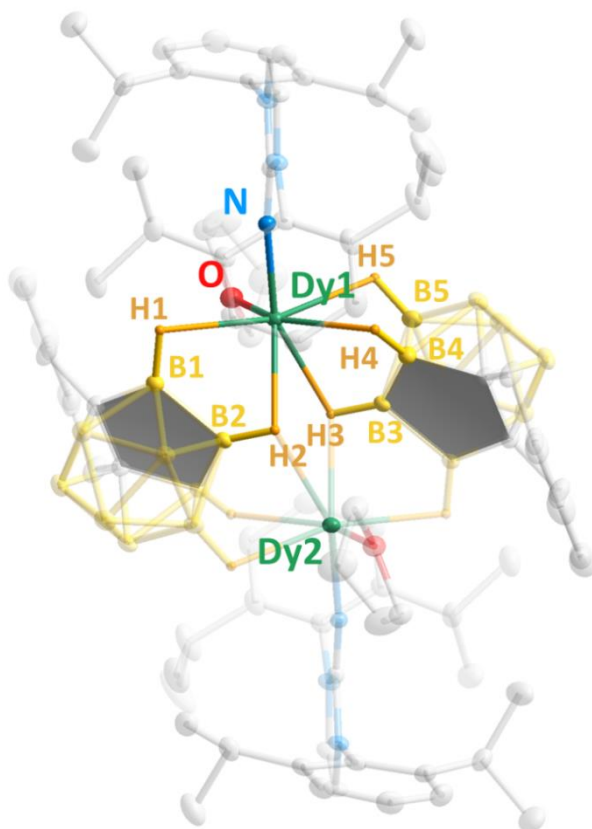
Figure S7 Thermal ellipsoid representation of the simplified molecular structure of 4Dy shown at the 30% probability level. All the hydrogen atoms are omitted for clarity except coordinated ones. Related to Figure 1.

Dy1-O	2.314(2)	Dy1-H5	2.549
Dy1-N	2.066(2)	Dy1-Dy2	4.162
Dy1-B1	2.781(3)	B1-Dy1-Cent (C_2B_3)	88.87
Dy1-B2	2.648(3)	B2-Dy1-Cent (C_2B_3)	89.93
Dy1-B3	2.804(3)	B3-Dy1-Cent (C_2B_3)	94.51
Dy1-B4	2.715(3)	H4-Dy1-Cent (C_2B_3)	100.01
Dy1-B5	2.904(3)	H5-Dy1-Cent (C_2B_3)	97.03
Dy1-H1	2.570		
Dy1-H2	2.415		
Dy1-H3	2.500		
Dy1-H4	2.306		

Table S5 Selected bond lengths (Å) and angles (°) for 4Dy. Related to Figure 1.
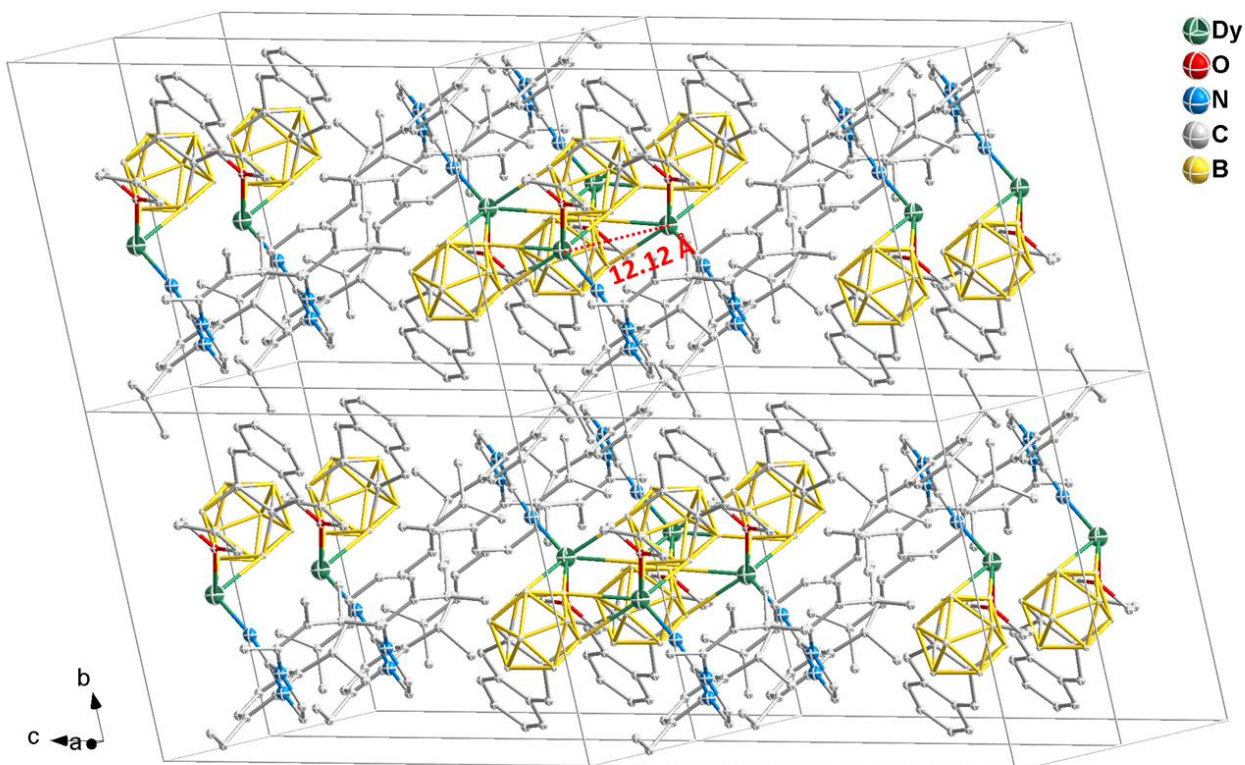
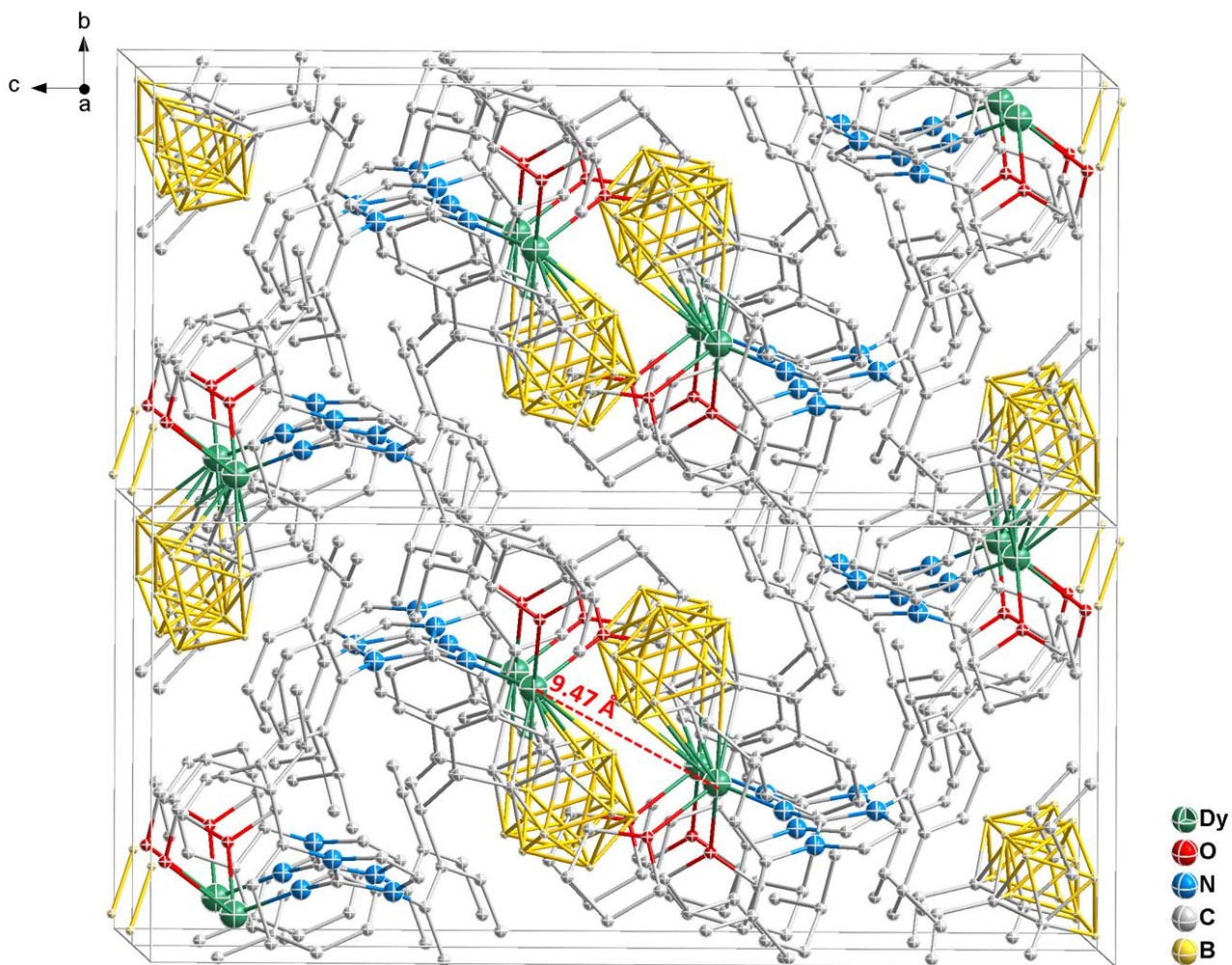**Figure S8 The crystal packing diagram for 4Dy**. Related to Figure 1.
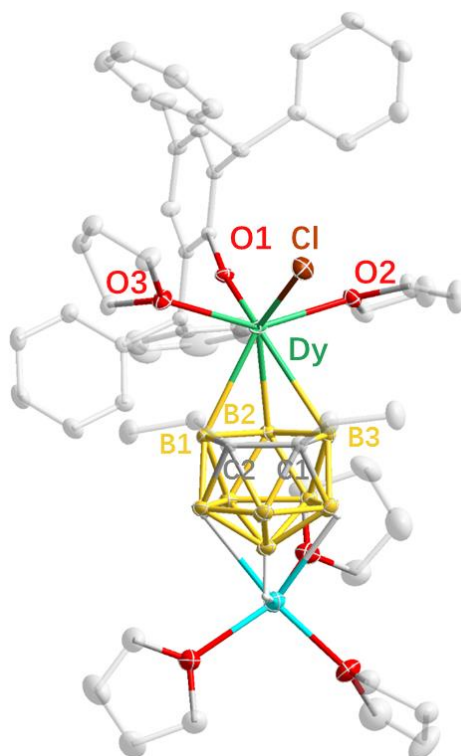
Figure S9 Thermal ellipsoid (30% probability) representation of the simplified molecular structure of 5Dy. All the hydrogen atoms are omitted for clarity. Related to Figure 1.

Dy-O1	2.112(2)
Dy-O2	2.455(2)
Dy-O3	2.432(3)
Dy-Cl	2.716(3)
Dy-B1	2.570(3)
Dy-B2	2.868(4)
Dy-B3	2.263(4)
Dy-C1	3.155(2)
Dy-C2	3.241(2)
Dy-C_2B_3 (centroid)	2.543

Table S6 Selected bond lengths (Å) for compound 5Dy. Related to Figure 1.
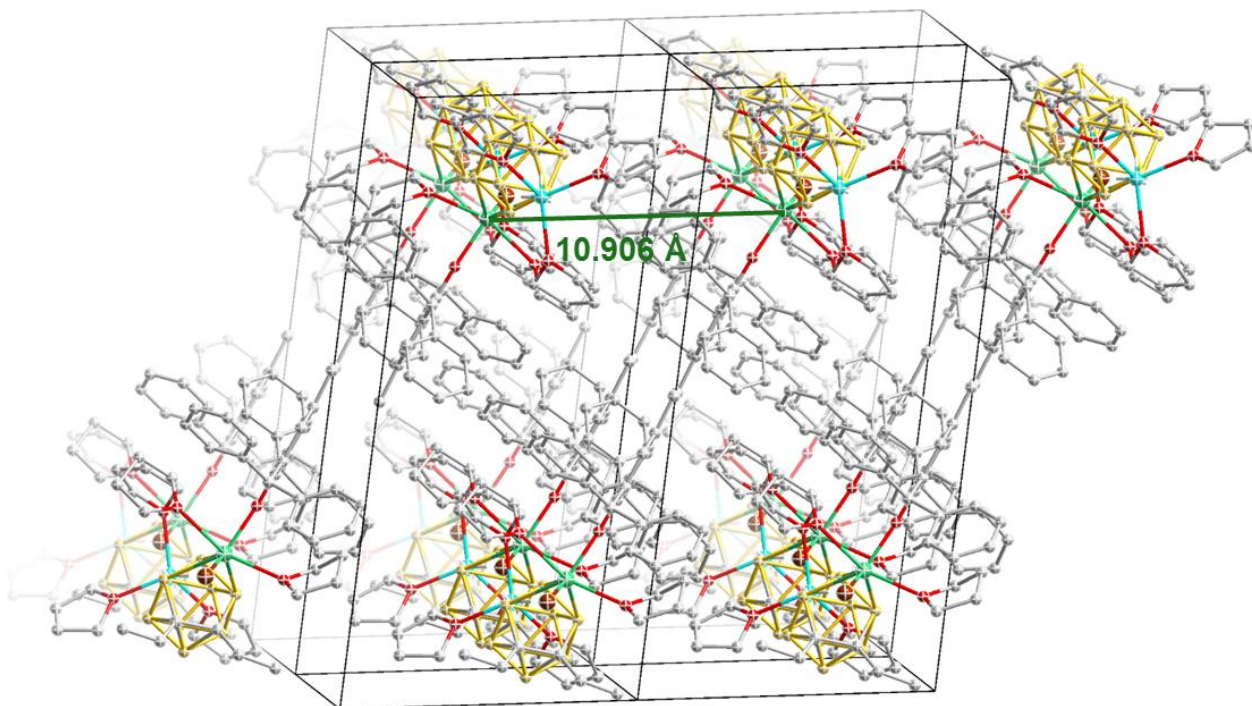
Figure S10 The crystal packing diagram for 5Dy. Related to Figure 1.
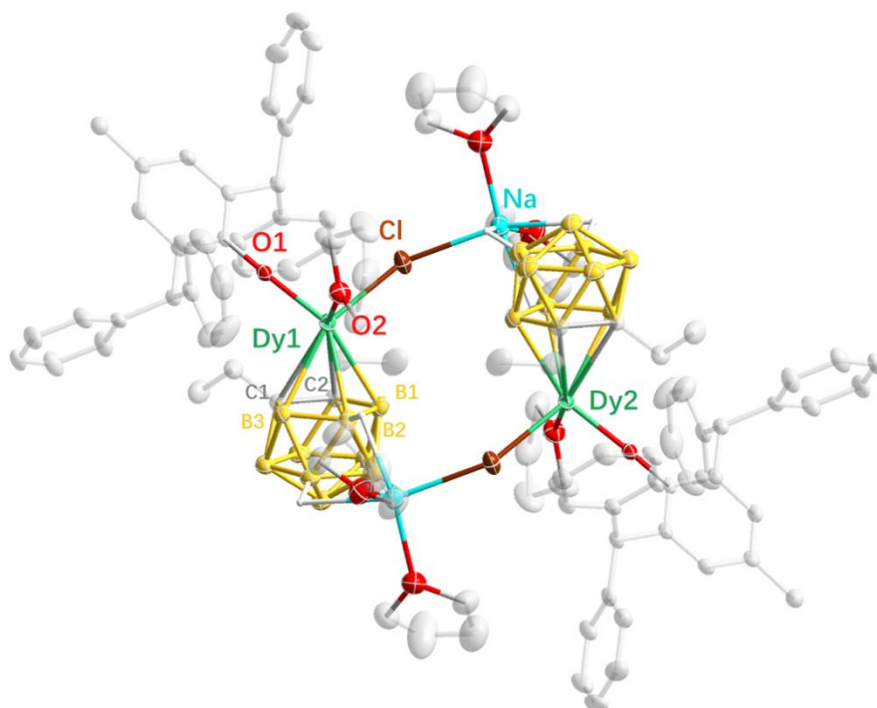
Figure S11 Thermal ellipsoid representation of the simplified molecular structure of 6Dy shown at the 30% probability level. All the hydrogen atoms are omitted for clarity except coordinated ones. Related to Figure 1.

Dy-O1	2.098(4)
Dy-O2	2.348(4)
Dy-Cl	2.626(3)
Dy1-C1	2.726(5)
Dy1-C2	2.702(6)
Dy1-B1	2.657(6)
Dy1-B2	2.689(7)
Dy1-B3	2.664(6)
Dy1-Dy2	6.907(4)
Na-Cl	2.738(3)
Dy-C_2B_3 (centroid)	2.268(2)

Table S7 Selected bond lengths (Å) and angles (°) for compound 6Dy. Related to Figure 1.
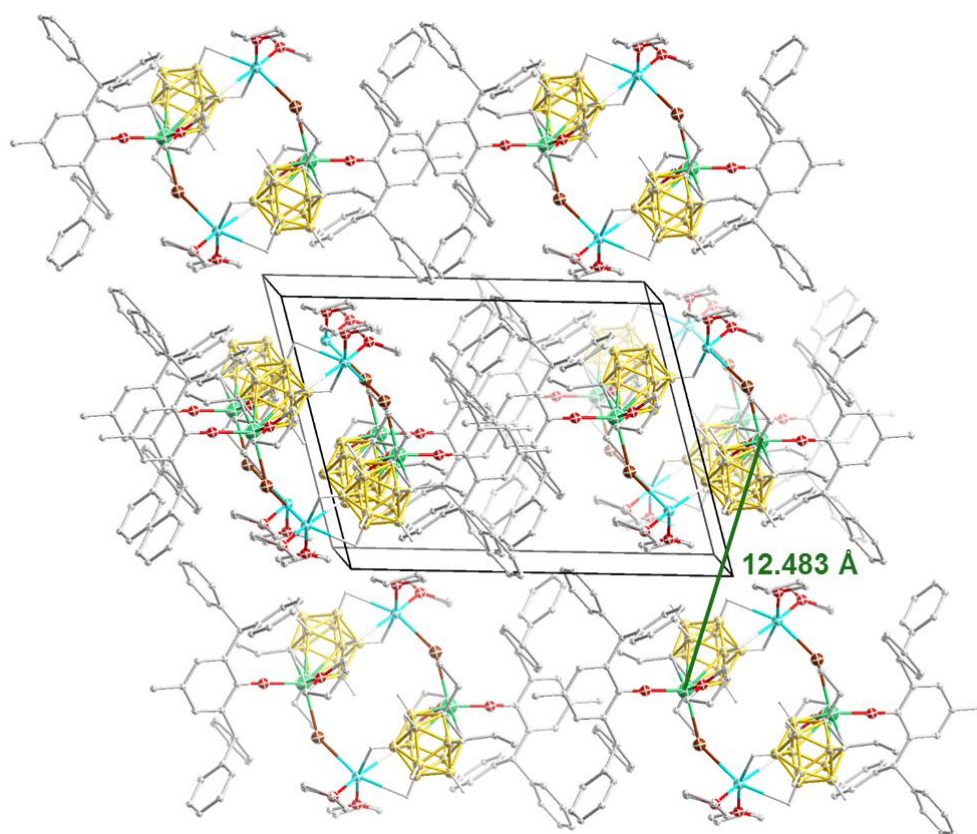
Figure S12 The crystal packing diagram for 6Dy. Related to Figure 1.
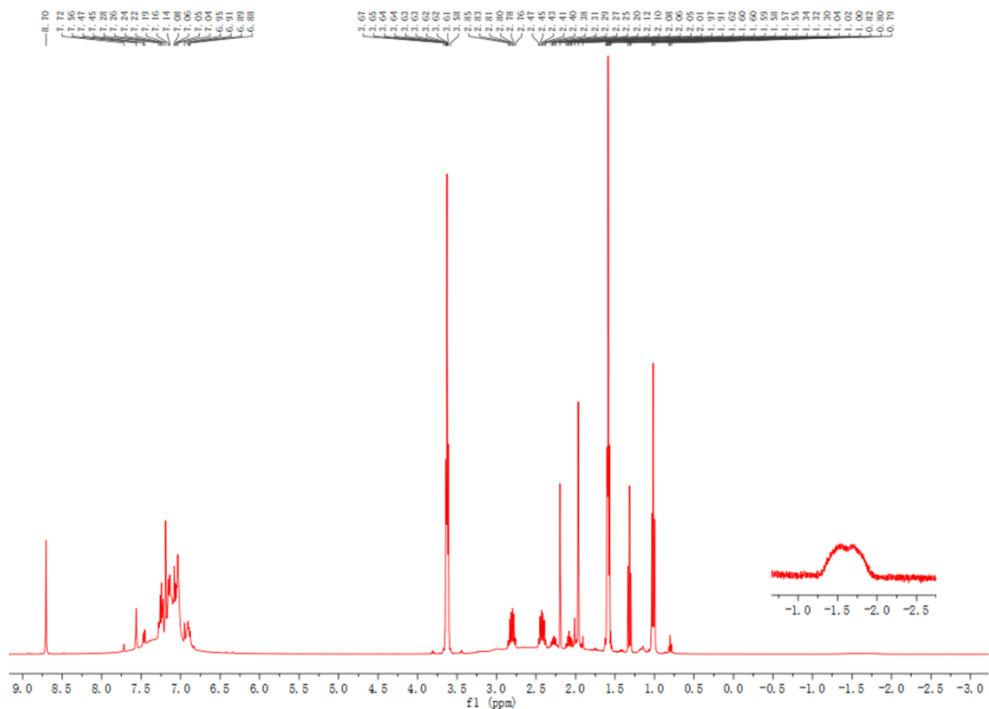
Figure S13 ^{1}H NMR spectrum (**Pyridine-d_5, 400 MHz**) **of 5Y**. Related to Figure 2.
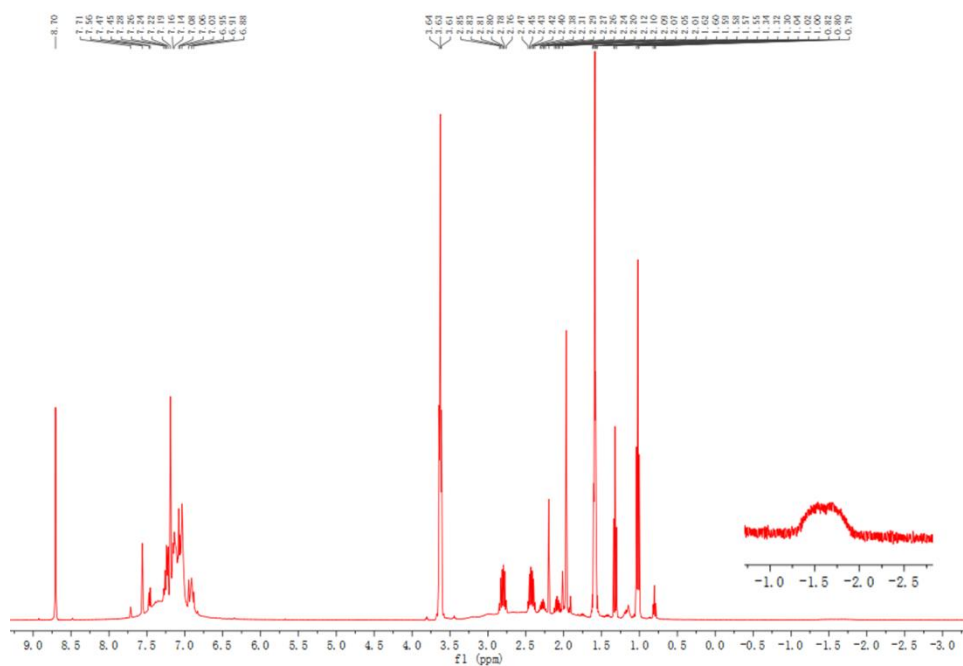
Figure S14 ^{1}H NMR spectrum (**Pyridine-d_5, 400 MHz**) **of 6Y**. Related to Figure 2.
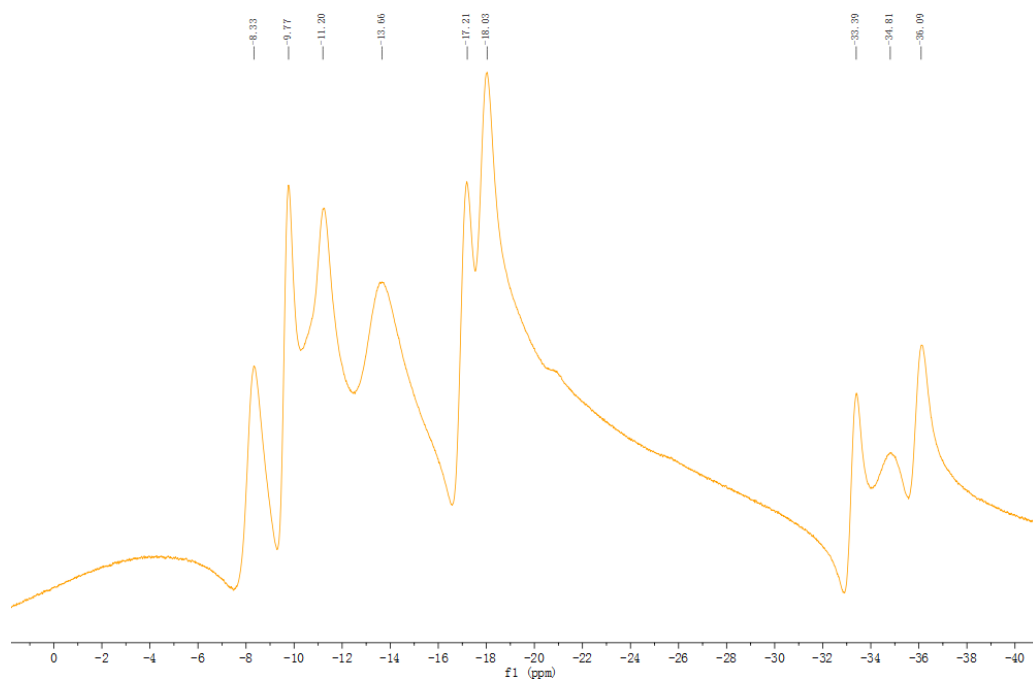
Figure S15 ^{11}B NMR spectrum (Pyridine-*d*5, 400 MHz) of 5Y. Related to Figure 2.
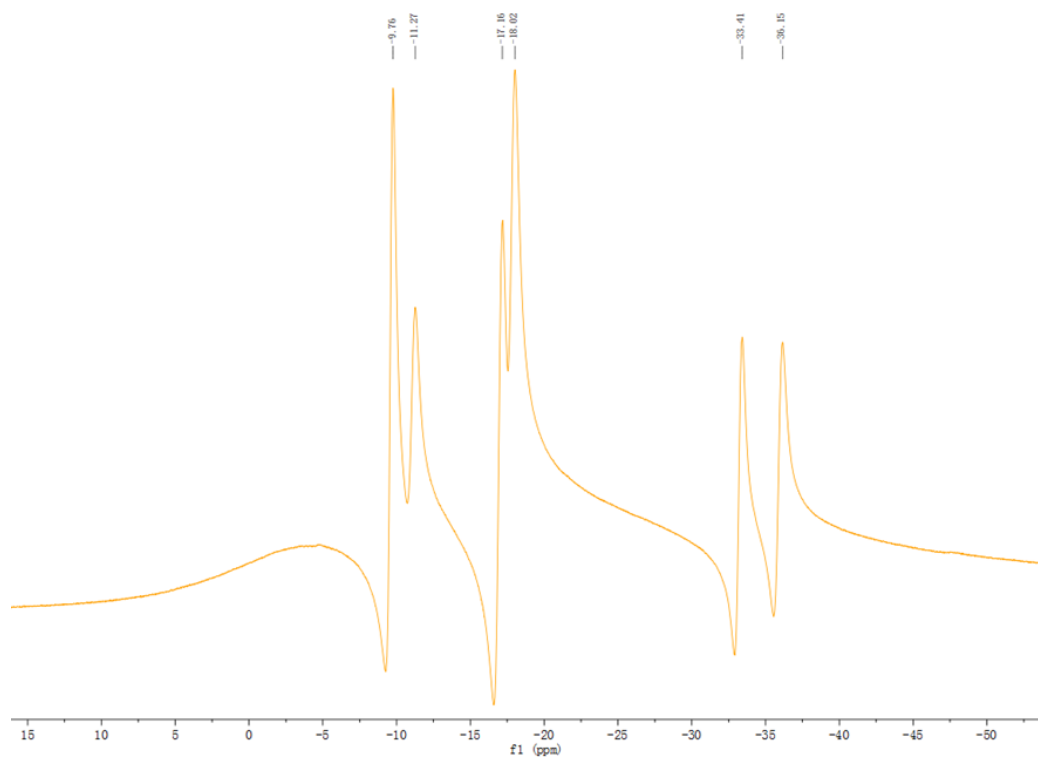
Figure S16 ^{11}B NMR spectrum (Pyridine-*d*5, 400 MHz) of 6Y. Related to Figure 2.
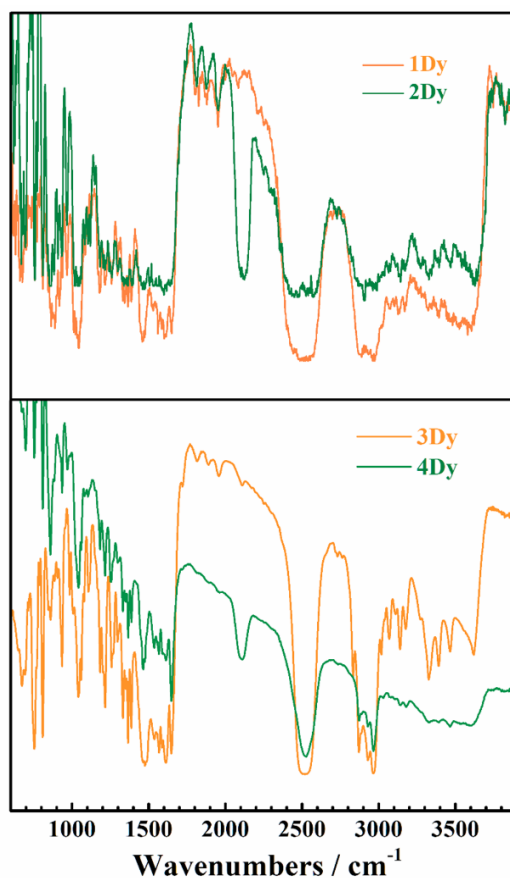
Figure S17 Infrared spectrum of complexes 1Dy and 3Dy (orange) and 2Y and 4Dy (green). Related to Figure 2.
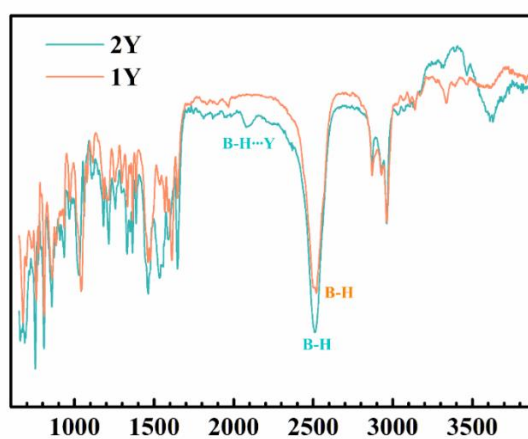
Figure S18 Infrared spectrum of complexes 1Y (orange) and 2Y (cyan). Related to Figure 2.
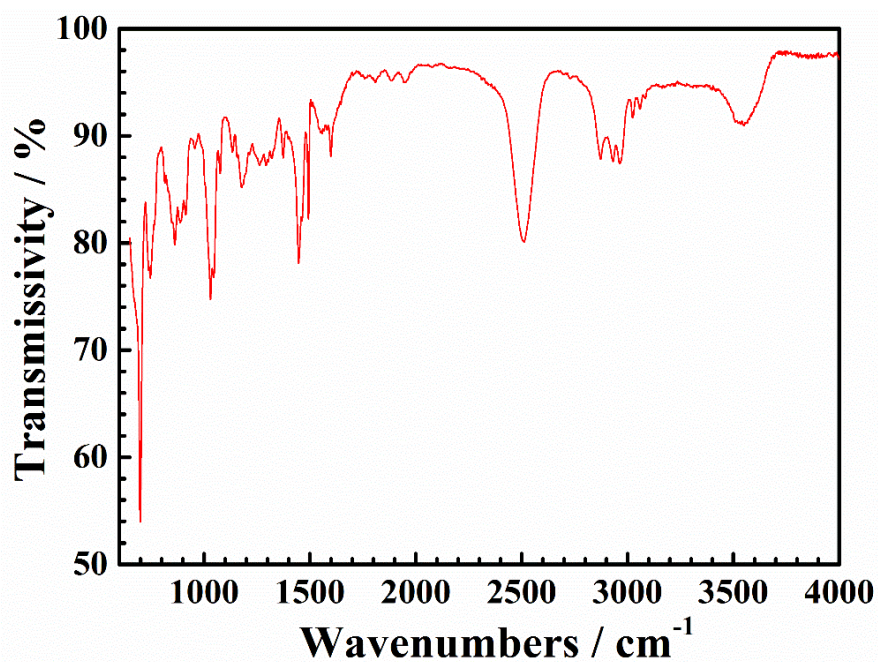
Figure S19 Infrared spectrum of compound 5Dy. Related to Figure 2.
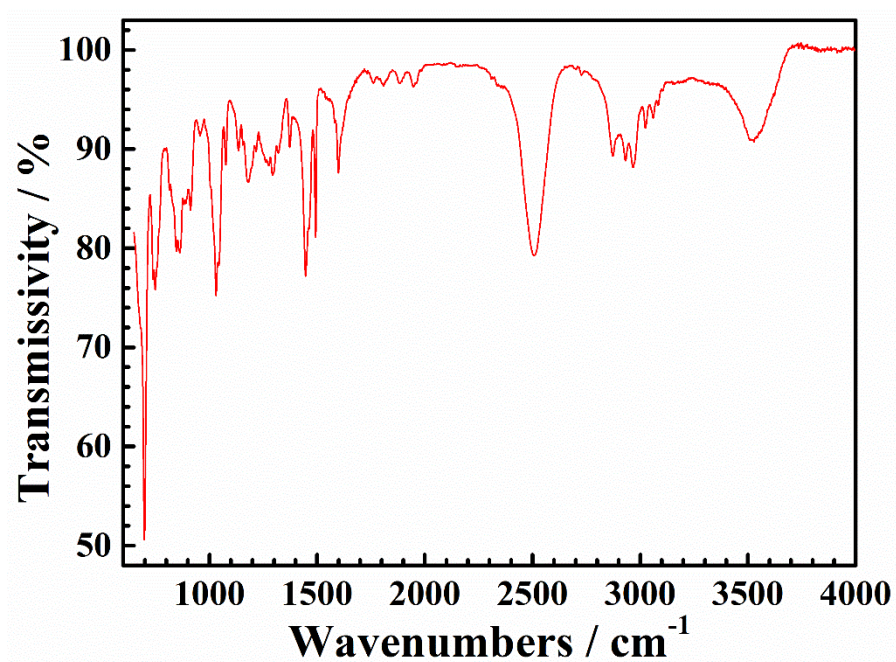
Figure S20 Infrared spectrum of compound 5Y. Related to Figure 2.
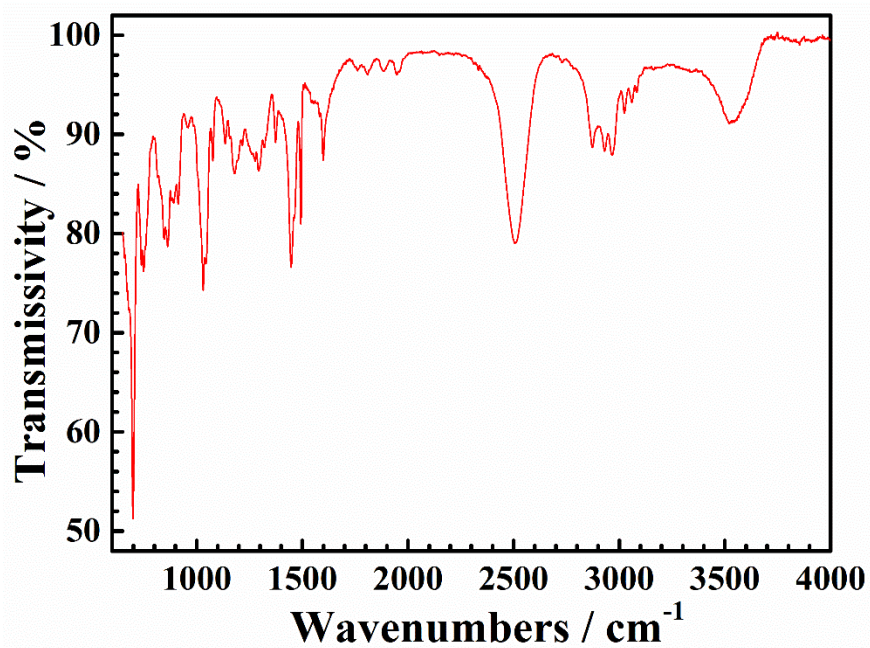
Figure S21 Infrared spectrum of compound 6Dy. Related to Figure 2.
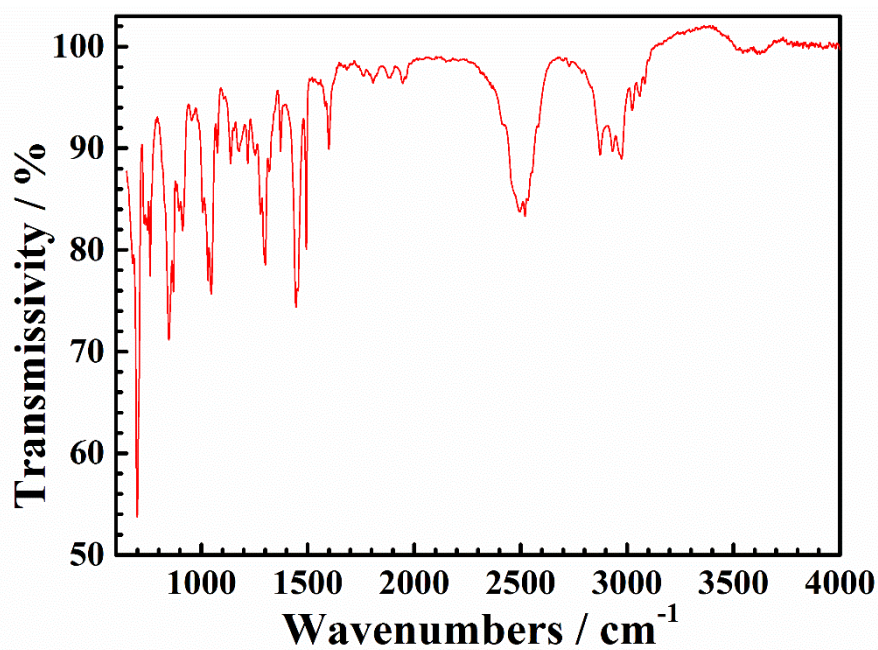
Figure S22 Infrared spectrum of compound 6Y. Related to Figure 2.
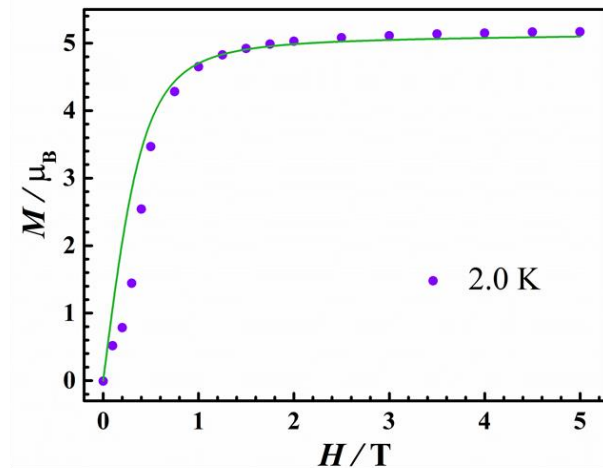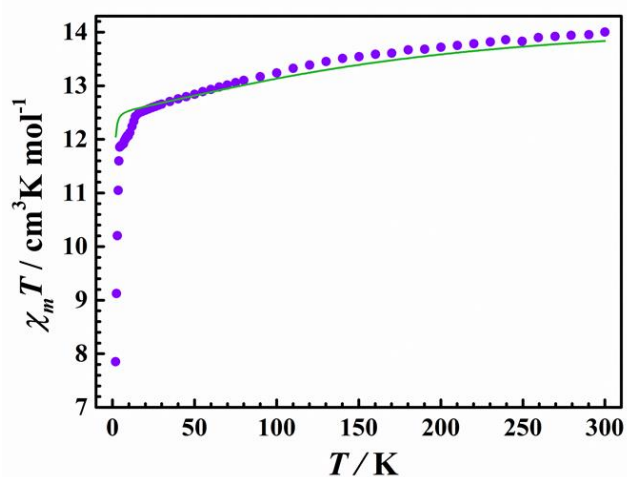
Figure S23 The temperature dependent susceptibility of $\chi_m T$ and the field dependent magnetization (*M/H*) for 1Dy. The $\chi_m T$ in an applied DC magnetic field of 1 kOe of polycrystalline sample (left), the *M/H* at 2.0 K up to 5 Tesla (right). The solid lines are best fits from *ab initio* calculations. Related to Figure 6.
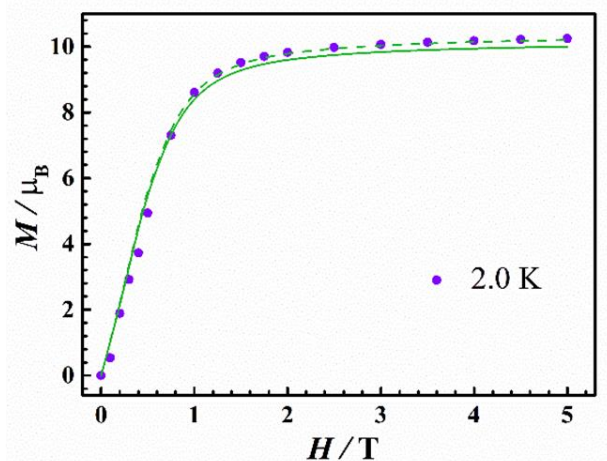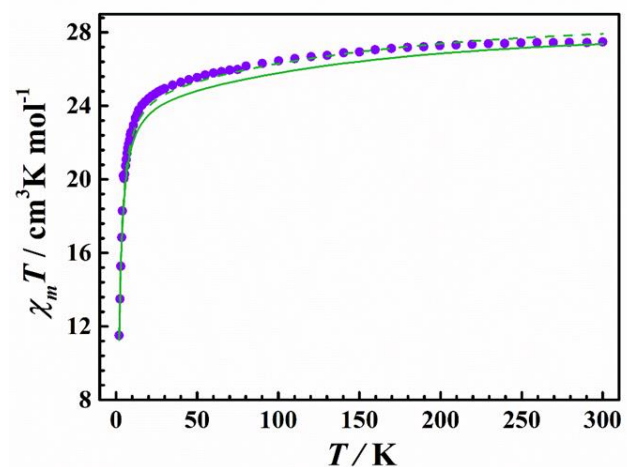
Figure S24 The temperature dependent susceptibility of $\chi_m T$ and the field dependent magnetization (*M/H*) for 2Dy. The $\chi_m T$ in an applied DC magnetic field of 1 kOe of polycrystalline sample (left), the *M/H* at 2.0 K up to 5 Tesla (right). The solid lines are best fits from *ab initio* calculations. Related to Figure 6.
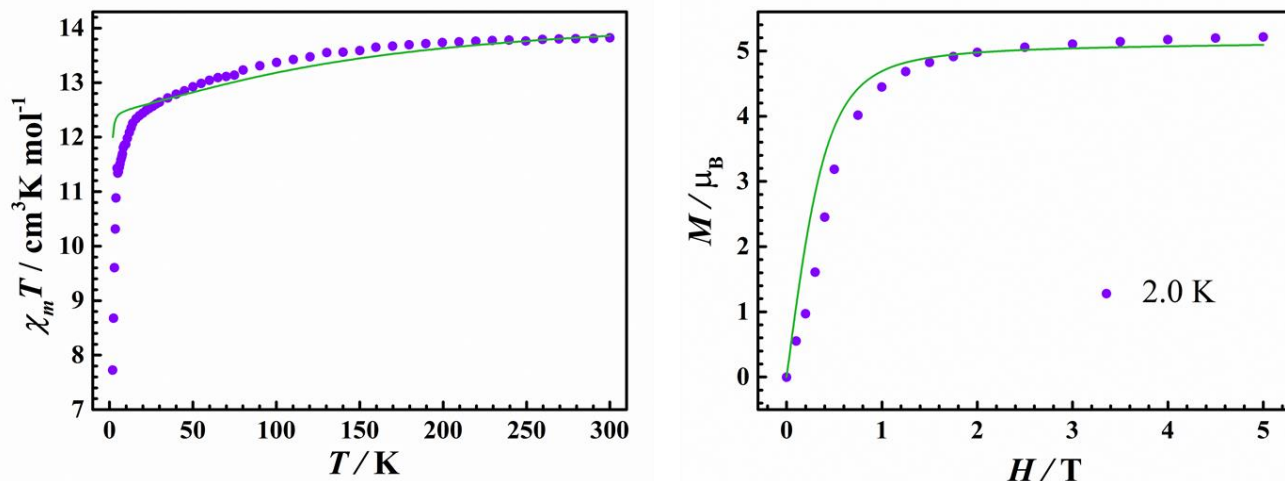
Figure S25 The temperature dependent susceptibility of $\chi_m T$ and the field dependent magnetization (*M/H*) for 3Dy. The $\chi_m T$ in an applied DC magnetic field of 1 kOe of polycrystalline sample (left), the *M/H* at 2.0 K up to 5 Tesla (right). The solid lines are best fits from *ab initio* calculations. Related to Figure 5.
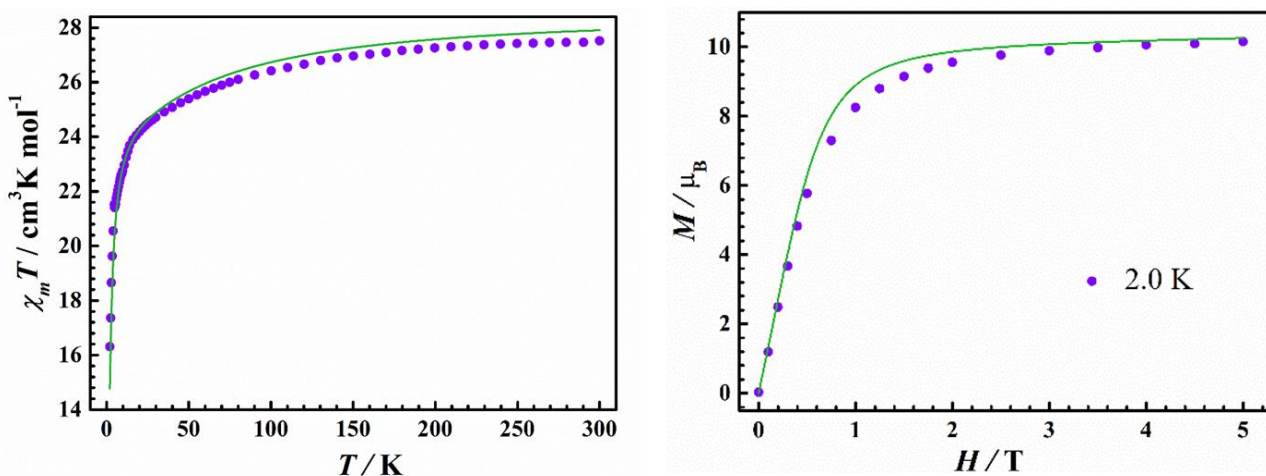
Figure S26 The temperature dependent susceptibility of $\chi_m T$ and the field dependent magnetization (*M/H*) for 4Dy. The $\chi_m T$ in an applied DC magnetic field of 1 kOe of polycrystalline sample (left), the *M/H* at 2.0 K up to 5 Tesla (right). The solid lines are best fits from *ab initio* calculations. Related to Figure 5.
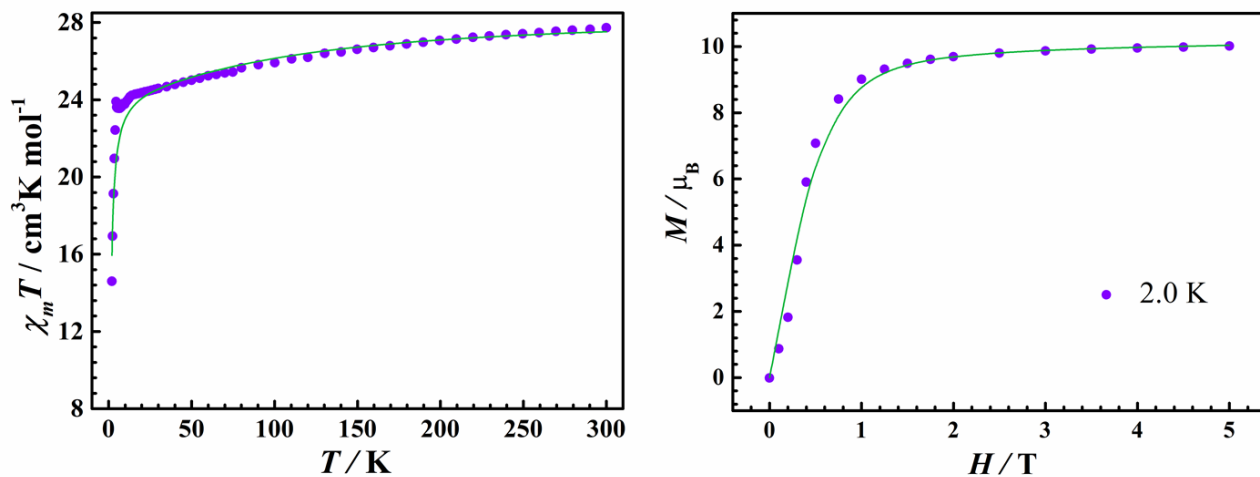
Figure S27 The temperature dependent susceptibility of $\chi_m T$ and the field dependent magnetization (*M/H*) for 6Dy. The $\chi_m T$ in an applied DC magnetic field of 1 kOe of polycrystalline sample (left), the *M/H* at 2.0 K up to 5 Tesla (right). The solid lines are best fits from *ab initio* calculations. Related to Figure 5.
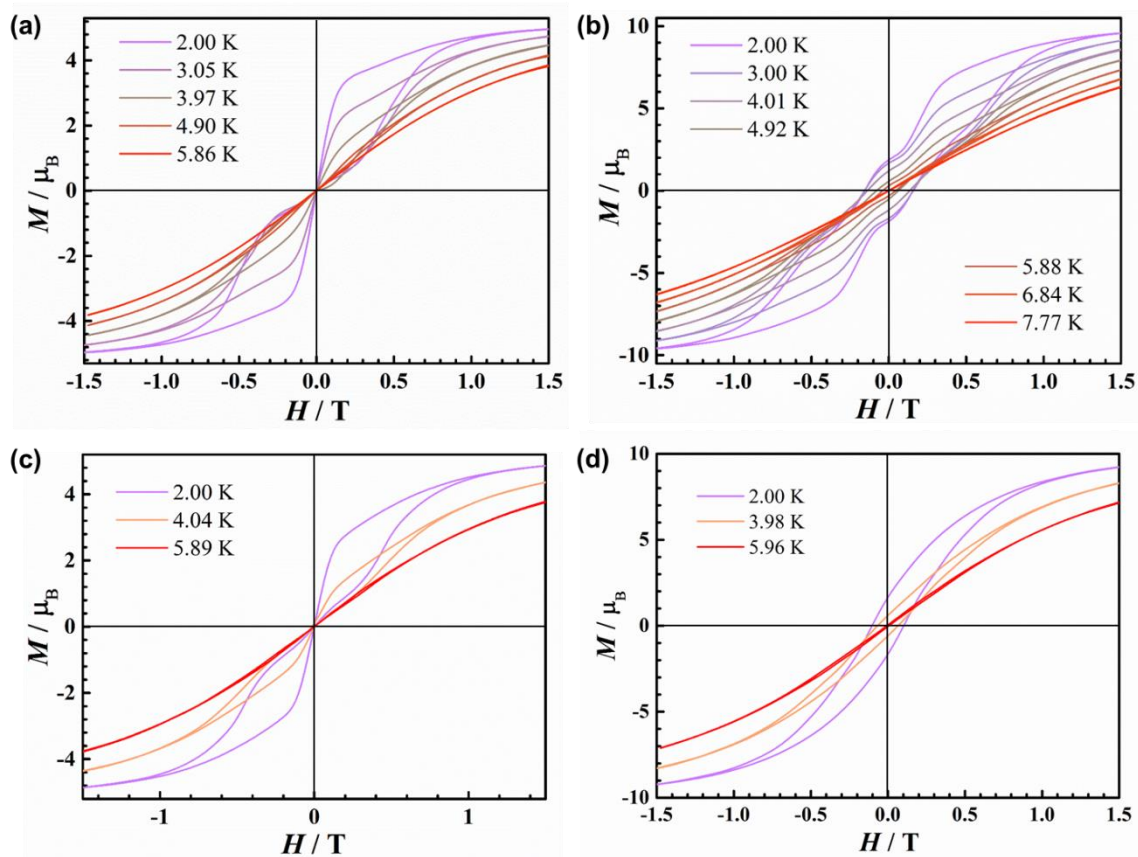
Figure S28 The magnetic hysteresis loop measurements. The magnetic hysteresis loop of polycrystalline samples 1Dy (a), 2Dy (b), 3Dy (c) and 4Dy (d) under an average sweep rate of 15 Oe s^{-1}. Related Figure 5 and Figure 6.
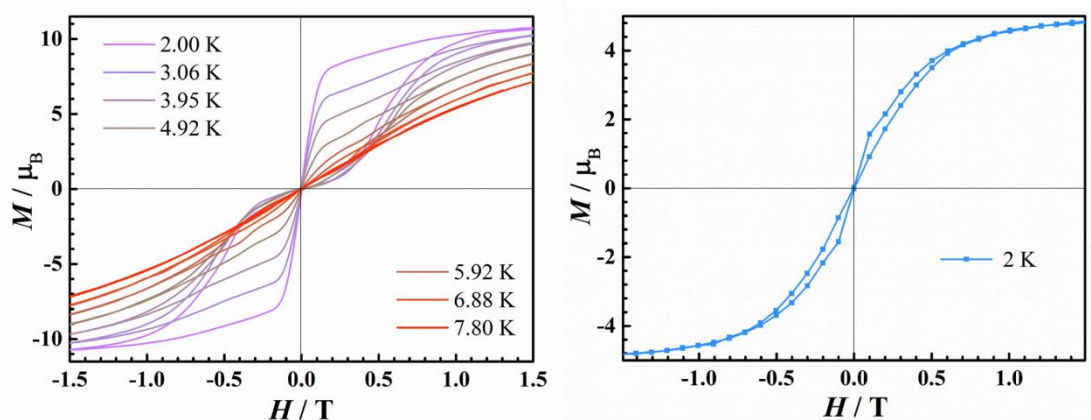
Figure S29 The magnetic hysteresis loop measurements. The magnetic hysteresis loop of polycrystalline samples **2Dy@2Y** (left) and **5Dy@5Y** (right) under an average sweep rate of 15 Oe s^{-1}. Related to Figure 5 and Figure 6.
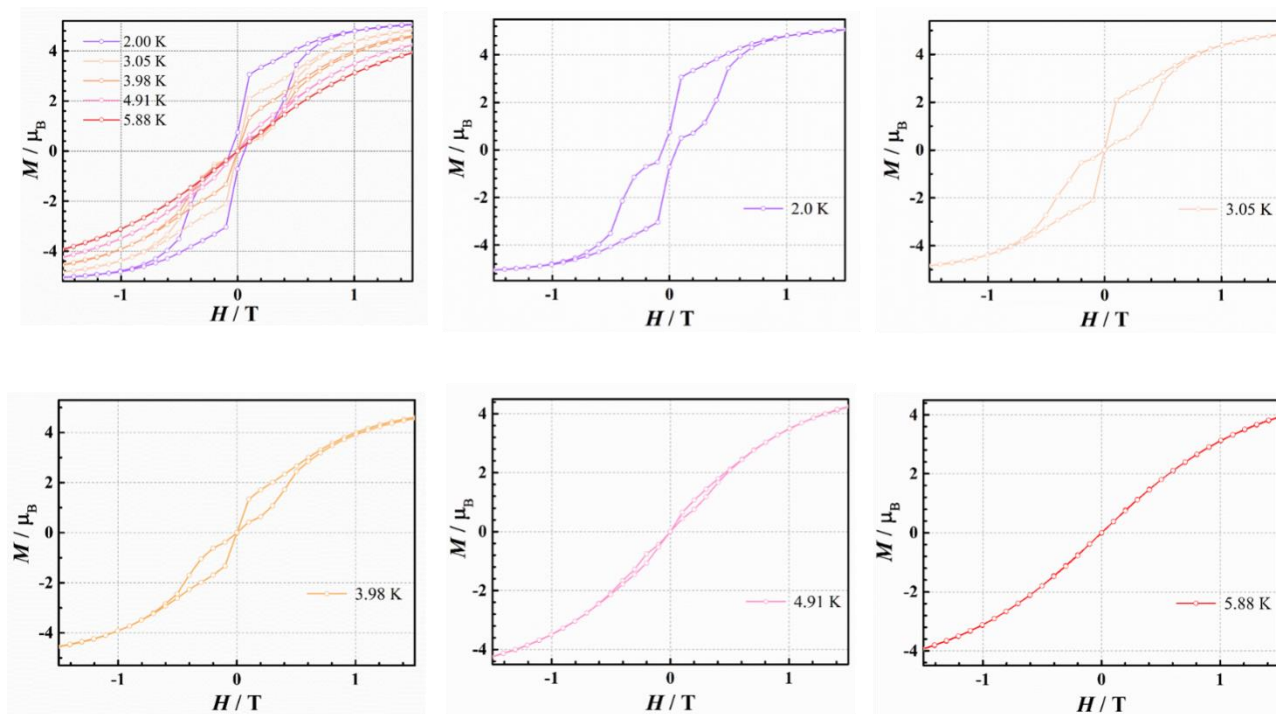
Figure S30 The magnetic hysteresis loop measurements. Magnetic hysteresis loops for **6Dy** with an average sweep rate of 15 Oe s^{-1}. Related to Figure 5.
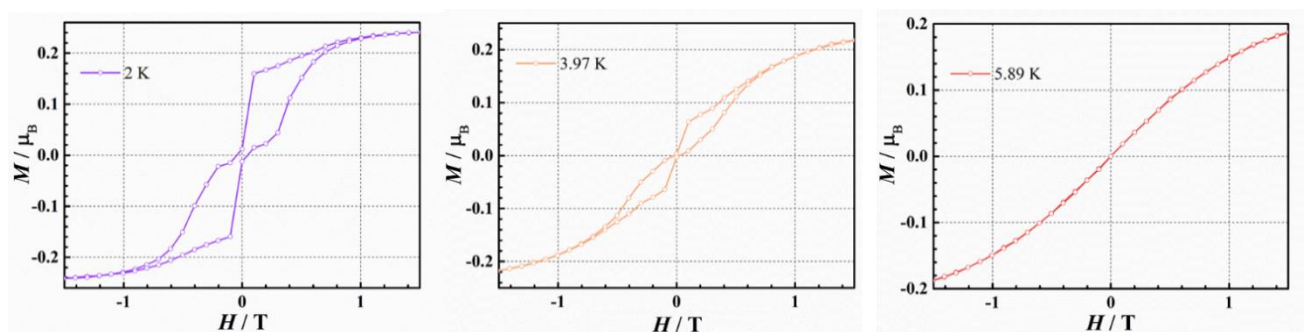
Figure S31 The magnetic hysteresis loop measurements. Magnetic hysteresis loops for **6Dy@6Y** with an average sweep rate of 15 Oe s^{-1}. Related to Figure 5.
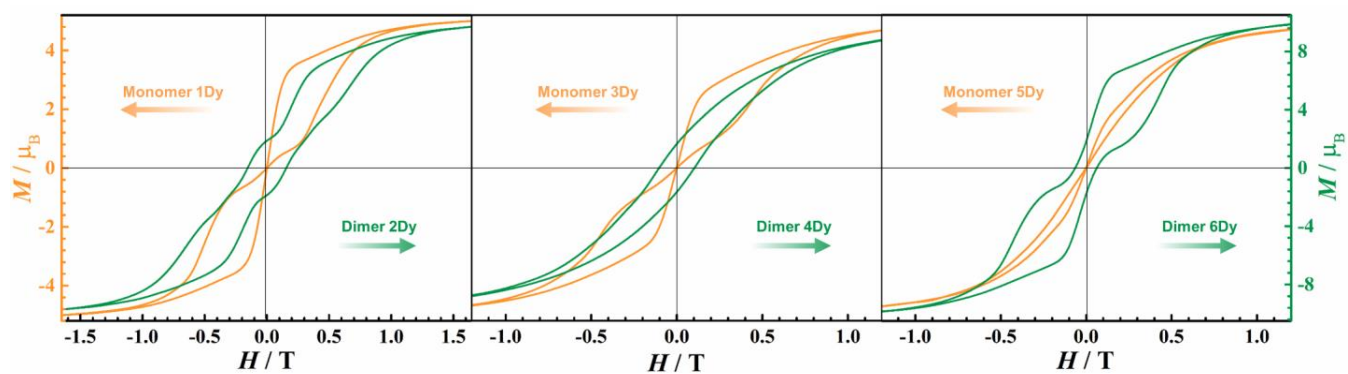
Figure S32 The magnetic hysteresis loop measurements. The comparison of magnetic hysteresis loops between polycrystalline samples **1Dy** and **2Dy** (left); **3Dy** and **4Dy** (middle); **5Dy** and **6Dy** (right) at 2 K under an average sweep rate of 15 Oe s^{-1}. Related to Figure 5 and Figure 6.
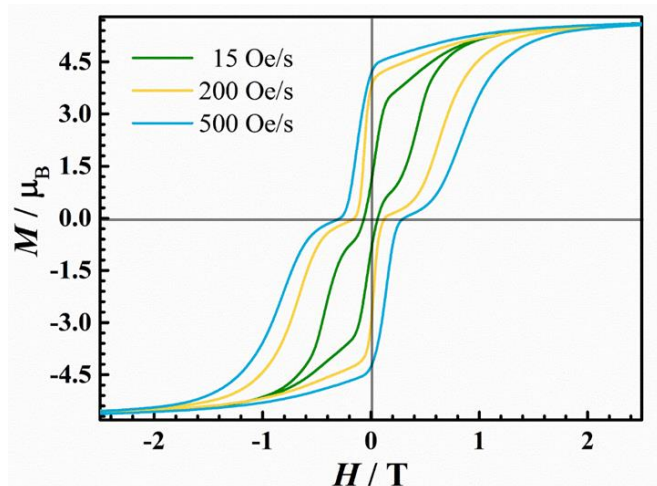
Figure S33 The magnetic hysteresis loop measurements. Magnetic hysteresis loop measurements for **6Dy** with accelerated magnetic field sweep rate from 15 Oe/s to 500 Oe/s at 2 K. Related to Figure 5.
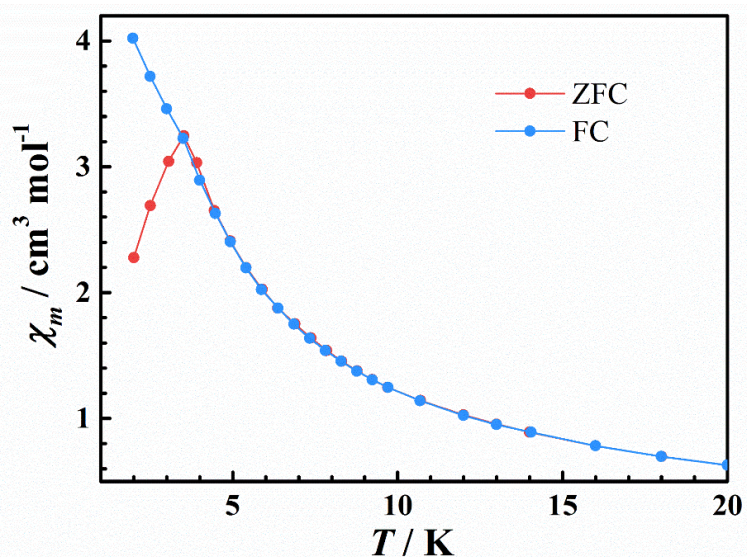
Figure S34 The Field-cooled (FC, blue line) and zero-field-cooled (ZFC, red line) variable-temperature magnetic susceptibility. The FC-ZFC for polycrystalline sample of **1Dy** with 2 KOe DC field in cool mode from 20 K to 2 K and in warm mode from 2 K to 20 K respectively. Related to Figure 5.
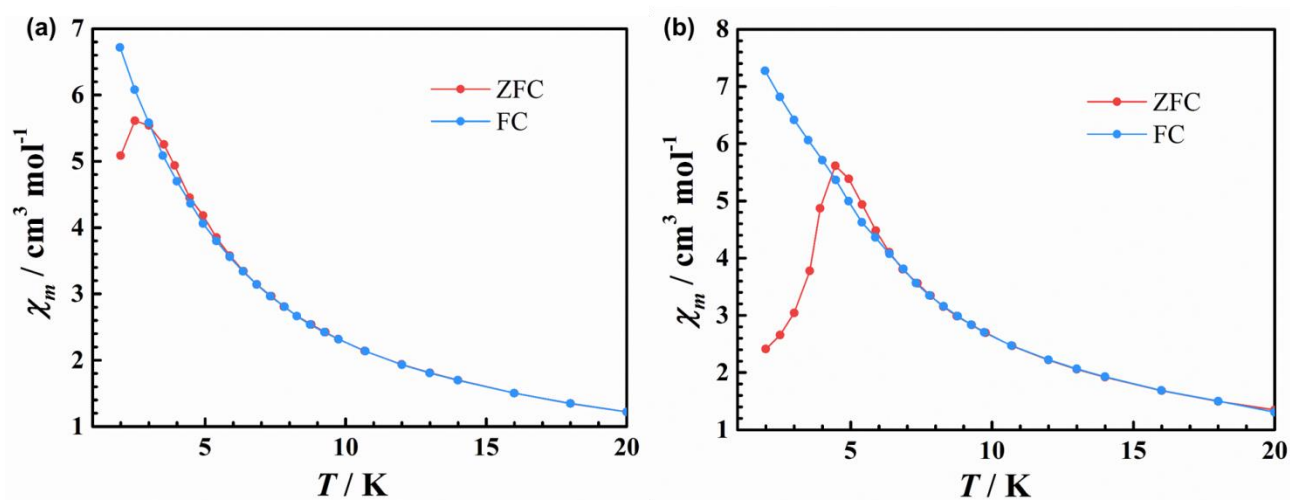
Figure S35 The Field-cooled (FC, blue line) and zero-field-cooled (ZFC, red line) variable-temperature magnetic susceptibility. The FC-ZFC for polycrystalline sample of **2Dy** (a) and **2Dy@2Y** (b) with 2 KOe DC field in cool mode from 20 to 2 K and in warm mode from 2 to 20 K respectively. Related to Figure 6.
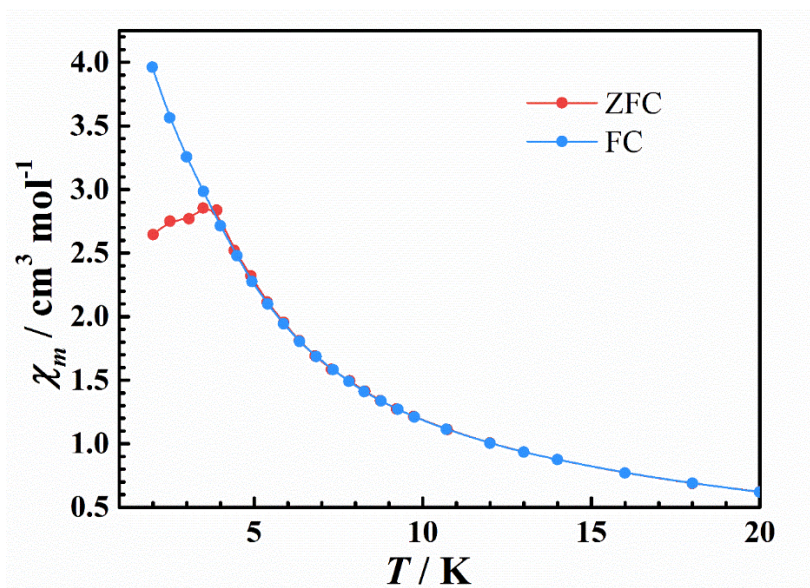
Figure S36 The Field-cooled (FC, blue line) and zero-field-cooled (ZFC, red line) variable-temperature magnetic susceptibility. The FC-ZFC for polycrystalline sample of **3Dy** with 2 KOe DC field in cool mode from 20 K to 2 K and in warm mode from 2 K to 20 K respectively. Related to Figure 5.
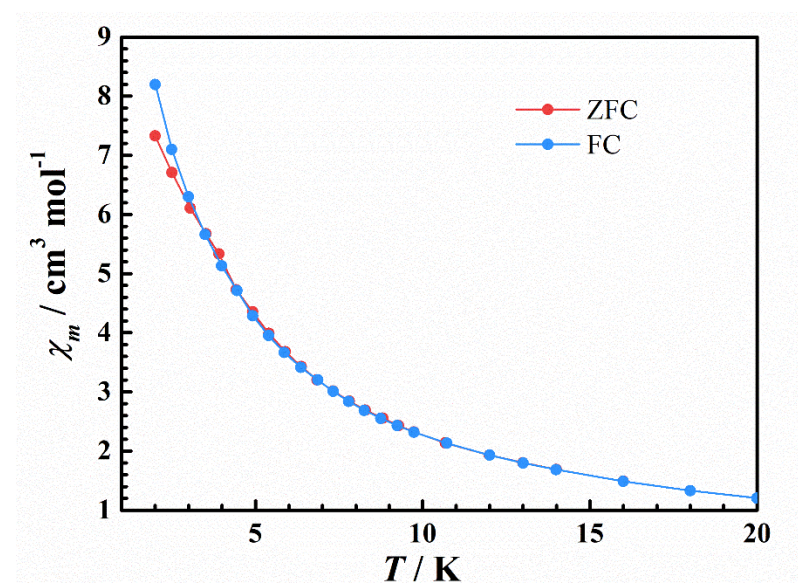
Figure S37 The Field-cooled (FC, blue line) and zero-field-cooled (ZFC, red line) variable-temperature magnetic susceptibility. The FC-ZFC for polycrystalline sample of **4Dy** with 2 KOe DC field in cool mode from 20 K to 2 K and in warm mode from 2 K to 20 K respectively. Related to Figure 5.
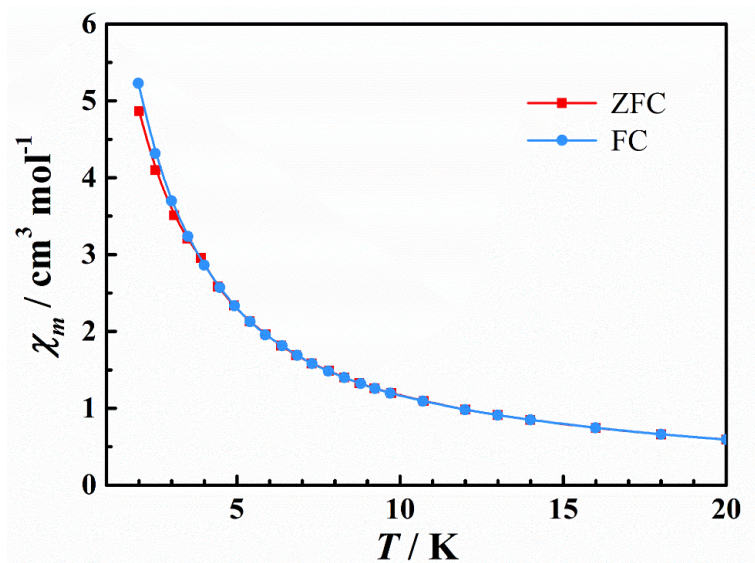
Figure S38 The Field-cooled (FC, blue line) and zero-field-cooled (ZFC, red line) variable-temperature magnetic susceptibility. The FC-ZFC for polycrystalline sample of **5Dy@5Y** with 2 KOe DC field in cool mode from 20 K to 2 K and in warm mode from 2 K to 20 K respectively. Related to Figure 5.
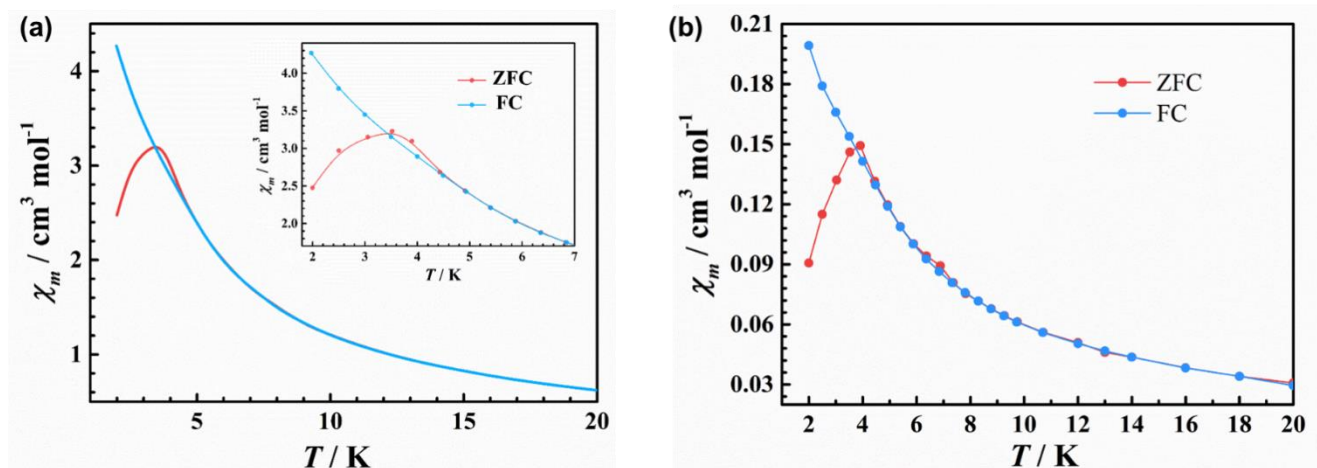
Figure S39 The Field-cooled (FC, blue line) and zero-field-cooled (ZFC, red line) variable-temperature magnetic susceptibility. The FC-ZFC for polycrystalline sample of **6Dy** (a) and **6Dy@6Y** (b) with 2 KOe DC field in cool mode from 20 K to 2 K and in warm mode from 2 K to 20 K respectively. Related to Figure 5.
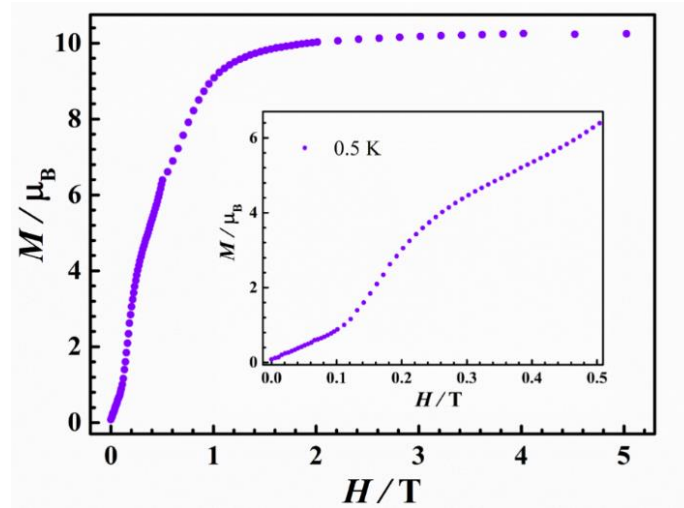
Figure S40 The field dependent magnetization (*M/H*). The *M/H* curve for polycrystalline sample of **2Dy** at 0.5 K up to 5 Tesla. Related to Figure 6.
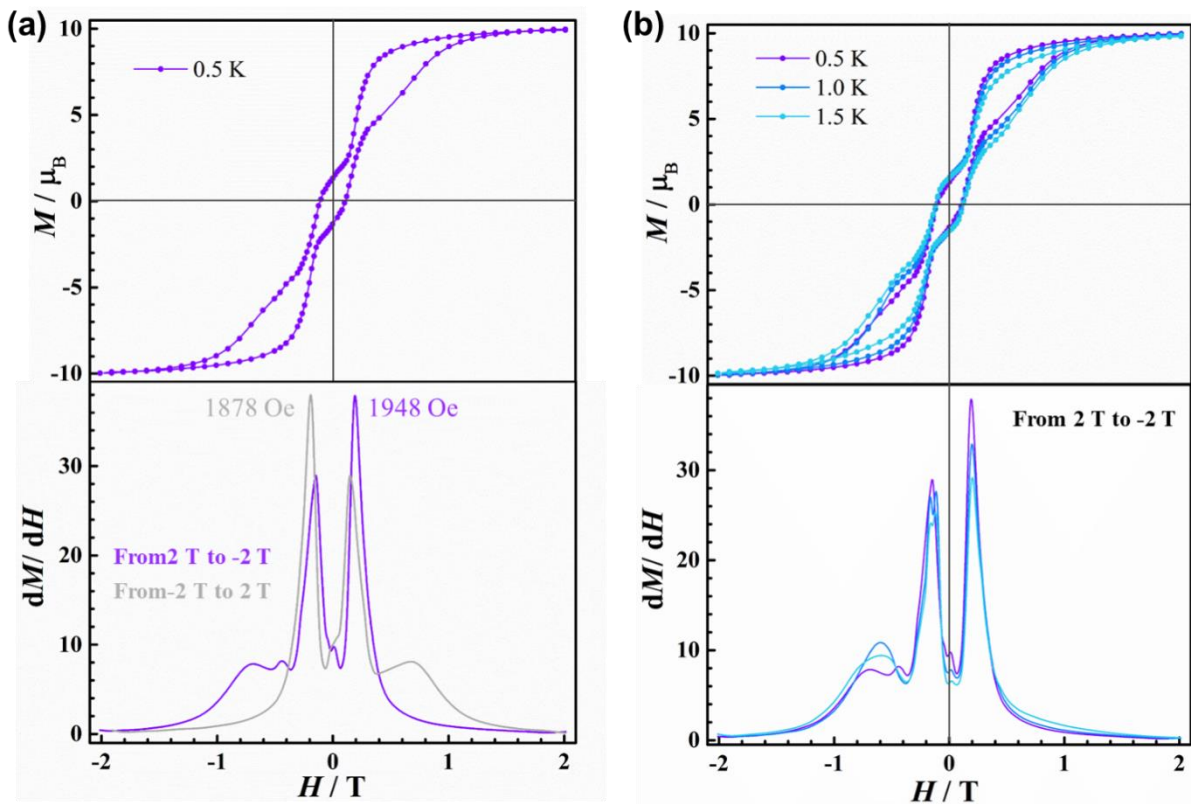
Figure S41 The magnetic hysteresis loop measurements of 2Dy. Magnetic hysteresis loops (top) and the first derivative of magnetization (*dM/dH*) versus magnetic field (bottom) for polycrystalline sample of **2Dy** at ultra-low temperature with an average sweep rate of 15 Oe s^{-1}. Related to Figure 6.
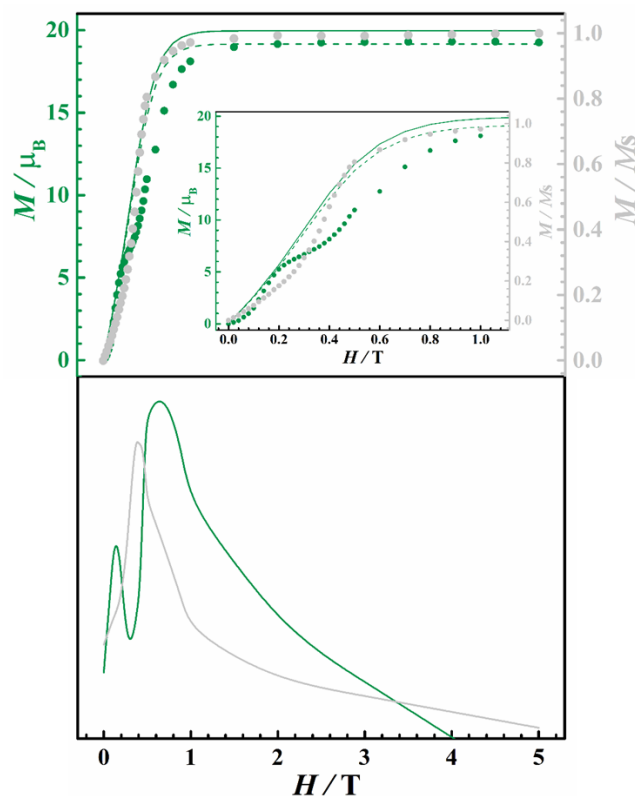
Figure S42 The field dependent magnetization (*M/H*). The field dependent magnetization measurements (top) and the first derivative of magnetization (*dM/dH*) versus magnetic field (bottom) at 2.0 K for single crystal sample of **2Dy** (green color) and **2Dy@2Y** (gray color). The solid green lines are the fits from POLY_ANISO and the green dash line represents the result of fitting data multiplied by a coefficient of 0.96. Related to Figure 6 and STAR Methods.
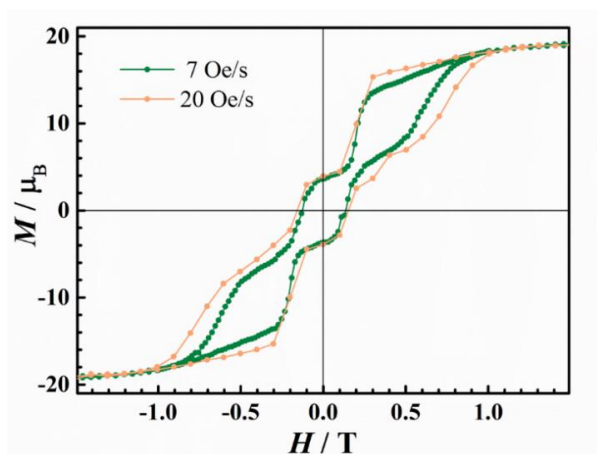
Figure S43 The magnetic hysteresis loop measurements of 2Dy. Magnetic hysteresis loop measurements for single crystal sample of **2Dy**. Related to Figure 6.
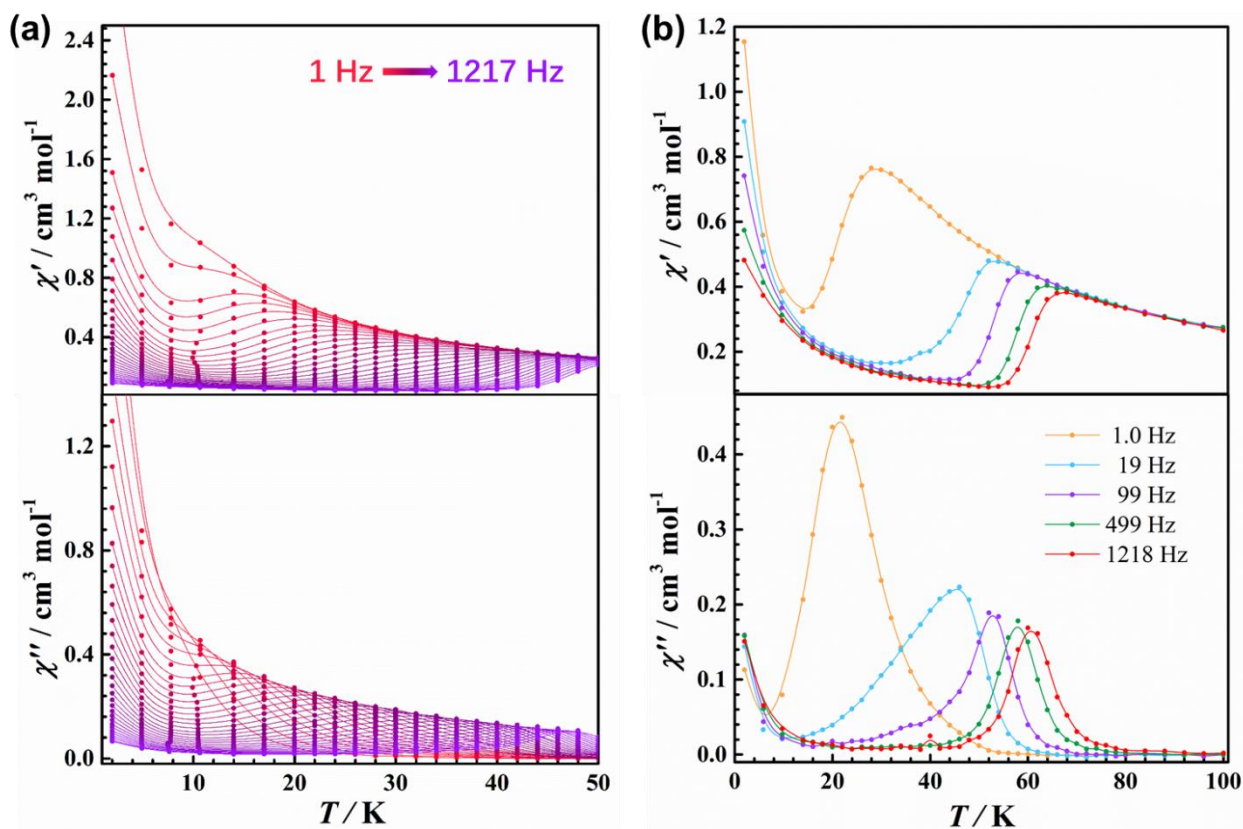
Figure S44 The ac susceptibility measurements. Variable-temperature magnetic susceptibility in-phase (χ', top) and out-of-phase (χ'', bottom) for polycrystalline sample of **1Dy** (a) and **2Dy** (b), at zero DC field and an oscillating field of 3.5 Oe. Related to Figure 7.
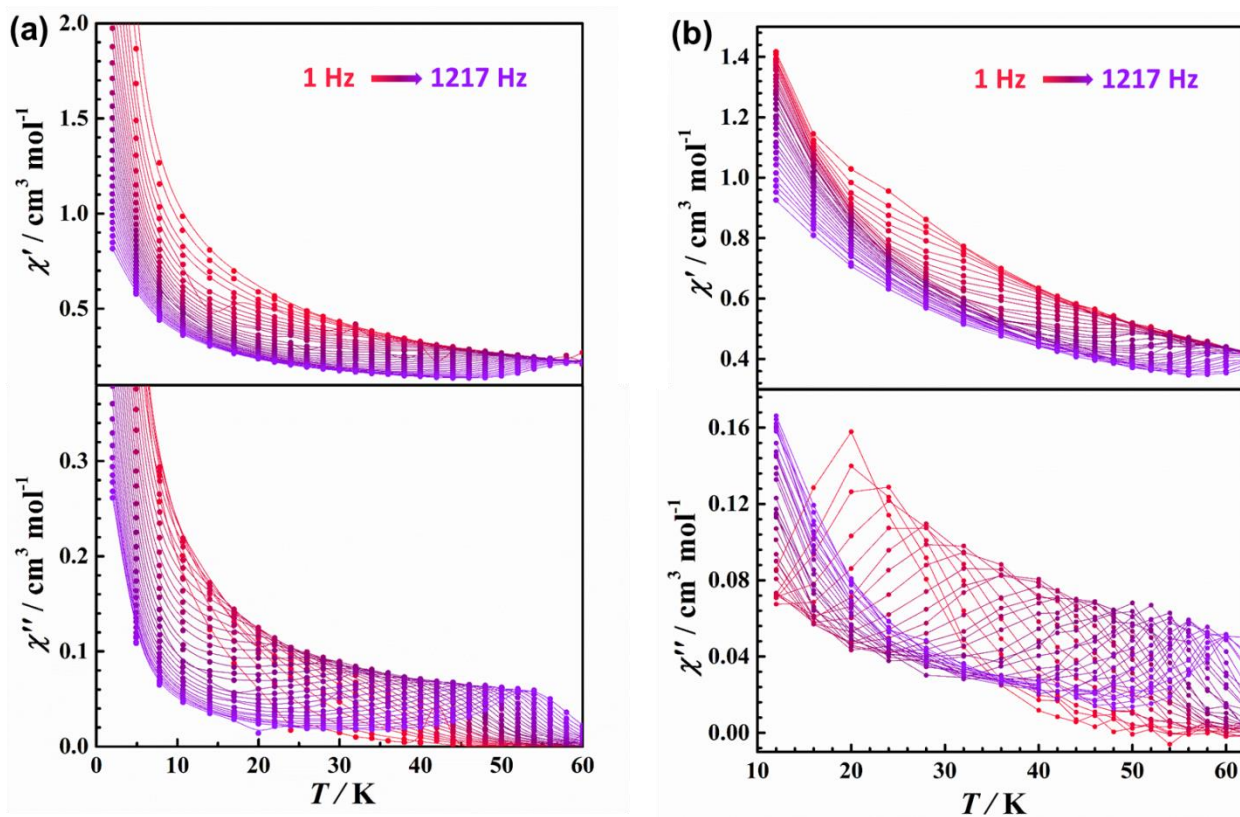
Figure S45 The ac susceptibility measurements. Variable-temperature magnetic susceptibility in-phase (χ', top) and out-of-phase (χ'', bottom) for polycrystalline sample of **3Dy** (a) and **4Dy** (b), at zero DC field and an oscillating field of 3.5 Oe. Related to Figure 7.
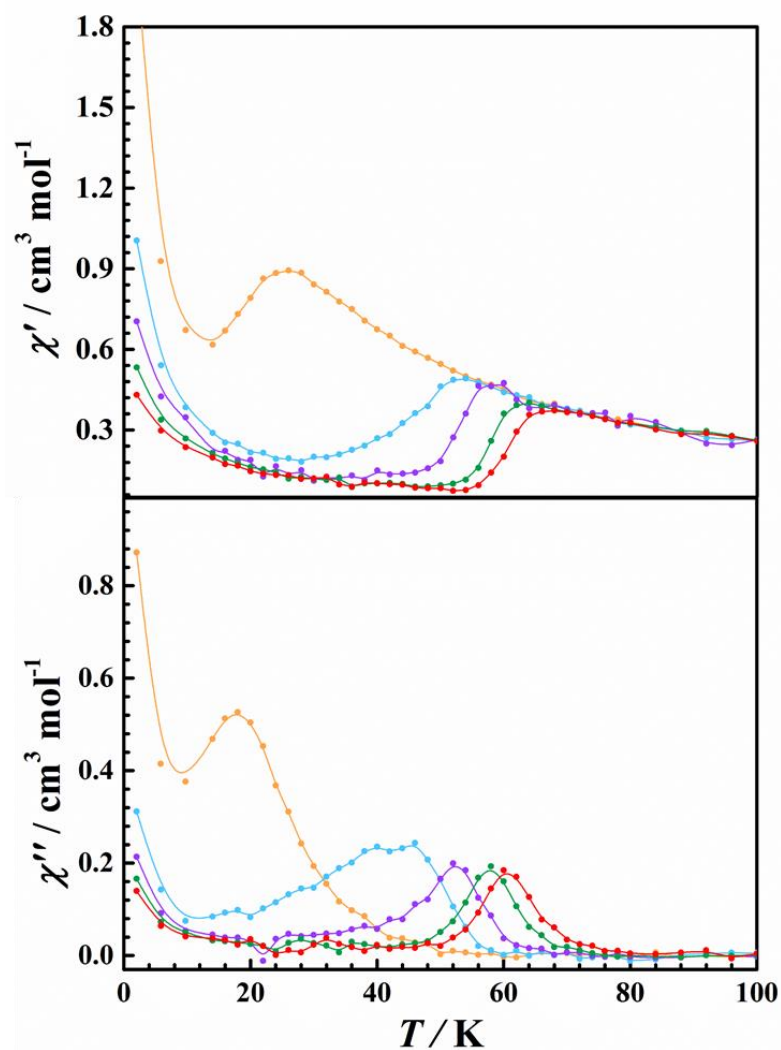
Figure S46 The ac susceptibility measurements. Variable-temperature magnetic susceptibility in-phase (χ', top) and out-of-phase (χ'', bottom) for polycrystalline sample of **2Dy@2Y**, at zero DC field and an oscillating field of 3.5 Oe. Related to Figure 7.
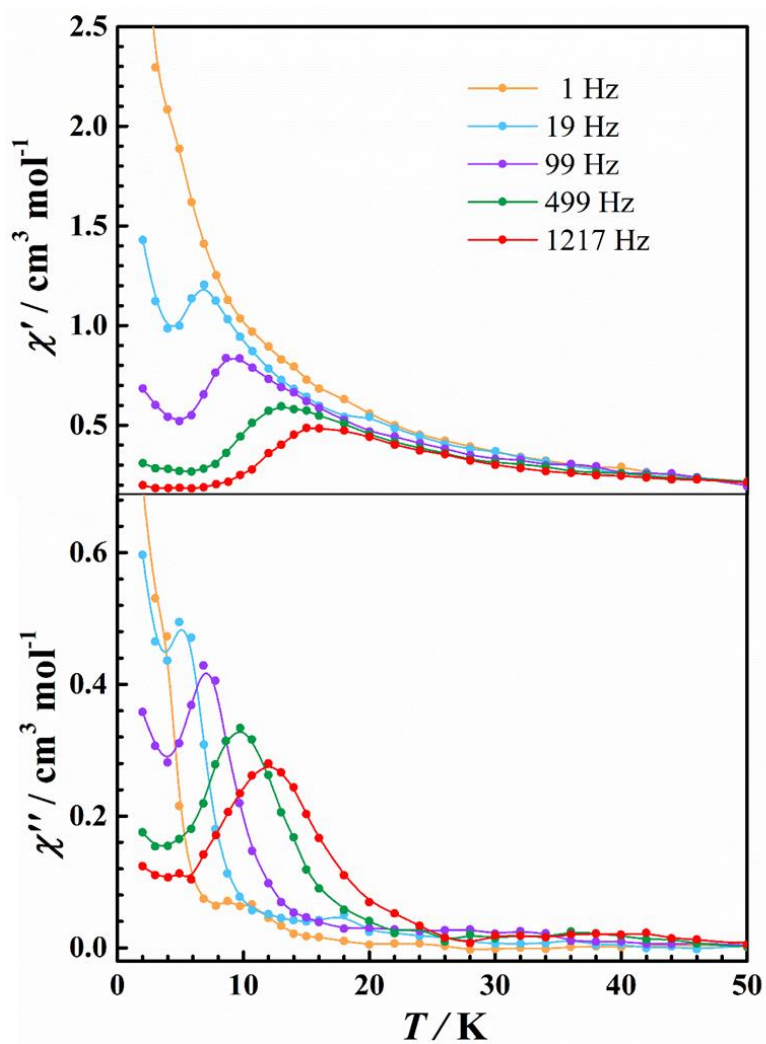
Figure S47 The ac susceptibility measurements. Variable-temperature magnetic susceptibility in-phase (χ', top) and out-of-phase (χ'', bottom) for **5Dy@5Y**, in zero DC field and an oscillating field of 3.5 Oe. Related to Figure 7.
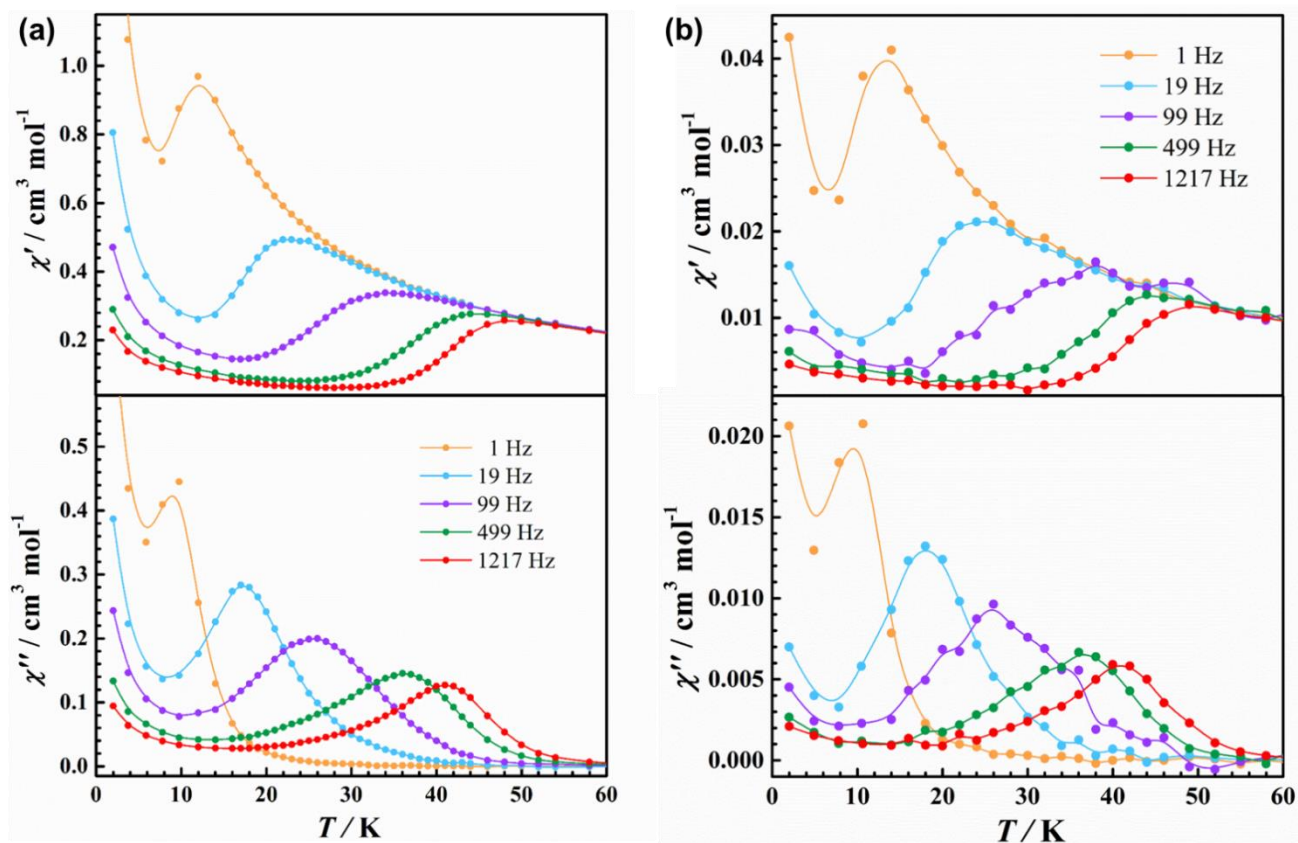
Figure S48 The ac susceptibility measurements. Variable-temperature magnetic susceptibility in-phase (χ', top) and out-of-phase (χ'', bottom) for **6Dy** (a) and **6Dy@6Y** (b) in zero DC field and an oscillating field of 3.5 Oe. Related to Figure 7.
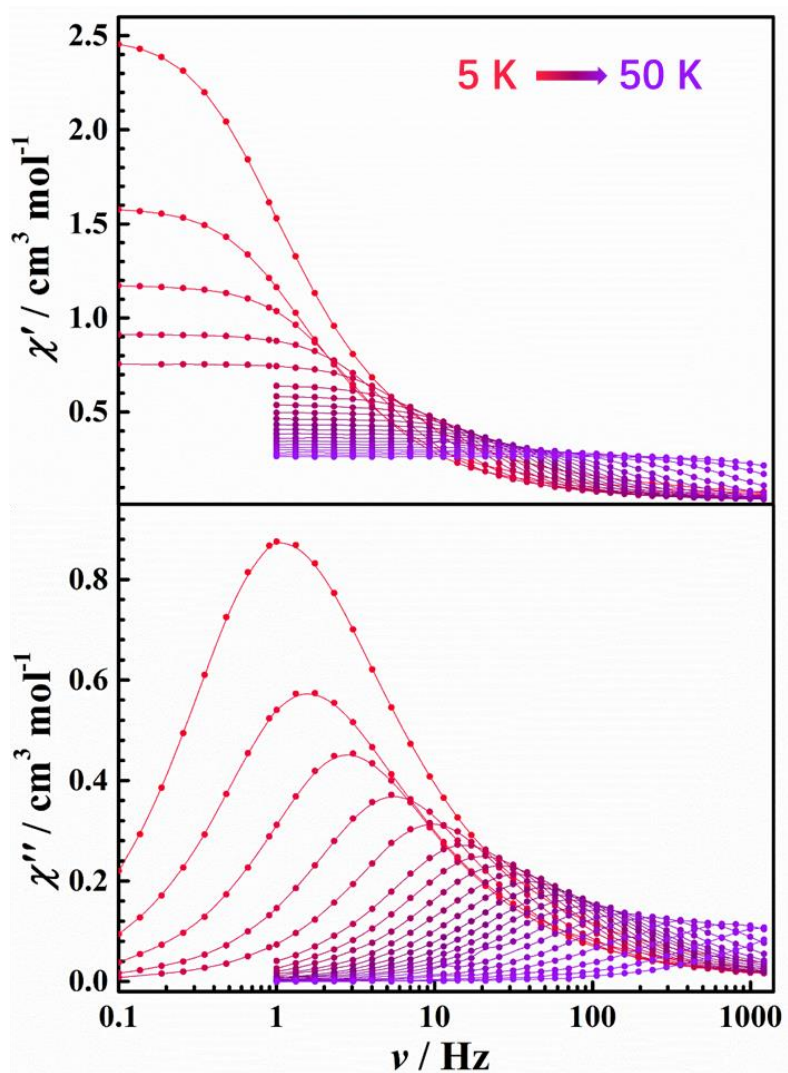
Figure S49 The ac susceptibility measurements. Frequency-dependence of the in-phase (χ', top) and out-of-phase (χ'', bottom) ac susceptibility signals for polycrystalline sample of **1Dy** in zero DC field and an oscillating field of 3.5 Oe. Related to Figure 7.
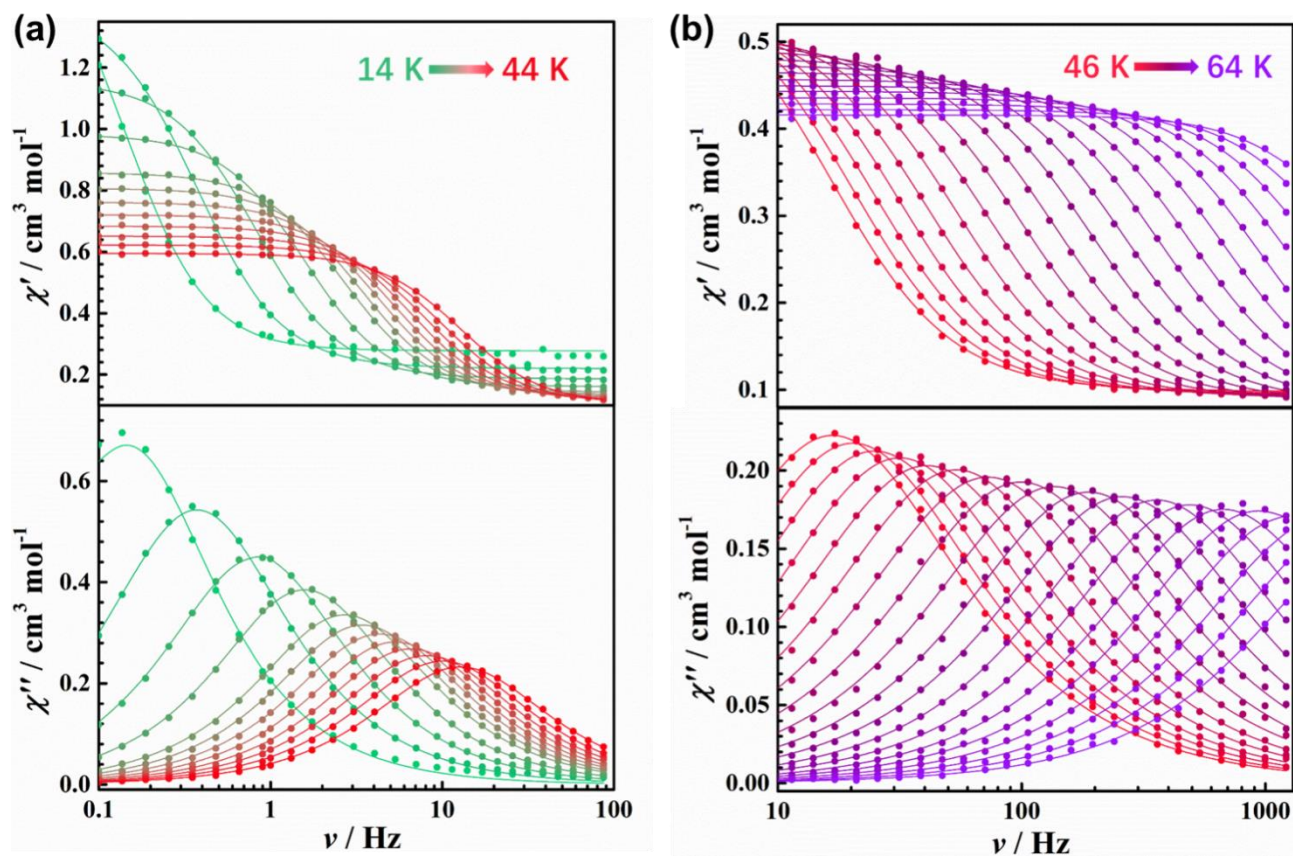
Figure S50 The ac susceptibility measurements. Frequency-dependence of the in-phase (χ', top) and out-of-phase (χ'', bottom) ac susceptibility signals for polycrystalline sample of **2Dy** in zero DC field and an oscillating field of 3.5 Oe. Related to Figure 7.
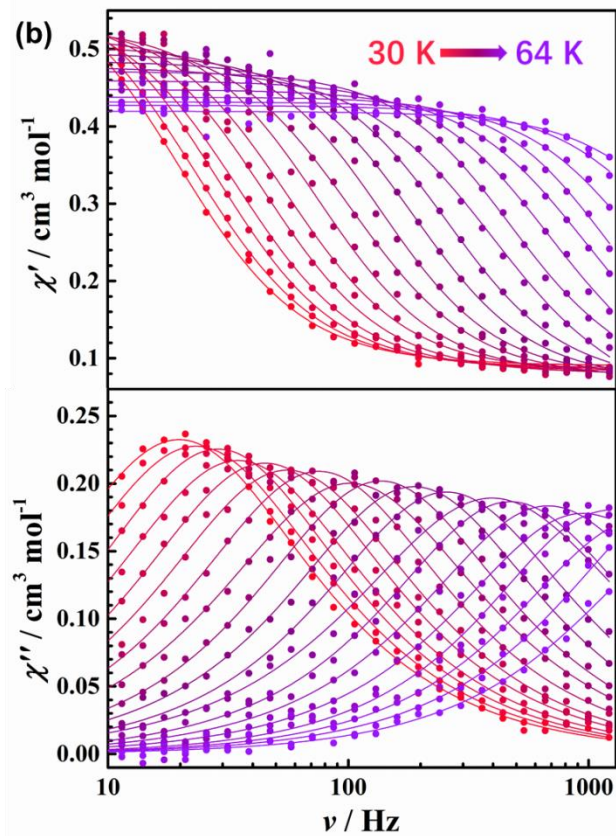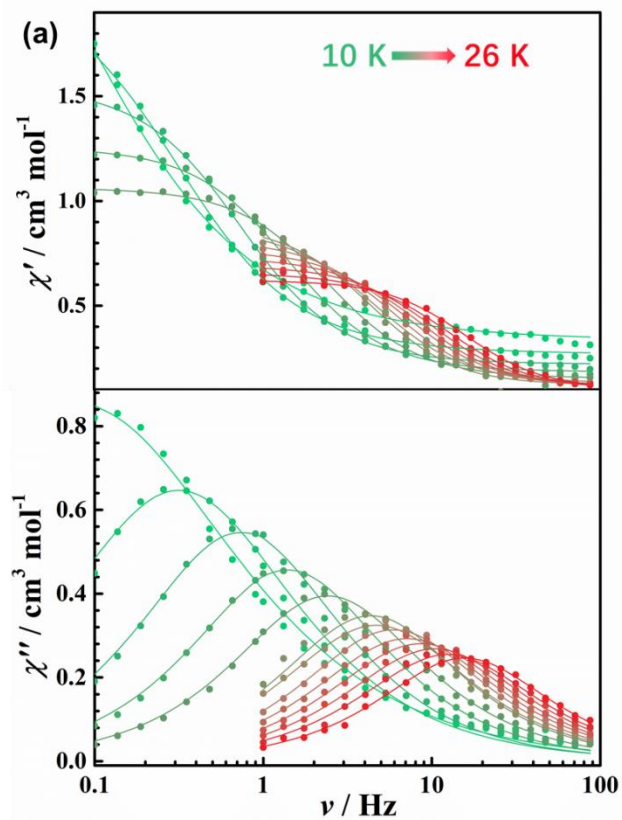
Figure S51 The ac susceptibility measurements. Frequency-dependence of the in-phase (χ', top) and out-of-phase (χ'', bottom) ac susceptibility signals for polycrystalline sample of **2Dy@2Y** in zero DC field and an oscillating field of 3.5 Oe. Related to Figure 7.
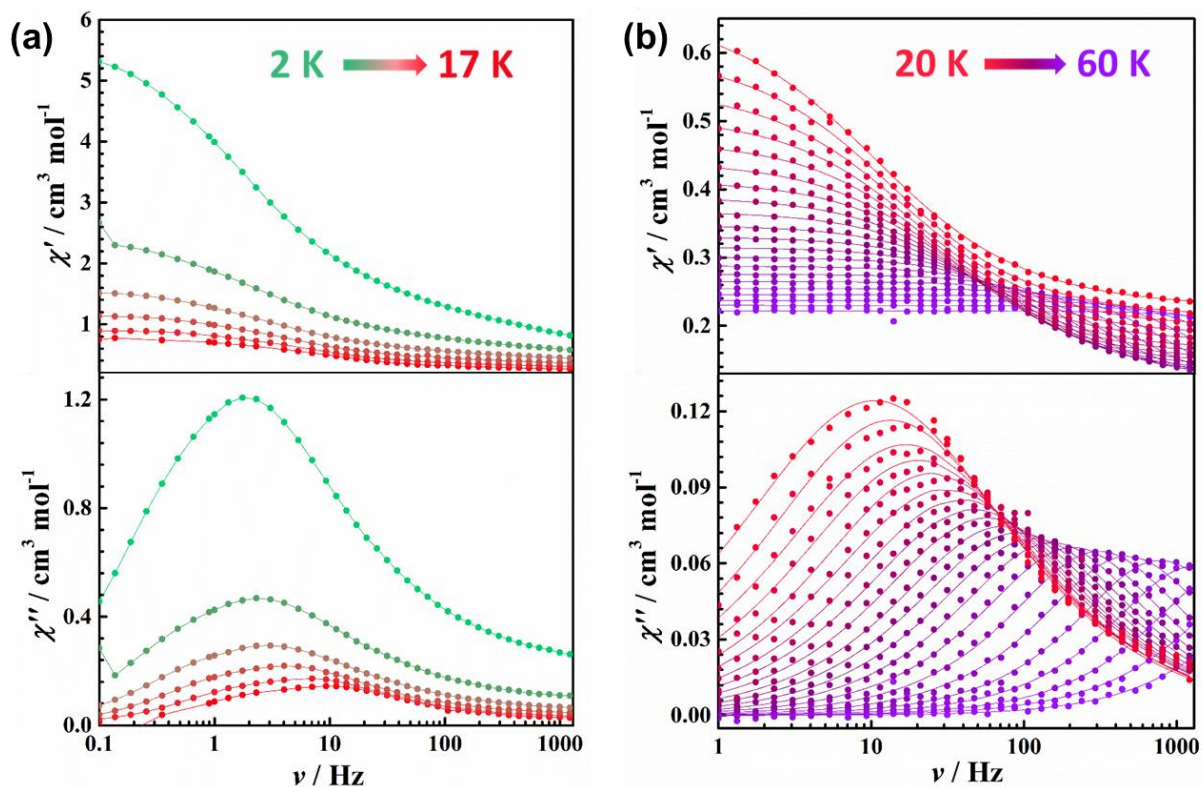
Figure S52 The ac susceptibility measurements. Frequency-dependence of the in-phase (χ', top) and out-of-phase (χ'', bottom) ac susceptibility signals for polycrystalline sample of **3Dy** in zero DC field and an oscillating field of 3.5 Oe. Related to Figure 7.
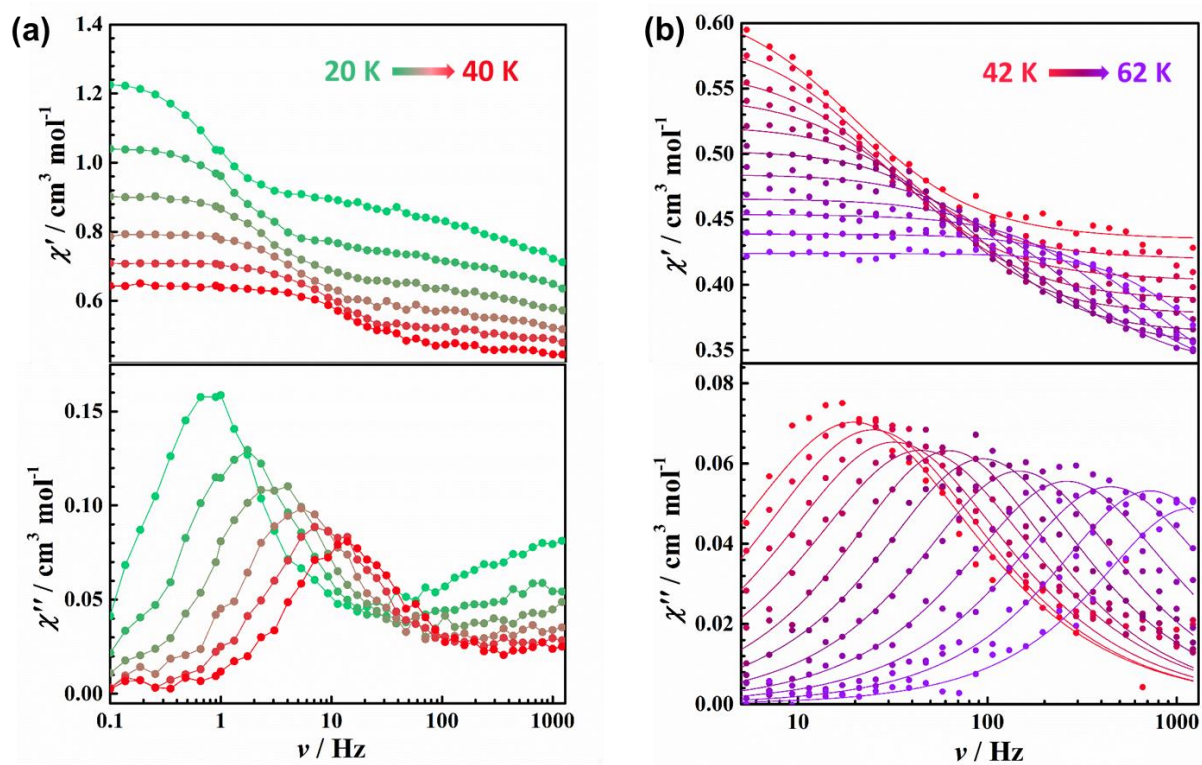
Figure S53 The ac susceptibility measurements. Frequency-dependence of the in-phase (χ', top) and out-of-phase (χ'', bottom) ac susceptibility signals for polycrystalline sample of **4Dy** in zero DC field and an oscillating field of 3.5 Oe. Related to Figure 7.
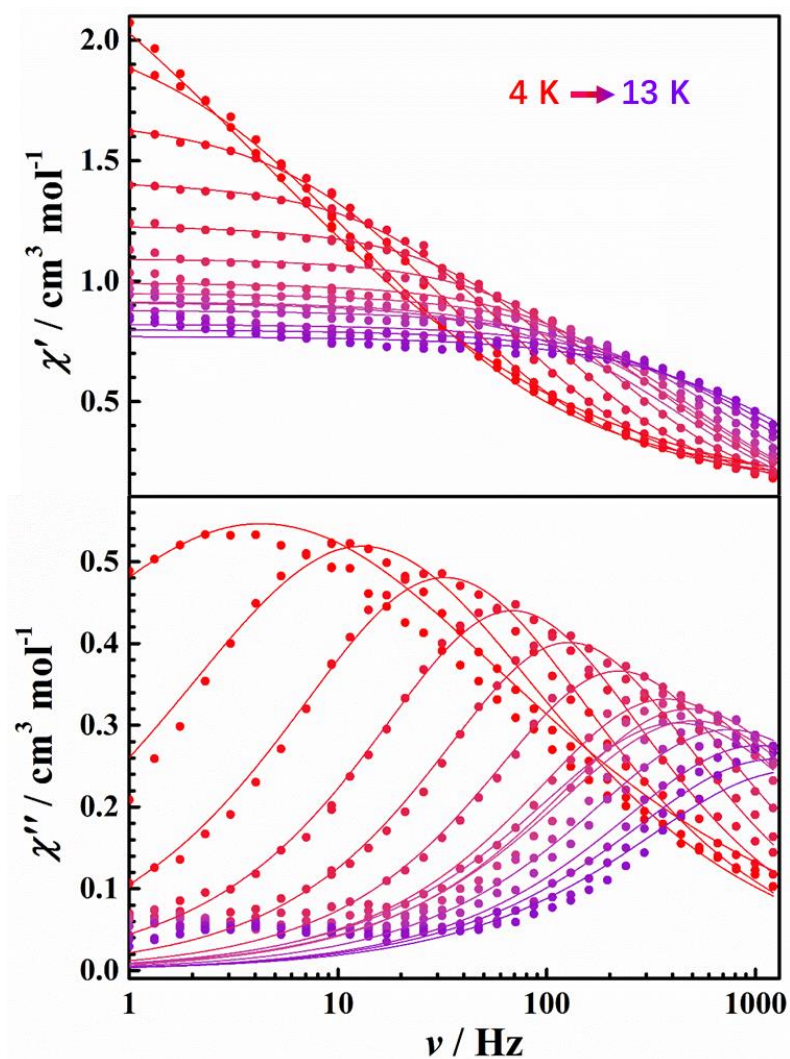
Figure S54 The ac susceptibility measurements. Frequency-dependence of the in-phase (χ', top) and out-of-phase (χ'', bottom) ac susceptibility signals for **5Dy@5Y** in zero DC field and an oscillating field of 3.5 Oe. Related to Figure 7.
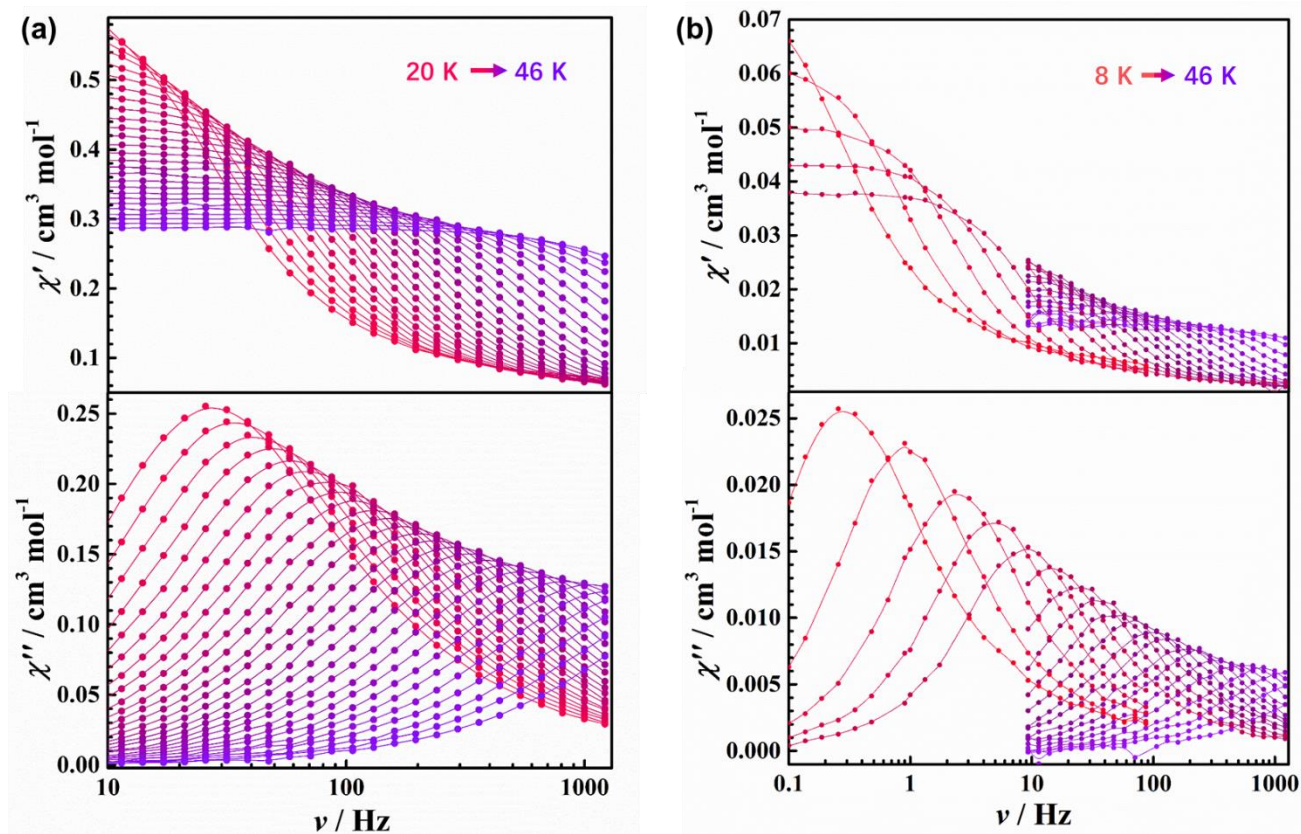
Figure S55 The ac susceptibility measurements. Frequency dependence of χ' and χ'' for **6Dy** (a) and **6Dy@6Y** (b) in zero DC field and an oscillating field of 3.5 Oe. Related to Figure 7.
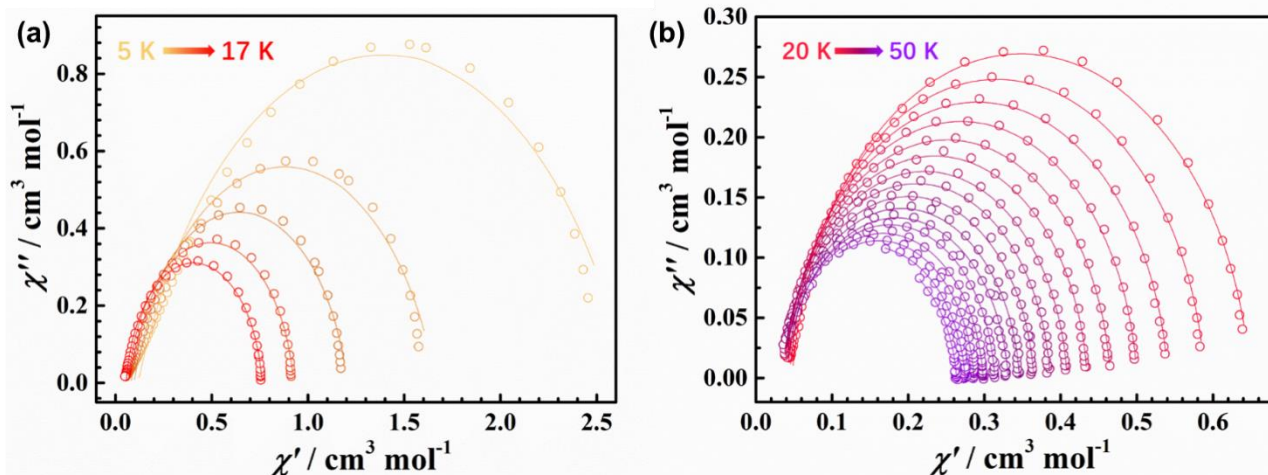
Figure S56 The Cole-Cole plots using the frequency-dependence ac susceptibility data under zero DC field. The plots for polycrystalline sample of **1Dy** from 4.0 K to 13 K. Related to Figure 8.
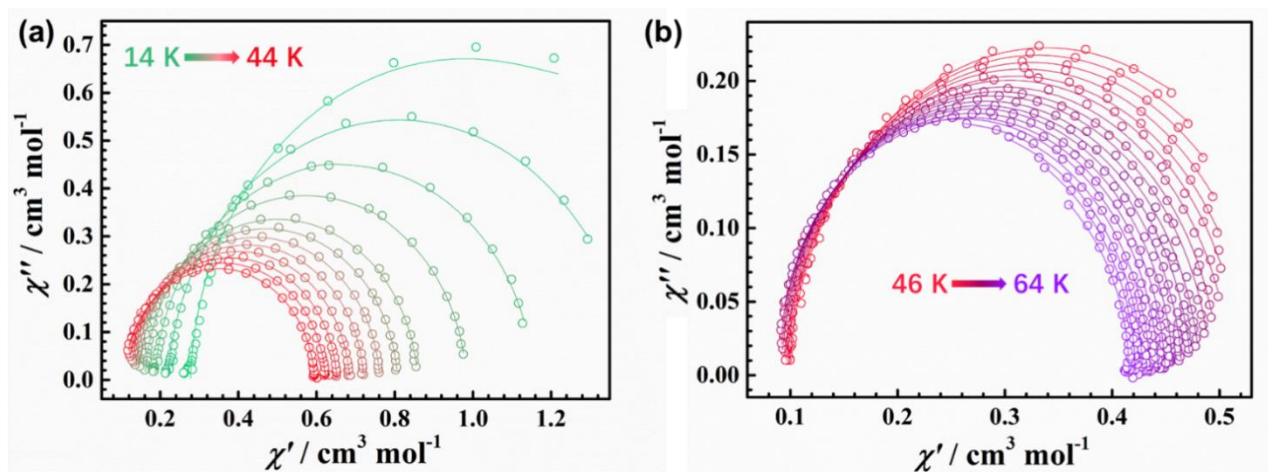
Figure S57 The Cole-Cole plots using the frequency-dependence ac susceptibility data under zero DC field. The plots for polycrystalline sample of **2Dy** from 4.0 K to 13 K. Related to Figure 8.
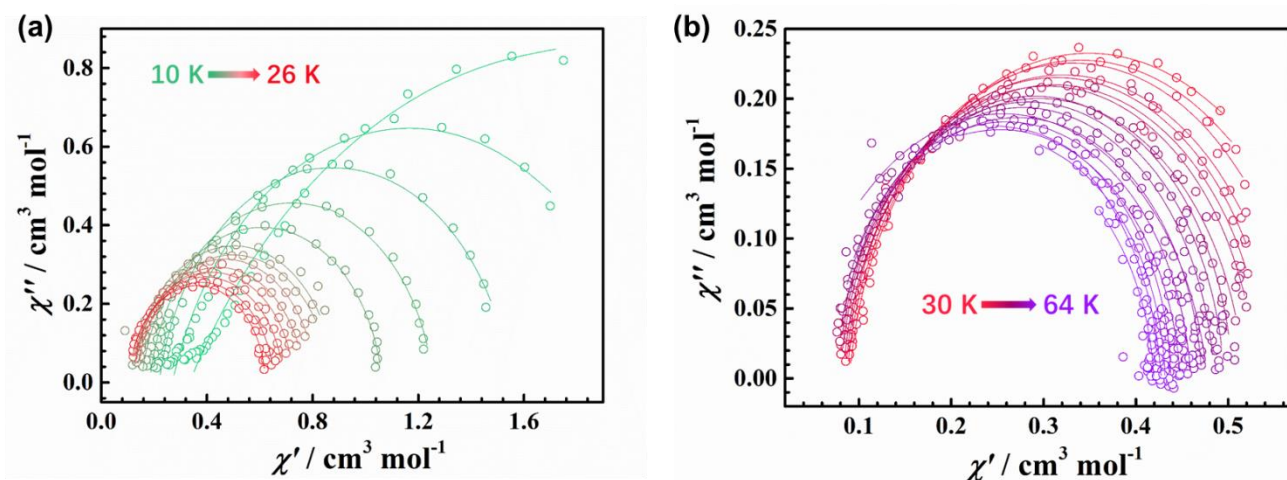
Figure S58 The Cole-Cole plots using the frequency-dependence ac susceptibility data under zero DC field. The plots for polycrystalline sample of **2Dy@2Y** from 8 K to 18 K (left), and from 20 K to 46K (right). Related to Figure 8.
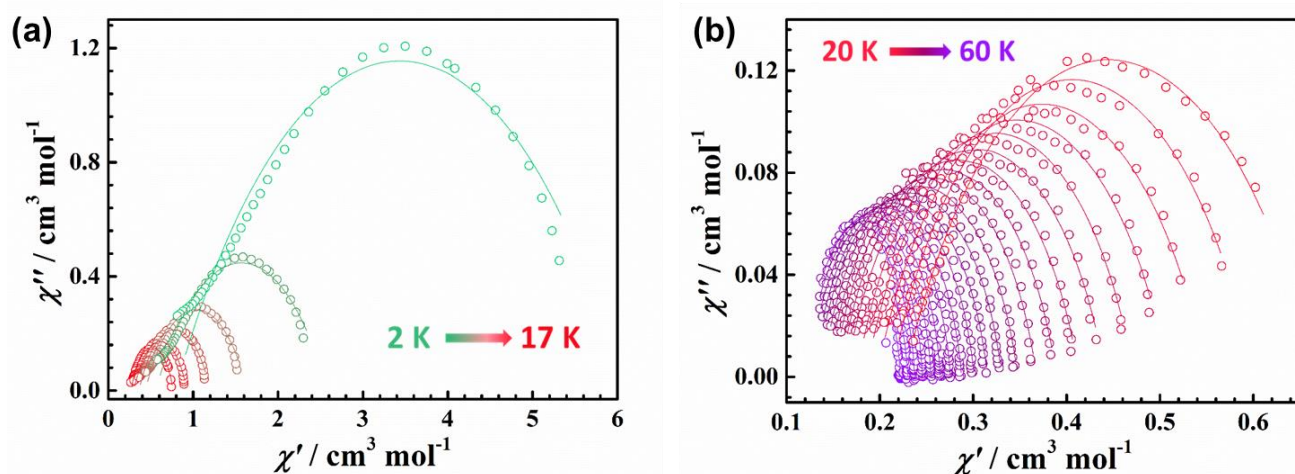
Figure S59 The Cole-Cole plots using the frequency-dependence ac susceptibility data under zero DC field. The plots for polycrystalline sample of **3Dy** from 8 K to 18 K (left), and from 20 K to 46K (right). Related to Figure 8.
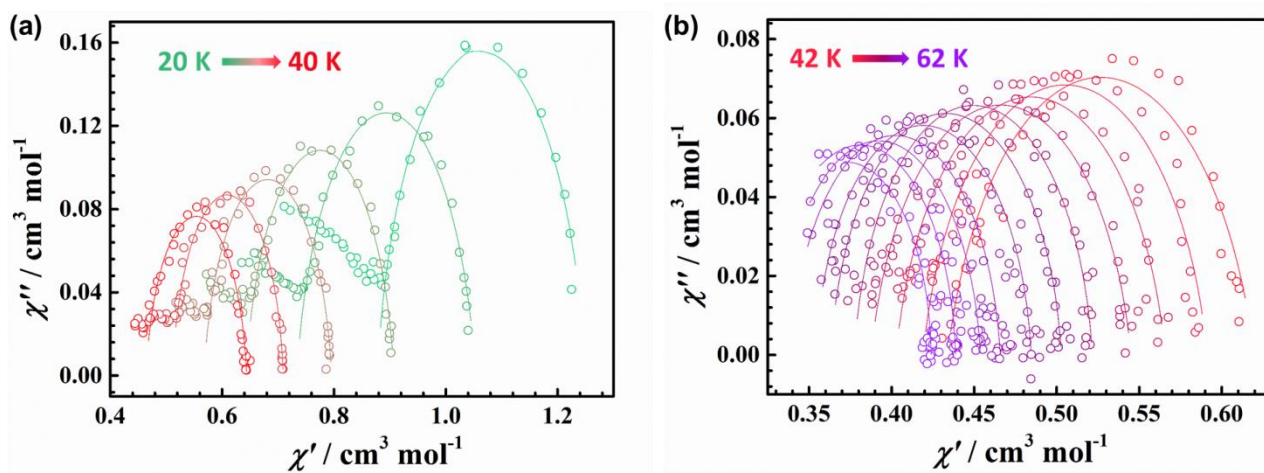
Figure S60 The Cole-Cole plots using the frequency-dependence ac susceptibility data under zero DC field. The plots for polycrystalline sample of **4Dy** from 8 K to 18 K (left), and from 20 K to 46K (right). Related to Figure 8.
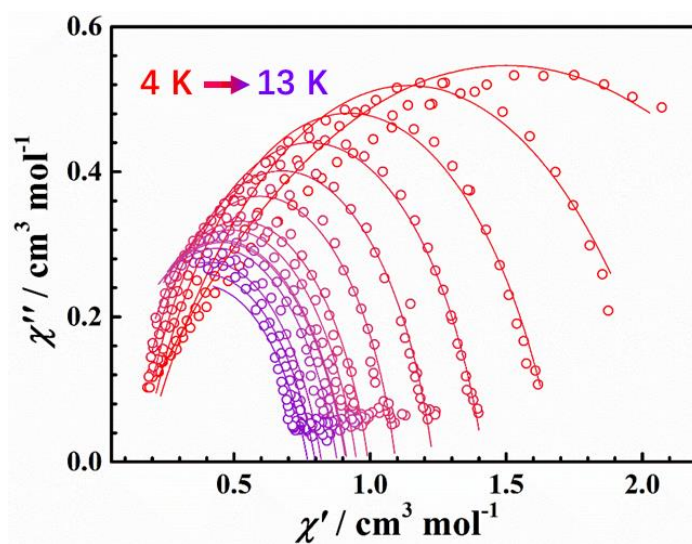
Figure S61 The Cole-Cole plots using the frequency-dependence ac susceptibility data under zero DC field. The plots for **5Dy@5Y** from 4.0 K to 13 K. Related to Figure 8.
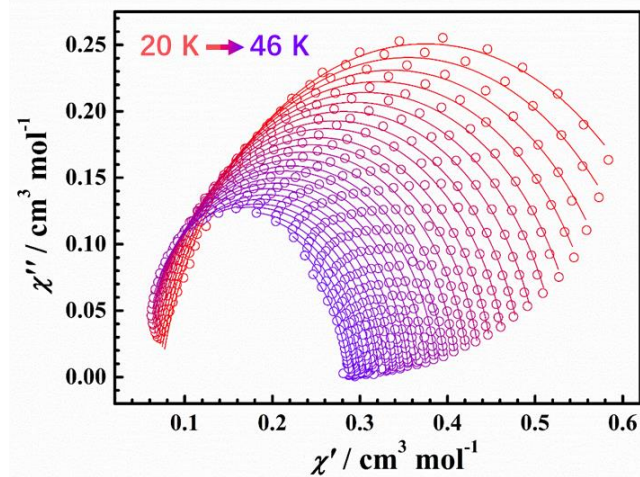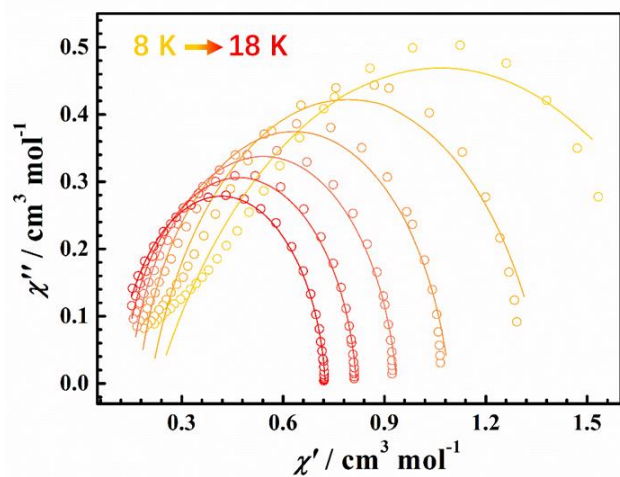
Figure S62 The Cole-Cole plots using the frequency-dependence ac susceptibility data under zero DC field. The plots for **6Dy** from 8 K to 18 K (left), and from 20 K to 46K (right). Related to Figure 8.
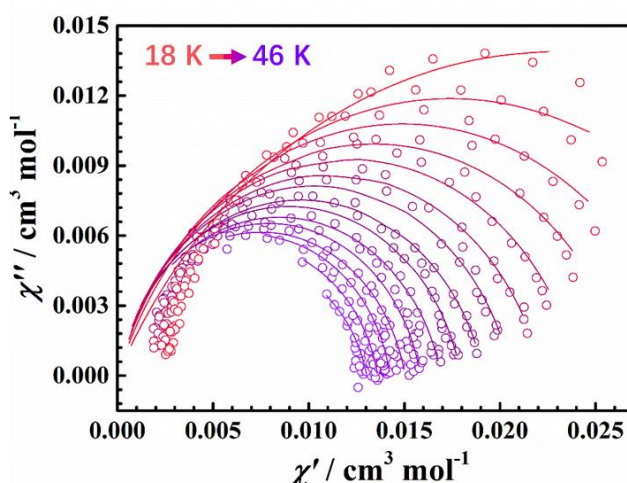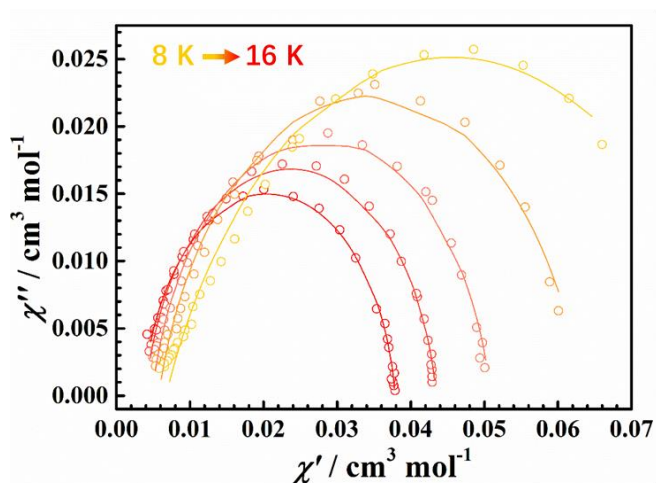
Figure S63 The Cole-Cole plots using the frequency-dependence ac susceptibility data under zero DC field. The plots for **6Dy@6Y** from 8 K to 16 K (left), and from 18 K to 46K (right). Related to Figure 8.
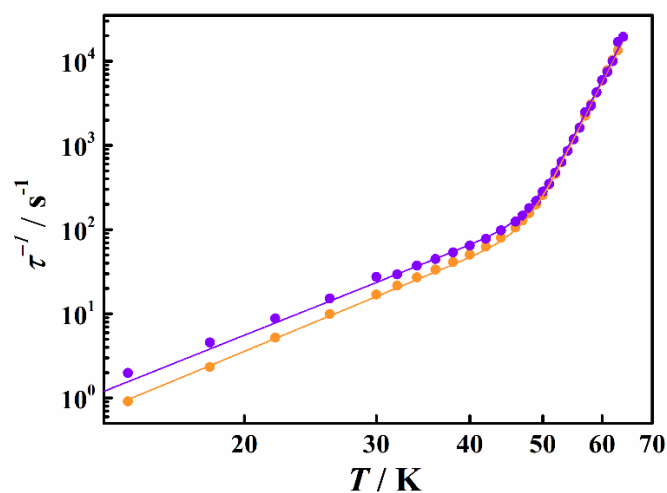
Figure S64 The slow magnetic relaxation plots. Plot of natural log of the inverse relaxation time *vs.* temperature for **2Dy** (orange) and **2Dy@2Y** (purple). The plots are from the ac susceptibility measurements. The solid lines are the best fit with equation 2, giving U_{eff} = 1089(6) K, $\tau_0 = 2.4(1) \times 10^{-12}$ s, $C = 5.5(2) \times 10^{-5}$ s^{-1} K $^{-n}$ and $n = 3.7(2)$ for **2Dy** and U_{eff} = 1089(6) K (Fixed), $\tau_0 = 2.3(1) \times 10^{-12}$ s, $C = 1.3(2) \times 10^{-4}$ s^{-1} K $^{-n}$ and $n = 3.56(2)$ for **2Dy@2Y** under zero dc magnetic field. Related to Figure 8.
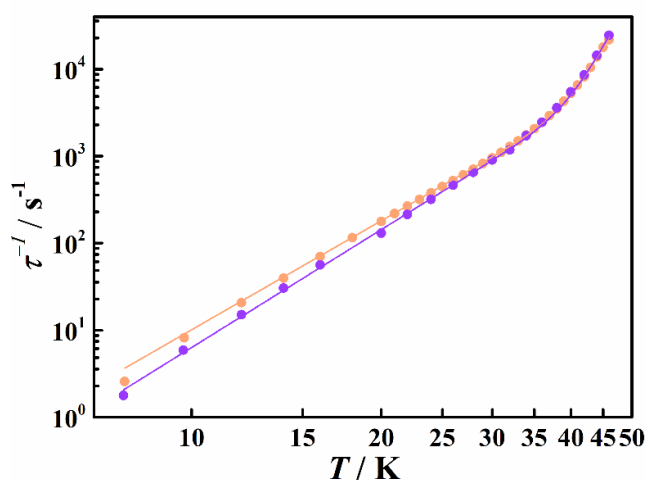
Figure S65 The slow magnetic relaxation plots. Plot of natural log of the inverse relaxation time *vs.* temperature for **6Dy** (orange) and **6Dy@6Y** (purple). The plots are from the ac susceptibility measurements. The solid lines are the best fit with equation 2, giving U_{eff} = 704(10) K, $\tau_0 = 1.28(2) \times 10^{-11}$ s, $C = 7.0(2) \times 10^{-4}$ s^{-1} K $^{-n}$ and $n = 4.16(2)$ for **6Dy** and U_{eff} = 704(10) K (Fixed), $\tau_0 = 1.25(1) \times 10^{-11}$ s, $C = 2.0(1) \times 10^{-4}$ s^{-1} K $^{-n}$ and $n = 4.5(1)$ for **6Dy@6Y** under zero dc magnetic field. Related to Figure 8.

Table S8 Relaxation fitting parameters for 1Dy from Figure S56. Related to Figure 8.

T / K	χ_S / cm^3 mol^{-1}	χ_T / cm^3 mol^{-1}	τ / s	α
5	0.11764	2.65999	0.12435	0.24767
8	0.09556	1.66284	0.08503	0.20735
11	0.08095	1.20376	0.04931	0.14641
14	0.06598	0.92518	0.02637	0.10123
17	0.05549	0.76076	0.01566	0.07648
20	0.04756	0.64878	0.01005	0.06678
22	0.04438	0.58905	0.00771	0.0559
24	0.04156	0.54056	0.00606	0.05066
26	0.03911	0.50005	0.00481	0.04626
28	0.03746	0.46517	0.00387	0.04607
30	0.03629	0.43484	0.00314	0.04586
32	0.03484	0.40864	0.00258	0.05087
34	0.03509	0.38618	0.00211	0.04983
36	0.03718	0.36466	0.00173	0.04919
38	0.03715	0.34604	0.00137	0.05511
40	0.03916	0.33108	0.00101	0.05545
42	0.03876	0.31332	6.7602E-4	0.04457
44	0.03651	0.29817	3.96933E-4	0.05091
46	0.0362	0.28616	2.17807E-4	0.05435
48	0.03222	0.27458	1.11934E-4	0.06716
50	0.03937	0.26324	6.12609E-5	0.06039

Table S9 Relaxation fitting parameters for 2Dy from Figure S57. Related to Figure 8.

T / K	χ_S / cm^3 mol^{-1}	χ_T / cm^3 mol^{-1}	τ / s	α
14	0.27756	1.68213	1.09635	0.01951
18	0.21959	1.40103	0.42718	0.04492
22	0.18571	1.15566	0.19227	0.04154
26	0.1602	0.9833	0.1007	0.03536
30	0.14238	0.85848	0.05893	0.03456
32	0.13475	0.8073	0.0464	0.03351
34	0.12791	0.76194	0.03689	0.03282
36	0.12256	0.721	0.0299	0.03075
38	0.11656	0.68408	0.02428	0.02888
40	0.11232	0.65174	0.01979	0.02956
42	0.10777	0.62278	0.01595	0.02963
44	0.10462	0.59511	0.01249	0.03001
46	0.098	0.57898	0.00947	0.0459
47	0.09616	0.56458	0.00782	0.04351
48	0.09434	0.55395	0.00638	0.04627
49	0.09303	0.54069	0.00503	0.04284
50	0.09078	0.53028	0.00389	0.04633
51	0.08947	0.52047	0.00294	0.04248
52	0.0879	0.51071	0.00219	0.04516
53	0.08681	0.49998	0.0016	0.04071
54	0.08592	0.49184	0.00117	0.0392
55	0.08502	0.48173	8.45494E-4	0.0365
56	0.08398	0.47359	6.12972E-4	0.0351
57	0.0846	0.4651	4.44719E-4	0.02761
58	0.08481	0.45688	3.23862E-4	0.02421
59	0.08504	0.44948	2.3674E-4	0.02127
60	0.07707	0.44334	1.70163E-4	0.028
61	0.08057	0.43564	1.28113E-4	0.02348
62	0.08355	0.42853	9.65619E-5	0.01993
63	0.09027	0.42185	7.46495E-5	0.01139

Table S10 Relaxation fitting parameters for 2Dy@2Y from Figure S58. Related to Figure 8.

T / K	χ_S / cm^3 mol^{-1}	χ_T / cm^3 mol^{-1}	τ / s	α
10	0.33436	3.3472	1.9123	0.34444
14	0.26935	2.06146	0.50494	0.19934
18	0.2195	1.55057	0.2184	0.11915
22	0.1829	1.25732	0.11361	0.09726
26	0.15217	1.06434	0.06587	0.08597
30	0.12008	0.88502	0.03655	0.05453
32	0.13023	0.86869	0.034	0.07588
34	0.12064	0.81235	0.02689	0.05546
36	0.11781	0.77056	0.02231	0.06292
38	0.11078	0.73018	0.01867	0.05687
40	0.10488	0.69119	0.01543	0.05166
42	0.10267	0.65503	0.01285	0.04789
44	0.10391	0.6215	0.01019	0.02728
46	0.0899	0.60829	0.00805	0.06564
47	0.087	0.59339	0.00685	0.06433
48	0.08522	0.57759	0.00555	0.05217
49	0.08254	0.55928	0.00458	0.05612
50	0.07951	0.54912	0.00354	0.05206
51	0.08289	0.54018	0.00286	0.05063
52	0.07737	0.5303	0.00211	0.04732
53	0.07327	0.51731	0.00156	0.06225
54	0.07619	0.50454	0.00116	0.0338
55	0.07168	0.49562	8.47501E-4	0.04051
56	0.0696	0.48478	6.194E-4	0.04025
57	0.03596	0.47763	4.01618E-4	0.09489
58	0.07212	0.47144	3.36833E-4	0.03933
59	0.0598	0.45957	2.34379E-4	0.05078
60	0.05989	0.44807	1.68601E-4	0.05163
61	0.06969	0.43778	1.34695E-4	0.01138
62	0.07114	0.4318	9.97785E-5	0.02687
63	0.0041	0.42743	5.89493E-5	0.05594
64	0.05761	0.41959	5.15616E-5	0.0491

Table S11 Relaxation fitting parameters for 3Dy from Figure S59. Related to Figure 8.

T/ K	χ_S / cm^3 mol^{-1}	χ_T / cm^3 mol^{-1}	τ / s	α
2	0.26807	0.76432	0.08153	0.30239
5	0.30366	0.92651	0.06292	0.35775
8	0.36201	1.20033	0.05054	0.39867
11	0.43554	1.63862	0.03879	0.43717
14	0.56084	2.57576	0.02674	0.46683
17	0.78827	6.07825	0.01913	0.47481
20	0.12944	0.22166	0.01526	0.04475
22	0.10068	0.23	0.01192	0.09407
24	0.10697	0.23722	0.00946	0.07472
26	0.11177	0.2457	0.00779	0.07943
28	0.11426	0.25484	0.00636	0.08516
30	0.11676	0.26487	0.00514	0.10217
32	0.1184	0.27559	0.00414	0.11969
34	0.1216	0.28762	0.00343	0.13992
36	0.12496	0.30105	0.00279	0.15929
38	0.12897	0.31531	0.0022	0.18014
40	0.13226	0.33082	0.00175	0.19903
42	0.13818	0.3478	0.00138	0.21097
44	0.14398	0.36793	0.00104	0.22414
46	0.14983	0.3894	7.55609E-4	0.23952
48	0.1567	0.41355	5.12736E-4	0.25281
50	0.16329	0.44165	3.35031E-4	0.27228
52	0.17509	0.47214	2.04301E-4	0.27141
54	0.18478	0.50915	1.22785E-4	0.29167
56	0.19659	0.55045	6.92201E-5	0.30725
58	0.21196	0.60015	3.76865E-5	0.31081
60	0.22634	0.66454	3.24435E-5	0.34208

Table S12 Relaxation fitting parameters for 4Dy from Figure S60. Related to Figure 8.

T / K	χ_S / cm^3 mol^{-1}	χ_T / cm^3 mol^{-1}	τ / s	α
20	0.87809	1.24936	0.199	0.10573
24	0.73342	1.05354	0.09309	0.1453
28	0.64286	0.90763	0.05322	0.1223
32	0.5677	0.79595	0.02894	0.11615
36	0.51144	0.70935	0.01775	0.07852
40	0.46433	0.64406	0.01083	0.0993
42	0.43403	0.61939	0.00807	0.17131
44	0.41912	0.59121	0.00642	0.14224
46	0.40278	0.56574	0.00497	0.13679
48	0.38777	0.54493	0.00359	0.13395
50	0.37748	0.52155	0.00254	0.07975
52	0.36313	0.5028	0.00169	0.08063
54	0.35407	0.48451	0.00109	0.06985
56	0.3388	0.46584	6.06035E-4	0.08144
58	0.33035	0.45385	3.59034E-4	0.07933
60	0.32361	0.43877	2.20183E-4	0.04675
62	0.32239	0.42398	1.36368E-4	0.02201

Table S13 Relaxation fitting parameters for 5Dy@5Y from Figure S61. Related to Figure 8.

T / K	χ_S / cm^3 mol^{-1}	χ_T / cm^3 mol^{-1}	τ / s	α
4	0.16156	1.68409	0.0049	0.28153
4.9	0.14622	1.41789	0.00232	0.2275
5.88	0.12387	1.23175	0.00125	0.19984
6.83	0.09827	1.0938	7.18059E-4	0.19031
7.81	0.05099	0.99332	4.26672E-4	0.21654
8.76	0.02512	0.95047	3.30228E-4	0.22818
9.7	5.48317E-14	0.9162	3.16071E-4	0.24991
10.21	6.67809E-14	0.91235	3.76711E-4	0.25246
11.16	1.08594E-13	0.87936	2.13138E-4	0.24681
12	1.95885E-13	0.82127	1.55663E-4	0.24695
12.5	2.9751E-13	0.79881	1.30362E-4	0.26774
13	4.357E-13	0.77161	1.07108E-4	0.28234

Table S14 Relaxation fitting parameters for 6Dy from Figure S62. Related to Figure 8.

T / K	χ_S / cm^3 mol^{-1}	χ_T / cm^3 mol^{-1}	τ / s	α
7.83	0.22663	1.90662	0.38756	0.34908
9.73	0.20727	1.37245	0.12209	0.19797
12	0.1722	1.09252	0.04839	0.12511
14	0.14708	0.93601	0.02528	0.09308
16	0.1268	0.81658	0.01423	0.07249
18	0.10956	0.72472	0.00865	0.05997
20	0.07243	0.67798	0.00563	0.11646
21	0.06953	0.6405	0.00457	0.10576
22	0.067	0.60605	0.00375	0.09473
23	0.06397	0.5776	0.00314	0.08838
24	0.06182	0.55169	0.00264	0.08194
25	0.05916	0.52819	0.00224	0.0766
26	0.05771	0.50643	0.00191	0.06993
27	0.05548	0.48749	0.00164	0.06889
28	0.05406	0.46984	0.00141	0.06407
29	0.05216	0.45309	0.00122	0.06421
30	0.05097	0.43813	0.00105	0.06145
31	0.04926	0.4244	9.06508E-4	0.06133
32	0.04692	0.41117	7.77495E-4	0.06349
33	0.04601	0.39823	6.66508E-4	0.06182
34	0.04511	0.38786	5.71306E-4	0.06006
35	0.04353	0.37647	4.83941E-4	0.06247
36	0.04306	0.36578	4.09886E-4	0.06028
37	0.04061	0.35606	3.42859E-4	0.06418
38	0.04147	0.34685	2.86911E-4	0.06438
39	0.03783	0.33834	2.3415E-4	0.07023
40	0.03658	0.32996	1.90651E-4	0.0722
41	0.03267	0.32239	1.52398E-4	0.07641
42	0.03334	0.31489	1.22241E-4	0.07967
43	0.03107	0.30781	9.59183E-5	0.08246
44	0.02574	0.30073	7.26615E-5	0.08841
45	0.02405	0.29433	5.61588E-5	0.09308
46	0.03504	0.28763	4.5974E-5	0.08907

Table S15 Relaxation fitting parameters for 6Dy@6Y from Figure S63. Related to Figure 8.

T / K	χ_S / cm^3 mol^{-1}	χ_T / cm^3 mol^{-1}	τ / s	α
7.8	0.00674	0.08432	0.56189	0.26432
9.7	0.00574	0.06327	0.16947	0.16002
12	0.00488	0.05085	0.06634	0.11741
14	0.00398	0.04343	0.03274	0.09522
16	1.9182E-24	0.04564	0.0175	0.30378
20	1.95816E-23	0.03482	0.00769	0.23628
22	3.1756E-23	0.02984	0.00467	0.20114
24	5.94493E-23	0.02682	0.00314	0.18674
26	6.53855E-18	0.0242	0.00216	0.16588
28	5.09343E-18	0.0222	0.00154	0.15818
30	7.85275E-18	0.0206	0.00111	0.14716
32	9.14172E-18	0.01916	8.49135E-4	0.14985
34	1.85246E-17	0.01796	5.8159E-4	0.13263
36	2.84999E-17	0.01692	4.07673E-4	0.13647
38	3.81425E-17	0.01584	2.7852E-4	0.11989
40	5.361E-17	0.01504	1.82873E-4	0.12449
42	7.1003E-17	0.01425	1.16444E-4	0.10558
44	1.04145E-16	0.01361	6.9486E-5	0.12164
46	6.3171E-4	0.01304	4.09291E-5	0.14488
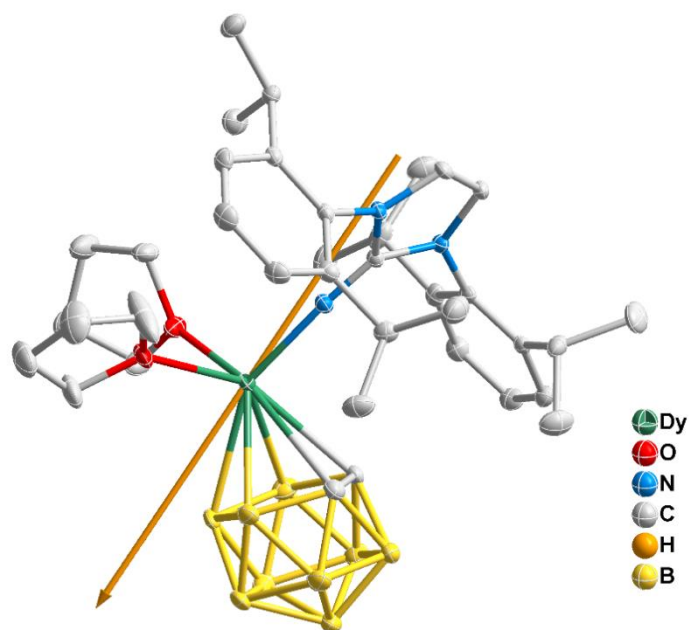
Figure S66 The local principal magnetization of the ground Kramer's doublet of 1Dy. Related to STAR Methods.
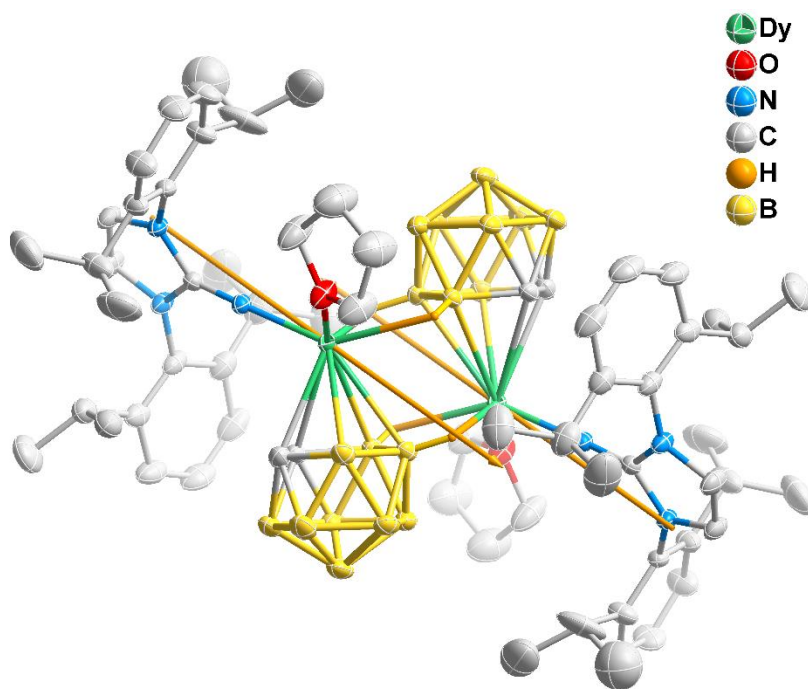
Figure S67 The local principal magnetizations of the ground Kramer's doublet of 2Dy. Related to STAR Methods.
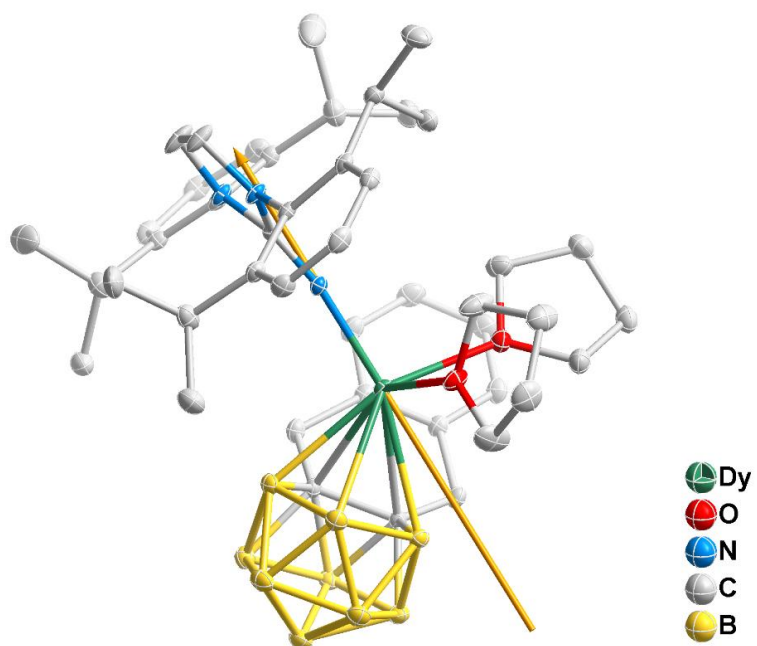
Figure S68 The local principal magnetizations of the ground Kramer's doublet of 3Dy. Related to STAR Methods.
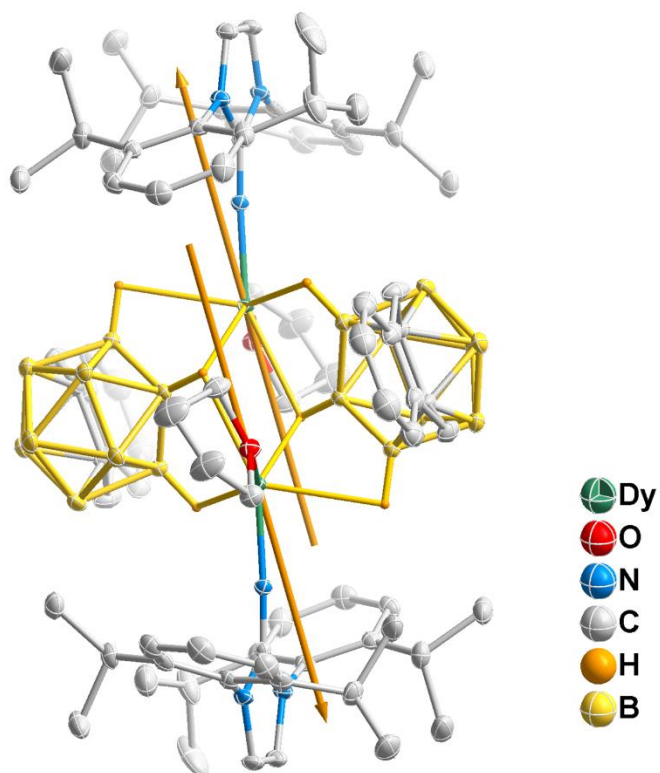
Figure S69 The local principal magnetizations of the ground Kramer's doublet of 4Dy. Related to STAR Methods.
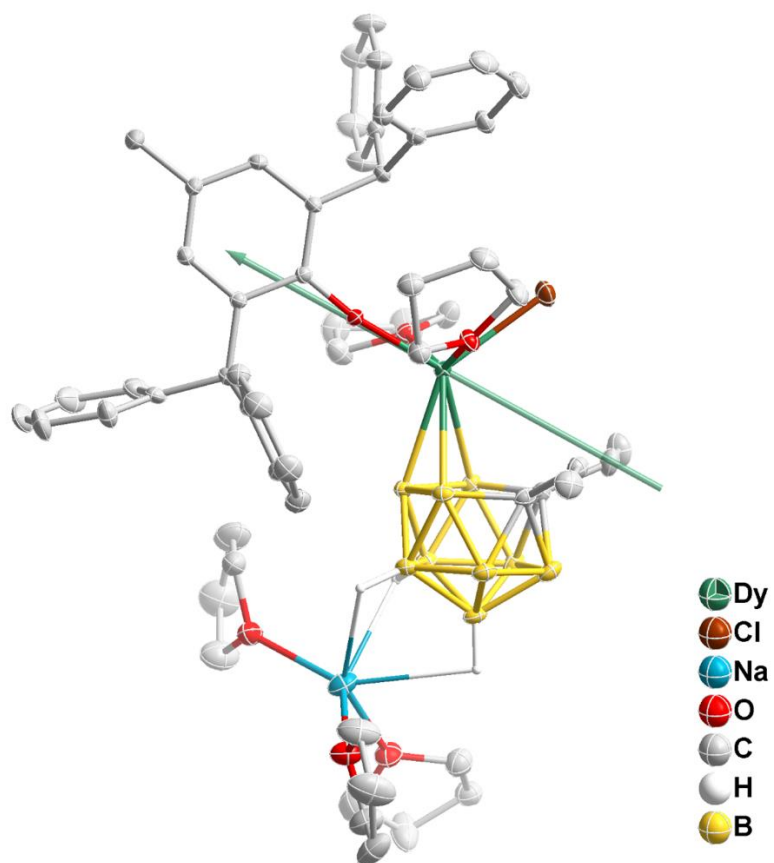
Figure S70 The local principal magnetizations of the ground Kramer's doublet of 5Dy. Related to STAR Methods.
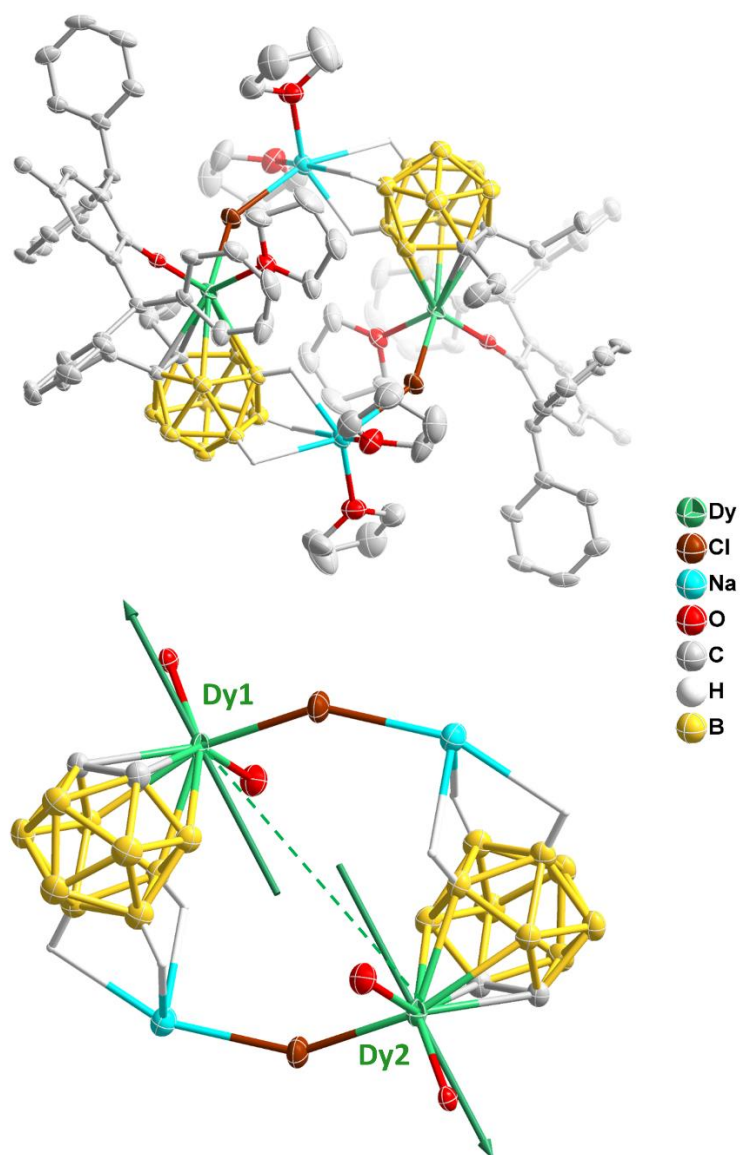
Figure S71 The local principal magnetizations of the ground Kramer's doublet of 6Dy. Related to STAR Methods.
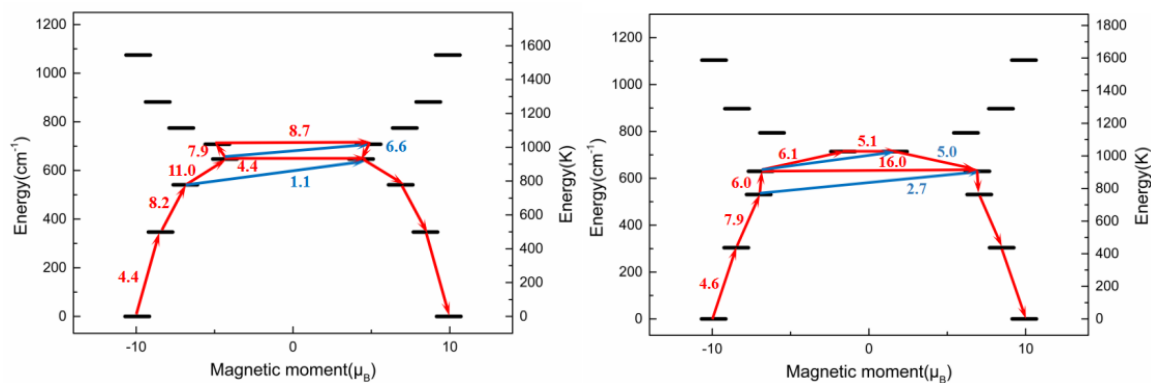
Figure S72 The *Ab initio* calculations. *Ab initio* calculated electronic states of the Dy(III) fragment from **1Dy**(left) and **3Dy**(right) with probability of transition between different substates. The numbers beside the arrows express the relative transition propensity. Related to STAR Methods.
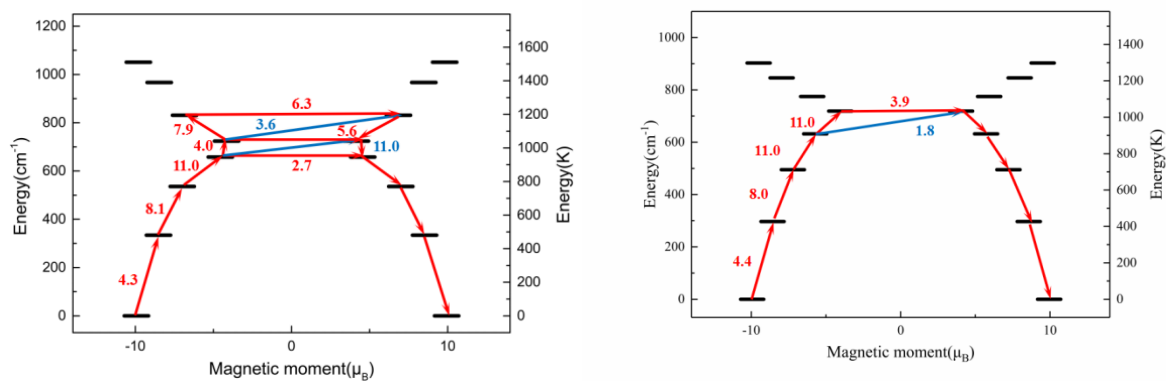
Figure S73 The *Ab initio* calculations. *Ab initio* calculated electronic states of the Dy(III) fragment from **2Dy**(left) and **4Dy**(right) with probability of transition between different substates. The numbers beside the arrows express the relative transition propensity. Related to STAR Methods.
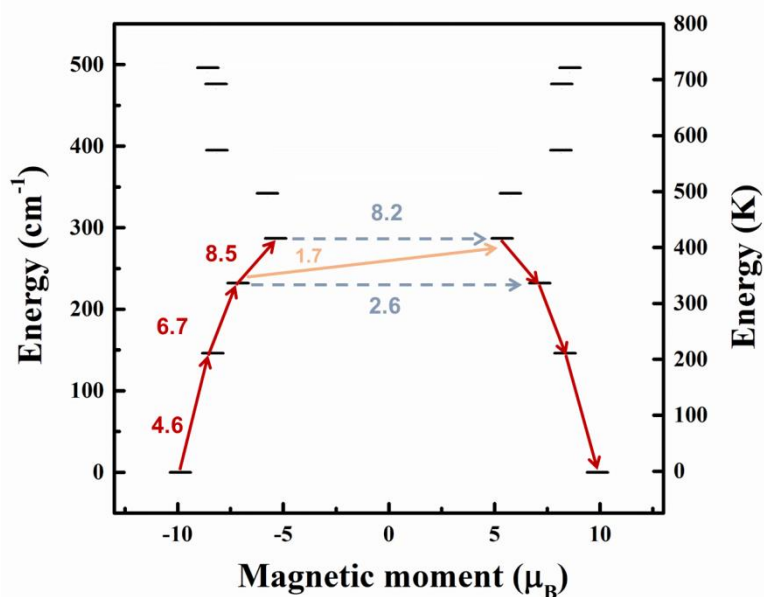
Figure S74 The *Ab initio* calculations. *Ab initio* calculated electronic states of the *J* = 15/2 manifold of the $^6H_{15/2}$ term of Dy^{III} for complex **5Dy**. Arrows depict the relaxation pathway for direct vertical transitions to the first-neighbor multiplet (red), Orbach/Raman relaxation (orange) and QTM (gray), while the number of the corresponding color represents probability of transition. Related to STAR Methods.
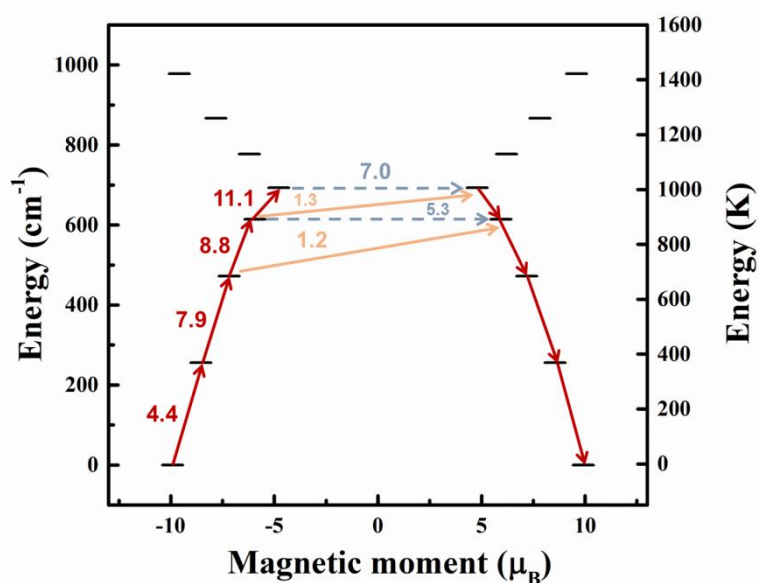
Figure S75 The *Ab initio* calculations. *Ab initio* calculated electronic states of the *J* = 15/2 manifold of the $^6H_{15/2}$ term of Dy^{III} for complex **6Dy**. Arrows depict the relaxation pathway for direct vertical transitions to the first-neighbor multiplet (red), Orbach/Raman relaxation (orange) and QTM (gray), while the number of the corresponding color represents probability of transition. Related to STAR Methods.

Table S16 *Ab initio* results for the *J* = 15/2 multiplet of Dy^{III} in 1Dy. Related to STAR Methods.

Ab initio Energy (cm^{-1})	Ab initio Energy (K)	g_x	g_y	g_z	g_z Angle (°)	Crystal field Wavefunction[a]
0	0	0.00	0.00	19.86	-	98.7%|±15/2>
347	499	0.03	0.04	16.90	5.99	95.1%|±13/2>
541	778	0.81	1.22	13.73	19.91	78.9%|±11/2>+15.0%|±7/2>
647	930	3.36	4.42	8.68	18.83	43.5%|±9/2>+30.1%|±5/2>
708	1018	2.97	4.46	9.65	88.89	13.5%|±9/2>+22.5%|±3/2>+18.5%|∓3/2>
775	1114	0.28	0.39	14.25	88.49	14.0%|±9/2>+19.5%|±1/2>+17.5%|∓1/2>+19.8%|∓7/2>
882	1268	0.06	0.09	17.26	89.33	17.3%|±7/2>+14.8%±5/2>+10.7%|±3/2>+17.9%|∓5/2>
1075	1545	0.01	0.01	19.75	86.73	11.8%|±5/2>+21.9%|±1/2>+10.4%|∓1/2>+20.7%|∓3/2>

[a] Only components with > 10% contribution are given, rounded to the nearest percent.

Table S17 *Ab initio* results for the *J* = 15/2 multiplet of Dy^{III} in 2Dy. Related to STAR Methods.

Ab initio Energy (cm^{-1})	Ab initio Energy (K)	g_x	g_y	g_z	g_z Angle (°)	Crystal field Wavefunction[a]
0	0	0.00	0.00	19.87	-	98.8%|±15/2>
334	480	0.02	0.03	17.05	8.22	96.7%|±13/2>
536	771	0.22	0.31	14.00	13.31	87.4%|±11/2>
658	946	2.30	4.93	9.12	11.84	56.5%|±9/2>+25.2%|±5/2>
724	1041	3.05	5.55	8.31	89.36	10.5%|±9/2>+12.4%|±1/2>+26.9%|∓3/2>+23.1%|∓7/2>
831	1195	0.10	0.14	13.70	89.67	13.5% |±9/2>+20.7%|±5/2>+15.7%|±1/2>+28.2%|∓7/2>
967	1390	0.05	0.06	16.95	86.81	20.8% |±7/2>+29.4% |±3/2>+36.7%|∓5/2>
1051	1511	0.01	0.01	19.62	87.25	20.2%|±3/2>+ 19.8%|±1/2>+ 12.4%|∓1/2>+30.5%|∓3/2>

[a] Only components with > 10% contribution are given, rounded to the nearest percent.

Table S18 *Ab initio* results for the *J* = 15/2 multiplet of Dy[III] in 3Dy. Related to STAR Methods.

Ab initio Energy (cm^{-1})	Ab initio Energy (K)	g_x	g_y	g_z	g_z Angle (°)	Crystal field Wavefunction[a]
0	0	0.00	0.00	19.82	-	97.3%|±15/2>
304	437	0.01	0.02	16.94	3.10	94.3%|±13/2>
531	763	0.43	0.64	14.07	19.11	83.2%|±11/2>
630	906	1.30	2.04	13.84	63.37	20.6%|±9/2>+18.7%|±5/2>+14.0%|±1/2>+13.3%|∓3/2>
714	1026	7.87	5.82	3.32	43.43	48.1%|±9/2>+12.9%|±3/2>+12.2%|∓1/2>
794	1141	2.67	4.07	12.37	87.03	36.5%|±7/2>+23.3%|∓1/2>+13.0%|∓5/2>
897	1290	0.45	0.78	16.83	85.56	18.2%|±7/2>+ 22.8%|±3/2>+35.2%|∓5/2>
1104	1587	0.02	0.03	19.77	86.23	18.7%|±5/2>+34.6%|±1/2> +26.7%|∓3/2>

[a] Only components with > 10% contribution are given, rounded to the nearest percent.

Table S19 *Ab initio* results for the *J* = 15/2 multiplet of Dy[III] in 4Dy. Related to STAR Methods.

Ab initio Energy (cm^{-1})	Ab initio Energy (K)	g_x	g_y	g_z	g_z Angle (°)	Crystal field Wavefunction[a]
0	0	0.00	0.00	19.88	-	96.7%|±15/2>
297	427	0.02	0.02	17.15	9.19	95.0%|±13/2>
495	712	0.20	0.23	14.44	16.76	93.8%|±11/2>
632	909	1.55	1.84	11.44	25.15	78.7%|±9/2>
719	1034	2.88	5.45	8.08	43.69	11.4%|±9/2>+46.2%|±7/2>
775	1114	2.61	4.50	11.85	83.45	21.4%|±7/2>+23.9%|±5/2>+14.3%|±3/2>+14.7%|∓1/2>+12.0%|∓5/2>
846	1216	0.49	0.70	15.94	84.41	28.7%|±5/2>+ 11.3%|±3/2>+12.3%|∓1/2>+22.7%|∓3/2>
903	1298	0.07	0.21	19.02	83.55	28.2%|±3/2> +30.1%|±1/2> +23.5%|∓1/2>

[a] Only components with > 10% contribution are given, rounded to the nearest percent.

Table S20 *Ab initio* **results for the** *J* **= 15/2 multiplet of Dy^{III} in 5Dy.** Related to STAR Methods.

Energy (cm^{-1})	Energy (K)	g_x	g_y	g_z	g_z Angle (°)	Wavefunction[a]
0	0	0.01	0.02	19.75	-	83.5%|∓15/2> + 15.3%|±13/2>
146	210	0.33	0.52	16.68	2.8	12.5%|∓15/2> + 65.5%|±13/2>
232	333	2.08	2.50	14.30	7.8	66.58%|∓11/2>
287	412	1.73	5.31	10.74	15	54.3%|9∓/2> + 10.3%|∓7/2>
342	492	2.34	5.01	11.50	12	25.5%|±7/2> + 18.8%|±5/2>
395	568	1.47	2.17	16.30	85	15.7%|±7/2> + 18.8%|∓5/2> + 27.3%|±3/2> + 10.7%|∓1/2>
476	684	0.13	1.04	16.38	88	11.1%|∓7/2> + 21.5%|∓5/2> + 10.4%|∓3/2> + 22.9%|∓1/2>
496	713	0.19	1.22	17.16	90	21.9%|∓3/2> + 23.9%|∓1/2>

[a] Only components with > 10% contribution are given, rounded to the nearest percent.

Table S21 *Ab initio* **results for the** *J* **= 15/2 multiplet of Dy^{III} in 6Dy.** Related to STAR Methods.

Energy (cm^{-1})	Energy (K)	g_x	g_y	g_z	g_z Angle (°)	Wavefunction[a]
0	0	0.00	0.00	19.82	-	94.3%|∓15/2>
256	368	0.00	0.00	17.11	10.34	92.5%|±13/2>
472	679	0.20	0.26	14.36	17.16	90.9%|∓11/2>
614	883	2.20	2.65	11.86	42.24	54.7%|∓9/2> + 17.3%|∓7/2>
693	997	2.65	6.04	9.59	70.78	24.2%|∓7/2> + 18.0%|±7/2> + 18.3%|∓5/2>
777	1118	1.73	3.22	12.41	88.12	14.8%|∓9/2 + 18.3%|∓5/2> + 12.5%|±3/2> + 17.4%|∓3/2> + 17.9%|±1/2>
867	1247	0.83	1.44	15.64	83.04	21.3%|∓5/2 + 13.8%|±3/2> + 10.4%|∓1/2> + 24.8%|±1/2>
978	1407	0.11	0.27	19.19	79.43	21.3%|∓5/2> + 13.8%|∓3/2> + 24.8%|∓1/2> + 10.4%|±1/2>

[a] Only components with > 10% contribution are given, rounded to the nearest percent

Table S22 Average transition magnetic moment elements between the states of 1Dy, given in μ_B^2. Related to STAR Methods.

	$\left\lvert +\frac{15}{2}\right\rangle$	$\left\lvert -\frac{15}{2}\right\rangle$	$\left\lvert +\frac{13}{2}\right\rangle$	$\left\lvert -\frac{13}{2}\right\rangle$	$\lvert +a\rangle$	$\lvert -a\rangle$	$\lvert +b\rangle$	$\lvert -b\rangle$	$\lvert +c\rangle$	$\lvert -c\rangle$	$\lvert +d\rangle$	$\lvert -d\rangle$	$\lvert +e\rangle$	$\lvert -e\rangle$	$\lvert +f\rangle$	$\lvert -f\rangle$
$\left\lvert +\frac{15}{2}\right\rangle$	--	7.2E-08	4.4E+00	2.9E-03	7.2E-02	6.9E-05	2.2E-02	4.7E-04	1.1E-02	1.2E-03	7.4E-03	8.6E-04	7.4E-04	5.4E-03	2.2E-04	1.6E-03
$\left\lvert -\frac{15}{2}\right\rangle$	7.2E-08	--	2.9E-03	4.4E+00	6.9E-05	7.2E-02	4.7E-04	2.2E-02	1.2E-03	1.1E-02	8.6E-04	7.4E-03	5.4E-03	7.4E-04	1.6E-03	2.2E-04
$\left\lvert +\frac{13}{2}\right\rangle$	4.4E+00	2.9E-03	--	6.6E-02	8.2E+00	2.3E-02	3.0E-01	1.2E-01	3.5E-02	8.9E-02	5.4E-03	8.2E-02	4.5E-02	1.5E-02	7.7E-03	7.4E-03
$\left\lvert -\frac{13}{2}\right\rangle$	2.9E-03	4.4E+00	6.6E-02	--	2.3E-02	8.2E+00	1.2E-01	3.0E-01	8.9E-02	3.5E-02	8.2E-02	5.4E-03	1.5E-02	4.5E-02	7.4E-03	7.7E-03
$\lvert +a\rangle$	7.2E-02	6.9E-05	8.2E+00	2.3E-02	--	2.7E-01	1.1E+01	1.1E+00	5.8E-01	3.6E-01	2.6E-01	1.3E-01	5.7E-02	1.4E-01	1.3E-02	3.0E-02
$\lvert -a\rangle$	6.9E-05	7.2E-02	2.3E-02	8.2E+00	2.7E-01	--	1.1E+00	1.1E+01	3.6E-01	5.8E-01	1.3E-01	2.6E-01	1.4E-01	5.7E-02	3.0E-02	1.3E-02
$\lvert +b\rangle$	2.2E-02	4.7E-04	3.0E-01	1.2E-01	1.1E+01	1.1E+00	--	4.4E+00	7.9E+00	6.6E+00	1.0E+00	3.4E-01	4.0E-01	2.0E-01	5.9E-03	4.2E-02
$\lvert -b\rangle$	4.7E-04	2.2E-02	1.2E-01	3.0E-01	1.1E+00	1.1E+01	4.4E+00	--	6.6E+00	7.9E+00	3.4E-01	1.0E+00	2.0E-01	4.0E-01	4.2E-02	5.9E-03
$\lvert +c\rangle$	1.1E-02	1.2E-03	3.5E-02	8.9E-02	5.8E-01	3.6E-01	7.9E+00	6.6E+00	--	8.7E+00	2.9E+00	8.4E+00	3.4E-01	1.0E-01	7.2E-02	2.7E-02
$\lvert -c\rangle$	1.2E-03	1.1E-02	8.9E-02	3.5E-02	3.6E-01	5.8E-01	6.6E+00	7.9E+00	8.7E+00	--	8.4E+00	2.9E+00	1.0E-01	3.4E-01	2.7E-02	7.2E-02
$\lvert +d\rangle$	7.4E-03	8.6E-04	5.4E-03	8.2E-02	2.6E-01	1.3E-01	1.0E+00	3.4E-01	2.9E+00	8.4E+00	--	1.7E+01	4.6E+00	2.6E+00	1.8E-01	8.6E-02
$\lvert -d\rangle$	8.6E-04	7.4E-03	8.2E-02	5.4E-03	1.3E-01	2.6E-01	3.4E-01	1.0E+00	8.4E+00	2.9E+00	1.7E+01	--	2.6E+00	4.6E+00	8.6E-02	1.8E-01
$\lvert +e\rangle$	7.4E-04	5.4E-03	4.5E-02	1.5E-02	5.7E-02	1.4E-01	4.0E-01	2.0E-01	3.4E-01	1.0E-01	4.6E+00	2.6E+00	--	1.9E+01	3.3E+00	9.6E-01
$\lvert -e\rangle$	5.4E-03	7.4E-04	1.5E-02	4.5E-02	1.4E-01	5.7E-02	2.0E-01	4.0E-01	1.0E-01	3.4E-01	2.6E+00	4.6E+00	1.9E+01	--	9.6E-01	3.3E+00
$\lvert +f\rangle$	2.2E-04	1.6E-03	7.7E-03	7.4E-03	1.3E-02	3.0E-02	5.9E-03	4.2E-02	7.2E-02	2.7E-02	1.8E-01	8.6E-02	3.3E+00	9.6E-01	--	1.6E+01
$\lvert -f\rangle$	1.6E-03	2.2E-04	7.4E-03	7.7E-03	3.0E-02	1.3E-02	4.2E-02	5.9E-03	2.7E-02	7.2E-02	8.6E-02	1.8E-01	9.6E-01	3.3E+00	1.6E+01	--

Table S23. **Average transition magnetic moment elements between the states of 2Dy, given in μ_B^2.** Related to STAR Methods.

	$\lvert+\tfrac{15}{2}\rangle$	$\lvert-\tfrac{15}{2}\rangle$	$\lvert+\tfrac{13}{2}\rangle$	$\lvert-\tfrac{13}{2}\rangle$	$\lvert+\tfrac{11}{2}\rangle$	$\lvert-\tfrac{11}{2}\rangle$	$\lvert+a\rangle$	$\lvert-a\rangle$	$\lvert+b\rangle$	$\lvert-b\rangle$	$\lvert+c\rangle$	$\lvert-c\rangle$	$\lvert+d\rangle$	$\lvert-d\rangle$	$\lvert+e\rangle$	$\lvert-e\rangle$
$\lvert+\tfrac{15}{2}\rangle$		7.2E-08	4.3E+00	9.2E-06	1.4E-01	8.4E-05	2.3E-02	1.1E-03	1.5E-03	1.0E-02	9.0E-04	4.9E-03	8.7E-04	5.1E-04	6.9E-05	1.2E-04
$\lvert-\tfrac{15}{2}\rangle$	7.2E-08		9.2E-06	4.3E+00	8.4E-05	1.4E-01	1.1E-03	2.3E-02	1.0E-02	1.5E-03	4.9E-03	9.0E-04	5.1E-04	8.7E-04	1.2E-04	6.9E-05
$\lvert+\tfrac{13}{2}\rangle$	4.3E+00	9.2E-06		3.9E-04	8.1E+00	4.2E-03	1.7E-01	8.5E-03	3.7E-02	1.4E-01	7.3E-03	5.1E-02	5.2E-03	5.0E-03	1.3E-03	1.1E-03
$\lvert-\tfrac{13}{2}\rangle$	9.2E-06	4.3E+00	3.9E-04		4.2E-03	8.1E+00	8.5E-03	1.7E-01	1.4E-01	3.7E-02	5.1E-02	7.3E-03	5.0E-03	5.2E-03	1.1E-03	1.3E-03
$\lvert+\tfrac{11}{2}\rangle$	1.4E-01	8.4E-05	8.1E+00	4.2E-03		3.8E-02	1.1E+01	2.2E-01	9.9E-01	3.2E-01	3.4E-01	1.3E-01	1.0E-02	3.6E-02	4.7E-03	6.1E-03
$\lvert-\tfrac{11}{2}\rangle$	8.4E-05	1.4E-01	4.2E-03	8.1E+00	3.8E-02		2.2E-01	1.1E+01	3.2E-01	9.9E-01	1.3E-01	3.4E-01	3.6E-02	1.0E-02	6.1E-03	4.7E-03
$\lvert+a\rangle$	2.3E-02	1.1E-03	1.7E-01	8.5E-03	1.1E+01	2.2E-01		2.7E+00	4.0E+00	1.1E+01	5.4E-01	9.3E-01	1.1E-01	3.1E-02	1.1E-02	5.8E-03
$\lvert-a\rangle$	1.1E-03	2.3E-02	8.5E-03	1.7E-01	2.2E-01	1.1E+01	2.7E+00		1.1E+01	4.0E+00	9.3E-01	5.4E-01	3.1E-02	1.1E-01	5.8E-03	1.1E-02
$\lvert+b\rangle$	1.5E-03	1.0E-02	3.7E-02	1.4E-01	9.9E-01	3.2E-01	4.0E+00	1.1E+01		5.6E+00	7.9E+00	3.6E+00	1.5E-01	3.9E-02	3.7E-02	2.7E-02
$\lvert-b\rangle$	1.0E-02	1.5E-03	1.4E-01	3.7E-02	3.2E-01	9.9E-01	1.1E+01	4.0E+00	5.6E+00		3.6E+00	7.9E+00	3.9E-02	1.5E-01	2.7E-02	3.7E-02
$\lvert+c\rangle$	9.0E-04	4.9E-03	7.3E-03	5.1E-02	3.4E-01	1.3E-01	5.4E-01	9.3E-01	7.9E+00	3.6E+00		6.3E+00	5.0E+00	3.4E+00	1.8E-01	1.1E-01
$\lvert-c\rangle$	4.9E-03	9.0E-04	5.1E-02	7.3E-03	1.3E-01	3.4E-01	9.3E-01	5.4E-01	3.6E+00	7.9E+00	6.3E+00		3.4E+00	5.0E+00	1.1E-01	1.8E-01
$\lvert+d\rangle$	8.7E-04	5.1E-04	5.2E-03	5.0E-03	1.0E-02	3.6E-02	1.1E-01	3.1E-02	1.5E-01	3.9E-02	5.0E+00	3.4E+00		2.4E+01	2.2E+00	2.6E+00
$\lvert-d\rangle$	5.1E-04	8.7E-04	5.0E-03	5.2E-03	3.6E-02	1.0E-02	3.1E-02	1.1E-01	3.9E-02	1.5E-01	3.4E+00	5.0E+00	2.4E+01		2.6E+00	2.2E+00
$\lvert+e\rangle$	6.9E-05	1.2E-04	1.3E-03	1.1E-03	4.7E-03	6.1E-03	1.1E-02	5.8E-03	3.7E-02	2.7E-02	1.8E-01	1.1E-01	2.2E+00	2.6E+00		3.2E+01
$\lvert-e\rangle$	1.2E-04	6.9E-05	1.1E-03	1.3E-03	6.1E-03	4.7E-03	5.8E-03	1.1E-02	2.7E-02	3.7E-02	1.1E-01	1.8E-01	2.6E+00	2.2E+00	3.2E+01	

Table S24 Average transition magnetic moment elements between the states of 3Dy, given in μ_B^2. Related to STAR Methods.

	$\lvert+\frac{15}{2}\rangle$	$\lvert-\frac{15}{2}\rangle$	$\lvert+\frac{13}{2}\rangle$	$\lvert-\frac{13}{2}\rangle$	$\lvert+\frac{11}{2}\rangle$	$\lvert-\frac{11}{2}\rangle$	$\lvert+a\rangle$	$\lvert-a\rangle$	$\lvert+b\rangle$	$\lvert-b\rangle$	$\lvert+c\rangle$	$\lvert-c\rangle$	$\lvert+d\rangle$	$\lvert-d\rangle$	$\lvert+e\rangle$	$\lvert-e\rangle$
$\lvert+\frac{15}{2}\rangle$	--	7.8E-08	4.6E+00	5.5E-05	4.6E-02	1.6E-04	1.7E-03	1.4E-03	4.1E-03	5.6E-04	2.3E-03	7.6E-04	1.2E-03	8.9E-04	2.1E-04	2.4E-04
$\lvert-\frac{15}{2}\rangle$	7.8E-08	--	5.5E-05	4.6E+00	1.6E-04	4.6E-02	1.4E-03	1.7E-03	5.6E-04	4.1E-03	7.6E-04	2.3E-03	8.9E-04	1.2E-03	2.4E-04	2.1E-04
$\lvert+\frac{13}{2}\rangle$	4.6E+00	5.5E-05	--	1.3E-03	7.9E+00	2.1E-02	3.1E-01	2.5E-01	6.4E-02	1.5E-02	1.1E-02	1.7E-02	7.1E-03	1.7E-02	4.1E-03	1.8E-03
$\lvert-\frac{13}{2}\rangle$	5.5E-05	4.6E+00	1.3E-03	--	2.1E-02	7.9E+00	2.5E-01	3.1E-01	1.5E-02	6.4E-02	1.7E-02	1.1E-02	1.7E-02	7.1E-03	1.8E-03	4.1E-03
$\lvert+\frac{11}{2}\rangle$	4.6E-02	1.6E-04	7.9E+00	2.1E-02	--	1.8E-01	6.0E+00	2.7E+00	3.3E+00	5.0E-02	3.4E-01	1.1E-01	1.1E-01	6.5E-02	1.1E-02	2.0E-02
$\lvert-\frac{11}{2}\rangle$	1.6E-04	4.6E-02	2.1E-02	7.9E+00	1.8E-01	--	2.7E+00	6.0E+00	5.0E-02	3.3E+00	1.1E-01	3.4E-01	6.5E-02	1.1E-01	2.0E-02	1.1E-02
$\lvert+a\rangle$	1.7E-03	1.4E-03	3.1E-01	2.5E-01	6.0E+00	2.7E+00	--	1.6E+01	6.1E+00	5.0E+00	5.1E-01	2.7E-01	9.9E-02	1.4E-01	1.5E-02	2.2E-02
$\lvert-a\rangle$	1.4E-03	1.7E-03	2.5E-01	3.1E-01	2.7E+00	6.0E+00	1.6E+01	--	5.0E+00	6.1E+00	2.7E-01	5.1E-01	1.4E-01	9.9E-02	2.2E-02	1.5E-02
$\lvert+b\rangle$	4.1E-03	5.6E-04	6.4E-02	1.5E-02	3.3E+00	5.0E-02	6.1E+00	5.0E+00	--	5.1E+00	1.0E+01	3.0E+00	6.2E-01	3.3E-01	9.2E-02	2.8E-02
$\lvert-b\rangle$	5.6E-04	4.1E-03	1.5E-02	6.4E-02	5.0E-02	3.3E+00	5.0E+00	6.1E+00	5.1E+00	--	3.0E+00	1.0E+01	3.3E-01	6.2E-01	2.8E-02	9.2E-02
$\lvert+c\rangle$	2.3E-03	7.6E-04	1.1E-02	1.7E-02	3.4E-01	1.1E-01	5.1E-01	2.7E-01	1.0E+01	3.0E+00	--	1.4E+01	2.3E+00	5.9E+00	1.0E-01	1.1E-01
$\lvert-c\rangle$	7.6E-04	2.3E-03	1.7E-02	1.1E-02	1.1E-01	3.4E-01	2.7E-01	5.1E-01	3.0E+00	1.0E+01	1.4E+01	--	5.9E+00	2.3E+00	1.1E-01	1.0E-01
$\lvert+d\rangle$	1.2E-03	8.9E-04	7.1E-03	1.7E-02	1.1E-01	6.5E-02	9.9E-02	1.4E-01	6.2E-01	3.3E-01	2.3E+00	5.9E+00	--	2.2E+01	1.6E+00	2.6E+00
$\lvert-d\rangle$	8.9E-04	1.2E-03	1.7E-02	7.1E-03	6.5E-02	1.1E-01	1.4E-01	9.9E-02	3.3E-01	6.2E-01	5.9E+00	2.3E+00	2.2E+01	--	2.6E+00	1.6E+00
$\lvert+e\rangle$	2.1E-04	2.4E-04	4.1E-03	1.8E-03	1.1E-02	2.0E-02	1.5E-02	2.2E-02	9.2E-02	2.8E-02	1.0E-01	1.1E-01	1.6E+00	2.6E+00	--	2.3E+01
$\lvert-e\rangle$	2.4E-04	2.1E-04	1.8E-03	4.1E-03	2.0E-02	1.1E-02	2.2E-02	1.5E-02	2.8E-02	9.2E-02	1.1E-01	1.0E-01	2.6E+00	1.6E+00	2.3E+01	--

Table S25 Average transition magnetic moment elements between the states of 4Dy, given in μ_B^2. Related to STAR Methods.

	$\lvert+\frac{15}{2}\rangle$	$\lvert-\frac{15}{2}\rangle$	$\lvert+\frac{13}{2}\rangle$	$\lvert-\frac{13}{2}\rangle$	$\lvert+\frac{11}{2}\rangle$	$\lvert-\frac{11}{2}\rangle$	$\lvert+\frac{9}{2}\rangle$	$\lvert-\frac{9}{2}\rangle$	$\lvert+a\rangle$	$\lvert-a\rangle$	$\lvert+b\rangle$	$\lvert-b\rangle$	$\lvert+c\rangle$	$\lvert-c\rangle$	$\lvert+d\rangle$	$\lvert-d\rangle$
$\lvert+\frac{15}{2}\rangle$		1.1E-07	4.3E+00	1.7E-05	1.6E-01	8.2E-06	7.3E-03	1.1E-04	2.3E-03	5.2E-04	3.9E-04	5.5E-04	4.2E-04	1.5E-04	2.2E-04	2.3E-05
$\lvert-\frac{15}{2}\rangle$	1.1E-07		1.7E-05	4.3E+00	8.2E-06	1.6E-01	1.1E-04	7.3E-03	5.2E-04	2.3E-03	5.5E-04	3.9E-04	1.5E-04	4.2E-04	2.3E-05	2.2E-04
$\lvert+\frac{13}{2}\rangle$	4.3E+00	1.7E-05		3.9E-04	8.0E+00	1.2E-03	2.7E-01	1.6E-03	2.0E-02	5.5E-03	3.3E-03	6.6E-03	2.4E-03	1.1E-03	2.0E-03	4.3E-04
$\lvert-\frac{13}{2}\rangle$	1.7E-05	4.3E+00	3.9E-04		1.2E-03	8.0E+00	1.6E-03	2.7E-01	5.5E-03	2.0E-02	6.6E-03	3.3E-03	1.1E-03	2.4E-03	4.3E-04	2.0E-03
$\lvert+\frac{11}{2}\rangle$	1.6E-01	8.2E-06	8.0E+00	1.2E-03		1.4E-02	1.1E+01	2.2E-01	4.1E-01	1.5E-01	3.7E-02	7.2E-02	2.0E-02	1.2E-02	9.8E-03	2.7E-03
$\lvert-\frac{11}{2}\rangle$	8.2E-06	1.6E-01	1.2E-03	8.0E+00	1.4E-02		2.2E-01	1.1E+01	1.5E-01	4.1E-01	7.2E-02	3.7E-02	1.2E-02	2.0E-02	2.7E-03	9.8E-03
$\lvert+\frac{9}{2}\rangle$	7.3E-03	1.1E-04	2.7E-01	1.6E-03	1.1E+01	2.2E-01		9.0E-01	1.1E+01	1.8E+00	6.0E-01	6.3E-01	1.9E-01	1.1E-01	4.0E-02	2.8E-02
$\lvert-\frac{9}{2}\rangle$	1.1E-04	7.3E-03	1.6E-03	2.7E-01	2.2E-01	1.1E+01	9.0E-01		1.8E+00	1.1E+01	6.3E-01	6.0E-01	1.1E-01	1.9E-01	2.8E-02	4.0E-02
$\lvert+a\rangle$	2.3E-03	5.2E-04	2.0E-02	5.5E-03	4.1E-01	1.5E-01	1.1E+01	1.8E+00		3.9E+00	2.0E+00	1.1E+01	4.3E-01	1.3E+00	1.1E-01	7.9E-02
$\lvert-a\rangle$	5.2E-04	2.3E-03	5.5E-03	2.0E-02	1.5E-01	4.1E-01	1.8E+00	1.1E+01	3.9E+00		1.1E+01	2.0E+00	1.3E+00	4.3E-01	7.9E-02	1.1E-01
$\lvert+b\rangle$	3.9E-04	5.5E-04	3.3E-03	6.6E-03	3.7E-02	7.2E-02	6.0E-01	6.3E-01	2.0E+00	1.1E+01		9.0E+00	3.1E+00	5.1E+00	4.5E-01	3.4E-01
$\lvert-b\rangle$	5.5E-04	3.9E-04	6.6E-03	3.3E-03	7.2E-02	3.7E-02	6.3E-01	6.0E-01	1.1E+01	2.0E+00	9.0E+00		5.1E+00	3.1E+00	3.4E-01	4.5E-01
$\lvert+c\rangle$	4.2E-04	1.5E-04	2.4E-03	1.1E-03	2.0E-02	1.2E-02	1.9E-01	1.1E-01	4.3E-01	1.3E+00	3.1E+00	5.1E+00		1.8E+01	3.9E+00	2.2E+00
$\lvert-c\rangle$	1.5E-04	4.2E-04	1.1E-03	2.4E-03	1.2E-02	2.0E-02	1.1E-01	1.9E-01	1.3E+00	4.3E-01	5.1E+00	3.1E+00	1.8E+01		2.2E+00	3.9E+00
$\lvert+d\rangle$	2.2E-04	2.3E-05	2.0E-03	4.3E-04	9.8E-03	2.7E-03	4.0E-02	2.8E-02	1.1E-01	7.9E-02	4.5E-01	3.4E-01	3.9E+00	2.2E+00		1.9E+00
$\lvert-d\rangle$	2.3E-05	2.2E-04	4.3E-04	2.0E-03	2.7E-03	9.8E-03	2.8E-02	4.0E-02	7.9E-02	1.1E-01	3.4E-01	4.5E-01	2.2E+00	3.9E+00	1.9E+00	

Table S26 Average transition magnetic moment elements between the states of 5Dy, given in $\mu_B{}^2$. Related to STAR Methods.

	$\left|+\frac{15}{2}\right>$	$\left|-\frac{15}{2}\right>$	$\left|+\frac{13}{2}\right>$	$\left|-\frac{13}{2}\right>$	$\left|+\frac{11}{2}\right>$	$\left|-\frac{11}{2}\right>$	$\left|+a\right>$	$\left|-a\right>$	$\left|+b\right>$	$\left|-b\right>$	$\left|+c\right>$	$\left|-c\right>$	$\left|+d\right>$	$\left|-d\right>$	$\left|+e\right>$	$\left|-e\right>$
$\left|+\frac{15}{2}\right>$	--	9.4E-05	3.0E-03	4.6E+00	1.3E-01	1.9E-02	3.3E-02	1.2E-02	9.4E-03	1.6E-02	3.8E-03	5.5E-03	7.9E-05	1.4E-02	4.3E-03	7.7E-04
$\left|-\frac{15}{2}\right>$	9.4E-05	--	4.6E+00	3.0E-03	1.9E-02	1.3E-01	1.2E-02	3.3E-02	1.6E-02	9.4E-03	5.5E-03	3.8E-03	1.4E-02	7.9E-05	7.7E-04	4.3E-03
$\left|+\frac{13}{2}\right>$	3.0E-03	4.6E+00	--	8.6E-02	6.2E-01	6.7E+00	3.6E-01	1.2E+00	1.4E-01	2.3E-01	3.2E-02	3.7E-02	7.8E-02	3.9E-03	1.2E-02	4.5E-02
$\left|-\frac{13}{2}\right>$	4.6E+00	3.0E-03	8.6E-02	--	6.7E+00	6.2E-01	1.2E+00	3.6E-01	2.3E-01	1.4E-01	3.7E-02	3.2E-02	3.9E-03	7.8E-02	4.5E-02	1.2E-02
$\left|+\frac{11}{2}\right>$	1.3E-01	1.9E-02	6.2E-01	6.7E+00	--	2.6E+00	8.5E+00	1.8E+00	6.0E-01	6.1E-01	4.6E-02	2.1E-01	2.9E-02	1.7E-01	6.9E-02	4.1E-02
$\left|-\frac{11}{2}\right>$	1.9E-02	1.3E-01	6.7E+00	6.2E-01	2.6E+00	--	1.8E+00	8.5E+00	6.1E-01	6.0E-01	2.1E-01	4.6E-02	1.7E-01	2.9E-02	4.1E-02	6.9E-02
$\left|+a\right>$	3.3E-02	1.2E-02	3.6E-01	1.2E+00	8.5E+00	1.8E+00	--	8.2E+00	5.3E+00	5.7E+00	6.2E-01	7.1E-01	1.3E-01	5.4E-01	9.2E-02	3.5E-01
$\left|-a\right>$	1.2E-02	3.3E-02	1.2E+00	3.6E-01	1.8E+00	8.5E+00	8.2E+00	--	5.7E+00	5.3E+00	7.1E-01	6.2E-01	5.4E-01	1.3E-01	3.5E-01	9.2E-02
$\left|+b\right>$	9.4E-03	1.6E-02	1.4E-01	2.3E-01	6.0E-01	6.1E-01	5.3E+00	5.7E+00	--	5.1E+00	3.0E+00	5.1E+00	1.7E+00	4.6E-01	6.8E-01	5.8E-01
$\left|-b\right>$	1.6E-02	9.4E-03	2.3E-01	1.4E-01	6.1E-01	6.0E-01	5.7E+00	5.3E+00	5.1E+00	--	5.1E+00	3.0E+00	4.6E-01	1.7E+00	5.8E-01	6.8E-01
$\left|+c\right>$	3.8E-03	5.5E-03	3.2E-02	3.7E-02	4.6E-02	2.1E-01	6.2E-01	7.1E-01	3.0E+00	5.1E+00	--	2.1E+01	1.0E+00	2.1E+00	1.2E+00	9.4E-01
$\left|-c\right>$	5.5E-03	3.8E-03	3.7E-02	3.2E-02	2.1E-01	4.6E-02	7.1E-01	6.2E-01	5.1E+00	3.0E+00	2.1E+01	--	2.1E+00	1.0E+00	9.4E-01	1.2E+00
$\left|+d\right>$	7.9E-05	1.4E-02	7.8E-02	3.9E-03	2.9E-02	1.7E-01	1.3E-01	5.4E-01	1.7E+00	4.6E-01	1.0E+00	2.1E+00	--	1.3E+00	1.1E+00	7.3E+00
$\left|-d\right>$	1.4E-02	7.9E-05	3.9E-03	7.8E-02	1.7E-01	2.9E-02	5.4E-01	1.3E-01	4.6E-01	1.7E+00	2.1E+00	1.0E+00	1.3E+00	--	7.3E+00	1.1E+00
$\left|+e\right>$	4.3E-03	7.7E-04	1.2E-02	4.5E-02	6.9E-02	4.1E-02	9.2E-02	3.5E-01	6.8E-01	5.8E-01	1.2E+00	9.4E-01	1.1E+00	7.3E+00	--	1.6E+01
$\left|-e\right>$	7.7E-04	4.3E-03	4.5E-02	1.2E-02	4.1E-02	6.9E-02	3.5E-01	9.2E-02	5.8E-01	6.8E-01	9.4E-01	1.2E+00	7.3E+00	1.1E+00	1.6E+01	--

Table S27 Average transition magnetic moment elements between the states of 6Dy, given in μ$_B^2$. Related to STAR Methods.

	$\lvert+\frac{15}{2}\rangle$	$\lvert-\frac{15}{2}\rangle$	$\lvert+\frac{13}{2}\rangle$	$\lvert-\frac{13}{2}\rangle$	$\lvert+\frac{11}{2}\rangle$	$\lvert-\frac{11}{2}\rangle$	|+a>	|-a>	|+b>	|-b>	|+c>	|-c>	|+d>	|-d>	|+e>	|-e>
$\lvert+\frac{15}{2}\rangle$	--	5.8E-09	8.9E-07	4.5E+00	1.6E-01	8.1E-05	2.1E-02	4.0E-03	2.9E-03	1.1E-03	2.6E-03	2.8E-04	1.0E-03	4.0E-04	5.6E-05	2.3E-04
$\lvert-\frac{15}{2}\rangle$	5.8E-09	--	4.5E+00	8.9E-07	8.1E-05	1.6E-01	4.0E-03	2.1E-02	1.1E-03	2.9E-03	2.8E-04	2.6E-03	4.0E-04	1.0E-03	2.3E-04	5.6E-05
$\lvert+\frac{13}{2}\rangle$	8.9E-07	4.5E+00	--	3.6E-05	3.1E-03	8.0E+00	4.3E-02	2.0E-01	4.9E-02	2.3E-02	7.8E-03	1.7E-02	1.6E-03	8.7E-03	1.8E-03	5.3E-04
$\lvert-\frac{13}{2}\rangle$	4.5E+00	8.9E-07	3.6E-05	--	8.0E+00	3.1E-03	2.0E-01	4.3E-02	2.3E-02	4.9E-02	1.7E-02	7.8E-03	8.7E-03	1.6E-03	5.3E-04	1.8E-03
$\lvert+\frac{11}{2}\rangle$	1.6E-01	8.1E-05	3.1E-03	8.0E+00	--	2.6E-02	8.9E+00	1.2E+00	3.5E-01	9.8E-01	2.1E-01	9.5E-02	7.3E-02	1.4E-02	3.8E-03	1.4E-02
$\lvert-\frac{11}{2}\rangle$	8.1E-05	1.6E-01	8.0E+00	3.1E-03	2.6E-02	--	1.2E+00	8.9E+00	9.8E-01	3.5E-01	9.5E-02	2.1E-01	1.4E-02	7.3E-02	1.4E-02	3.8E-03
|+a>	2.1E-02	4.0E-03	4.3E-02	2.0E-01	8.9E+00	1.2E+00	--	5.3E+00	1.3E+00	1.1E+01	9.3E-01	7.1E-01	1.4E-01	1.1E-01	1.7E-02	3.6E-02
|-a>	4.0E-03	2.1E-02	2.0E-01	4.3E-02	1.2E+00	8.9E+00	5.3E+00	--	1.1E+01	1.3E+00	7.1E-01	9.3E-01	1.1E-01	1.4E-01	3.6E-02	1.7E-02
|+b>	2.9E-03	1.1E-03	4.9E-02	2.3E-02	3.5E-01	9.8E-01	1.3E+00	1.1E+01	--	7.0E+00	5.9E+00	5.5E+00	5.7E-01	5.8E-01	3.7E-02	1.3E-02
|-b>	1.1E-03	2.9E-03	2.3E-02	4.9E-02	9.8E-01	3.5E-01	1.1E+01	1.3E+00	7.0E+00	--	5.5E+00	5.9E+00	5.8E-01	5.7E-01	1.3E-02	3.7E-02
|+c>	2.6E-03	2.8E-04	7.8E-03	1.7E-02	2.1E-01	9.5E-02	9.3E-01	7.1E-01	5.9E+00	5.5E+00	--	3.5E+00	8.2E+00	1.4E+00	3.5E-02	6.4E-01
|-c>	2.8E-04	2.6E-03	1.7E-02	7.8E-03	9.5E-02	2.1E-01	7.1E-01	9.3E-01	5.5E+00	5.9E+00	3.5E+00	--	1.4E+00	8.2E+00	6.4E-01	3.5E-02
|+d>	1.0E-03	4.0E-04	1.6E-03	8.7E-03	7.3E-02	1.4E-02	1.4E-01	1.1E-01	5.7E-01	5.8E-01	8.2E+00	1.4E+00	--	1.2E+01	9.8E-01	4.7E+00
|-d>	4.0E-04	1.0E-03	8.7E-03	1.6E-03	1.4E-02	7.3E-02	1.1E-01	1.4E-01	5.8E-01	5.7E-01	1.4E+00	8.2E+00	1.2E+01	--	4.7E+00	9.8E-01
|+e>	5.6E-05	2.3E-04	1.8E-03	5.3E-04	3.8E-03	1.4E-02	1.7E-02	3.6E-02	3.7E-02	1.3E-02	3.5E-02	6.4E-01	9.8E-01	4.7E+00	--	1.9E+00
|-e>	2.3E-04	5.6E-05	5.3E-04	1.8E-03	1.4E-02	3.8E-03	3.6E-02	1.7E-02	1.3E-02	3.7E-02	6.4E-01	3.5E-02	4.7E+00	9.8E-01	1.9E+00	--

Table S28 The calculated energies of spin-orbit states (cm⁻¹). The tunneling splittings (cm⁻¹) and g_z values of the low-lying exchange doublet states of **2Dy**. Related to STAR Methods.

E	Δ_{tun}	g_z
0.000	4.0E-9	0.000
1.676	2.8E-9	39.748
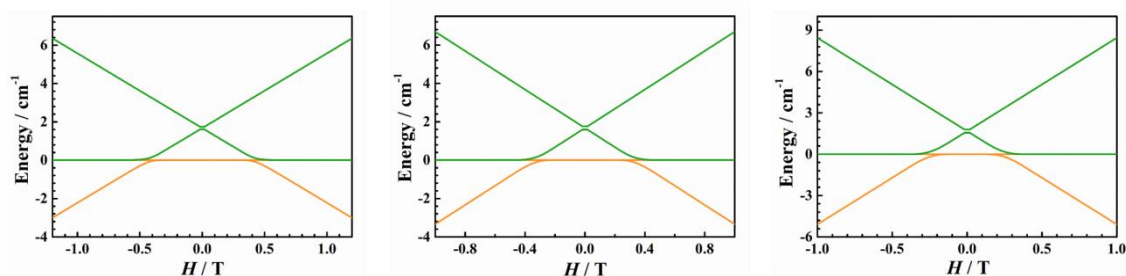
Figure S76 The simulated Zeeman diagram of 2Dy. The directions of applied magnetic field is the molecule's x-axis (left), y-axis (center) and z-axis (right). Related to Figure 6 and STAR Methods.

Table S29 The calculated energies of spin-orbit states (cm⁻¹). The tunneling splittings (cm⁻¹) and g_z values of the low-lying exchange doublet states of **4Dy**. Related to STAR Methods.

E	Δ_{tun}	g_z
0.000	5.5E-9	0.000
1.036	1.2E-9	39.757

Table S30 The calculated energies of spin-orbit states (cm⁻¹). The tunneling splittings (cm⁻¹) and g_z values of the low-lying exchange doublet states of **6Dy**. Related to STAR Methods.

E	Δ_{tun}	g_z
0.000	3.0E-10	0.000
1.006	1.0E-10	39.650
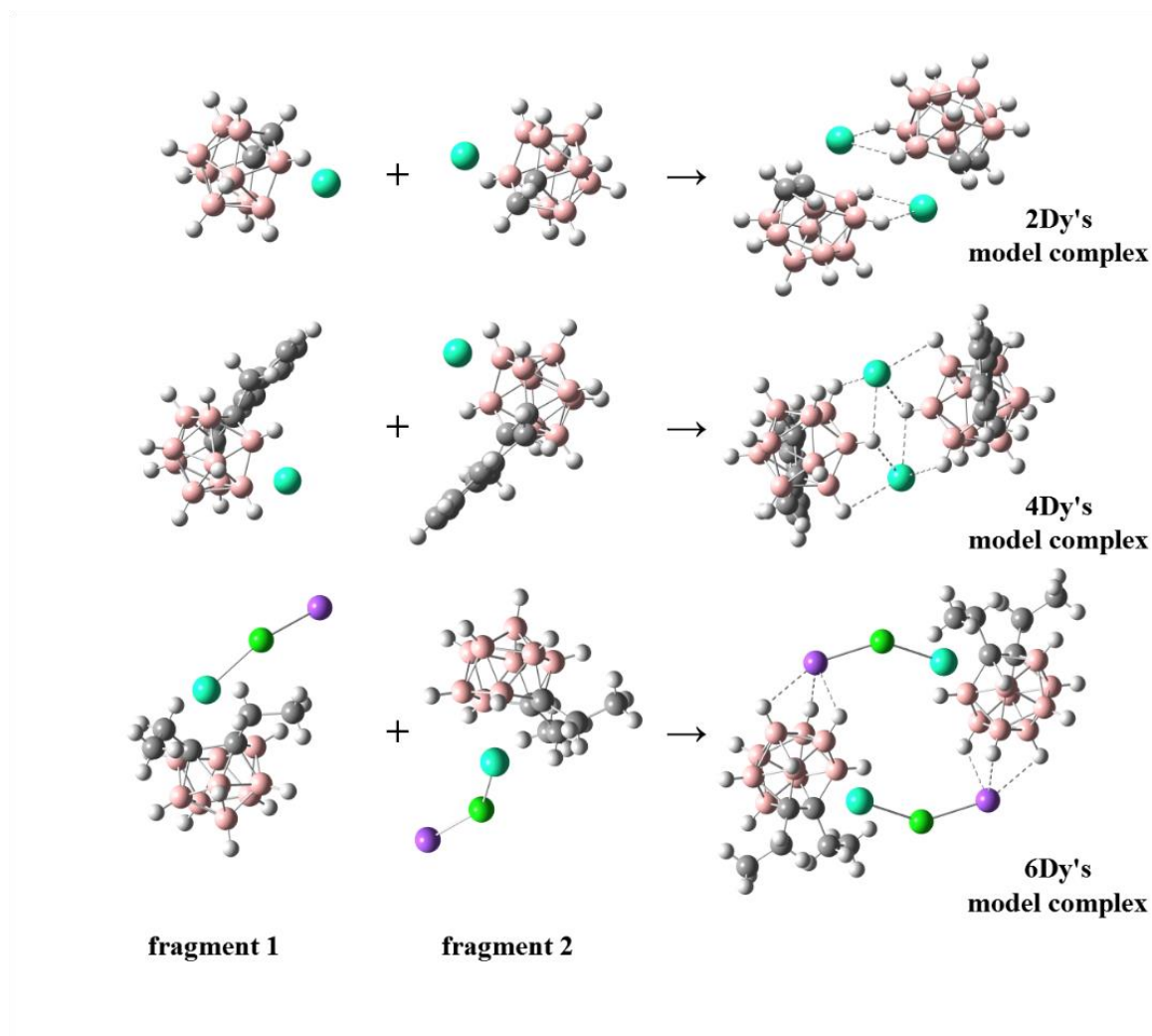
Figure S77 The structure of the model complexes of 2Dy, 4Dy and 6Dy in DFT calculations to quantify the bonding energy between fragments. (cyan for Dy, pink for B, grey for C, green for Cl, purple for Na and white for H). Related to Figure 3.

Table S31 Geometry coordinates of model compound for 2Dy in population analysis calculations. Related to Figure 3.

Dy	-0.1078	1.6920	9.9410
C	-2.6152	2.5950	9.5018
C	-2.0000	3.3872	10.7043
B	-2.8093	1.0135	9.8727
B	-2.2875	0.8393	11.5419
B	-1.7172	2.4252	12.0025
H	-1.4251	4.1395	10.5575
B	-4.2382	2.0840	9.8177
B	-3.6696	3.6713	10.3374
H	-2.4168	2.9404	8.6824
B	-3.0959	3.5385	12.0087
B	-4.0193	0.9492	11.1812
H	-2.9042	0.2712	9.0697
B	-3.3398	1.8628	12.5386
H	-2.0614	-0.0571	11.9638
H	-0.9280	2.5636	12.7566
H	-5.0456	1.9698	9.0819
B	-4.5416	2.6578	11.4685
H	-4.0984	4.6005	9.9338
H	-3.1543	4.3864	12.7077
H	-4.6936	0.0928	11.3320
H	-3.5798	1.6101	13.5821
H	-5.5519	2.9205	11.8130
B	0.3678	-1.0135	10.5086
B	-0.1540	-0.8393	8.8394
H	0.4627	-0.2712	11.3116
H	-0.3801	0.0571	8.4175
Dy	-2.3337	-1.6920	10.4403
C	0.1737	-2.5950	10.8795
B	1.7967	-2.0840	10.5636
B	1.5778	-0.9492	9.2001
B	-0.7244	-2.4252	8.3787
B	0.8983	-1.8628	7.8427
C	-0.4415	-3.3872	9.6770
H	-1.0164	-4.1395	9.8238
B	1.2281	-3.6713	10.0439
H	-0.0247	-2.9404	11.6989
H	2.6041	-1.9698	11.2994
B	2.1001	-2.6578	8.9127
H	2.2521	-0.0928	9.0493
H	-1.5135	-2.5636	7.6246
B	0.6544	-3.5385	8.3726
H	1.1383	-1.6101	6.7992
H	1.6569	-4.6005	10.4474
H	3.1104	-2.9205	8.5683
H	0.7128	-4.3864	7.6736

Table S32 Geometry coordinates of fragment 1 for 2Dy in population analysis calculations. Related to Figure 3.

Dy	-0.1078	1.6920	9.9410
C	-2.6152	2.5950	9.5018
C	-2.0000	3.3872	10.7043
B	-2.8093	1.0135	9.8727
B	-2.2875	0.8393	11.5419
B	-1.7172	2.4252	12.0025
H	-1.4251	4.1395	10.5575
B	-4.2382	2.0840	9.8177
B	-3.6696	3.6713	10.3374
H	-2.4168	2.9404	8.6824
B	-3.0959	3.5385	12.0087
B	-4.0193	0.9492	11.1812
H	-2.9042	0.2712	9.0697
B	-3.3398	1.8628	12.5386
H	-2.0614	-0.0571	11.9638
H	-0.9280	2.5636	12.7566
H	-5.0456	1.9698	9.0819
B	-4.5416	2.6578	11.4685
H	-4.0984	4.6005	9.9338
H	-3.1543	4.3864	12.7077
H	-4.6936	0.0928	11.3320
H	-3.5798	1.6101	13.5821
H	-5.5519	2.9205	11.8130

Table S33 Geometry coordinates of fragment 2 for 2Dy in population analysis calculations. Related to Figure 3.

B	0.3678	-1.0135	10.5086
B	-0.1540	-0.8393	8.8394
H	0.4627	-0.2712	11.3116
H	-0.3801	0.0571	8.4175
Dy	-2.3337	-1.6920	10.4403
C	0.1737	-2.5950	10.8795
B	1.7967	-2.0840	10.5636
B	1.5778	-0.9492	9.2001
B	-0.7244	-2.4252	8.3787
B	0.8983	-1.8628	7.8427
C	-0.4415	-3.3872	9.6770
H	-1.0164	-4.1395	9.8238
B	1.2281	-3.6713	10.0439
H	-0.0247	-2.9404	11.6989
H	2.6041	-1.9698	11.2994
B	2.1001	-2.6578	8.9127
H	2.2521	-0.0928	9.0493
H	-1.5135	-2.5636	7.6246
B	0.6544	-3.5385	8.3726
H	1.1383	-1.6101	6.7992
H	1.6569	-4.6005	10.4474
H	3.1104	-2.9205	8.5683
H	0.7128	-4.3864	7.6736

Table S34 Geometry coordinates of model compound for 4Dy in population analysis calculations. Related to Figure 3.

Dy	7.88906	7.22636	1.65443
Dy	9.87078	5.66319	-1.65443
B	7.55895	6.83087	-1.10201
B	7.63472	6.82152	-2.83556
B	10.20089	6.05868	1.10201
B	10.0116	4.36452	0.72501
B	11.63183	5.15704	0.59892
B	7.74824	8.52503	-0.72501
B	6.12801	7.73251	-0.59892
B	10.12512	6.06803	2.83556
B	11.71396	6.28798	2.00007
B	11.61944	5.31094	3.46427
B	6.23815	9.36925	-1.23724
B	6.04588	6.60156	-2.00007
B	11.50042	3.61846	2.98671
B	12.54861	4.70154	2.07415
B	6.25942	9.27109	-2.98671
B	5.21123	8.18801	-2.07415
B	11.52169	3.52029	1.23724
B	6.1404	7.5786	-3.46427
C	10.07895	4.52637	3.32857
C	7.74612	9.34268	-2.11261
C	10.01372	3.54687	2.11261
C	9.3674	4.10346	4.61482
C	7.68089	8.36318	-3.32857
C	8.49837	10.64643	-2.28062
C	9.26146	2.24312	2.28062
C	8.24413	3.11309	4.43215
C	8.39244	8.78608	-4.61482
C	9.55453	10.64991	-3.34449
C	8.20531	2.23963	3.34449
C	7.25065	3.0108	5.41391
C	9.51571	9.77645	-4.43215
C	10.59292	11.59766	-3.26883
C	7.16692	1.29188	3.26883
C	6.25142	2.06376	5.33037
C	10.50919	9.87874	-5.41391
C	11.54745	11.68857	-4.24759
C	6.21239	1.20098	4.24759
C	11.50842	10.82578	-5.33037
H	9.98832	6.93218	0.49647
H	7.77152	5.95737	-0.49647
H	5.68962	7.55743	0.40979
H	8.16371	8.97078	0.1718
H	9.70857	6.90236	3.44063
H	12.07022	5.33211	-0.40979
H	9.59613	3.91876	-0.1718
H	8.05127	5.98718	-3.44063

H	12.27221	7.23516	1.97958
H	12.11071	5.62518	4.39575
H	5.80586	10.22794	-0.70452
H	5.48763	5.65439	-1.97958
H	10.02258	3.71553	5.21532
H	9.01118	4.89655	5.04352
H	11.90907	2.81088	3.61242
H	13.6452	4.61891	2.08991
H	8.91671	10.87067	-1.43425
H	7.85757	11.34577	-2.48236
H	5.85076	10.07866	-3.61242
H	4.11464	8.27064	-2.08991
H	11.95398	2.6616	0.70452
H	5.64913	7.26436	-4.39575
H	8.84313	2.01888	1.43425
H	9.90227	1.54377	2.48236
H	7.73726	9.17401	-5.21532
H	8.74866	7.99299	-5.04352
H	7.26515	3.59482	6.13891
H	10.63081	12.17417	-2.54067
H	7.12903	0.71537	2.54067
H	5.60782	2.00431	5.99864
H	10.49469	9.29473	-6.13891
H	12.22045	12.32734	-4.18455
H	5.53939	0.56221	4.18455
H	12.15202	10.88523	-5.99864

Table S35 Geometry coordinates of fragment 1 for 4Dy in population analysis calculations. Related to Figure 3.

Dy	7.88906	7.22636	1.65443
B	7.55895	6.83087	-1.10201
B	7.63472	6.82152	-2.83556
B	7.74824	8.52503	-0.72501
B	6.12801	7.73251	-0.59892
B	6.23815	9.36925	-1.23724
B	6.04588	6.60156	-2.00007
B	6.25942	9.27109	-2.98671
B	5.21123	8.18801	-2.07415
B	6.1404	7.5786	-3.46427
C	7.74612	9.34268	-2.11261
C	7.68089	8.36318	-3.32857
C	8.49837	10.64643	-2.28062
C	8.39244	8.78608	-4.61482
C	9.55453	10.64991	-3.34449
C	9.51571	9.77645	-4.43215
C	10.59292	11.59766	-3.26883
C	10.50919	9.87874	-5.41391
C	11.54745	11.68857	-4.24759
C	11.50842	10.82578	-5.33037
H	7.77152	5.95737	-0.49647
H	5.68962	7.55743	0.40979

H	8.16371	8.97078	0.1718
H	8.05127	5.98718	-3.44063
H	5.80586	10.22794	-0.70452
H	5.48763	5.65439	-1.97958
H	8.91671	10.87067	-1.43425
H	7.85757	11.34577	-2.48236
H	5.85076	10.07866	-3.61242
H	4.11464	8.27064	-2.08991
H	5.64913	7.26436	-4.39575
H	7.73726	9.17401	-5.21532
H	8.74866	7.99299	-5.04352
H	10.63081	12.17417	-2.54067
H	10.49469	9.29473	-6.13891
H	12.22045	12.32734	-4.18455
H	12.15202	10.88523	-5.99864

Table S36 Geometry coordinates of fragment 2 for 4Dy in population analysis calculations. Related to Figure 3.

Dy	9.87078	5.66319	-1.65443
B	10.20089	6.05868	1.10201
B	10.0116	4.36452	0.72501
B	11.63183	5.15704	0.59892
B	10.12512	6.06803	2.83556
B	11.71396	6.28798	2.00007
B	11.61944	5.31094	3.46427
B	11.50042	3.61846	2.98671
B	12.54861	4.70154	2.07415
B	11.52169	3.52029	1.23724
C	10.07895	4.52637	3.32857
C	10.01372	3.54687	2.11261
C	9.3674	4.10346	4.61482
C	9.26146	2.24312	2.28062
C	8.24413	3.11309	4.43215
C	8.20531	2.23963	3.34449
C	7.25065	3.0108	5.41391
C	7.16692	1.29188	3.26883
C	6.25142	2.06376	5.33037
C	6.21239	1.20098	4.24759
H	9.98832	6.93218	0.49647
H	9.70857	6.90236	3.44063
H	12.07022	5.33211	-0.40979
H	9.59613	3.91876	-0.1718
H	12.27221	7.23516	1.97958
H	12.11071	5.62518	4.39575
H	10.02258	3.71553	5.21532
H	9.01118	4.89655	5.04352
H	11.90907	2.81088	3.61242
H	13.6452	4.61891	2.08991
H	11.95398	2.6616	0.70452
H	8.84313	2.01888	1.43425
H	9.90227	1.54377	2.48236

H	7.26515	3.59482	6.13891
H	7.12903	0.71537	2.54067
H	5.60782	2.00431	5.99864
H	5.53939	0.56221	4.18455

Table S37 Geometry coordinates of model compound for 6Dy in population analysis calculations. Related to Figure 3.

Dy	5.3342	5.3451	3.1506
Cl	5.7674	7.9348	3.198
C	3.0475	3.8672	3.2816
C	2.6768	5.3177	2.662
B	4.1741	3.1108	2.2816
B	4.4649	4.1551	0.9002
B	3.4958	5.5871	1.2472
Na	6.8276	10.0984	1.8975
C	3.0813	3.6593	4.8055
B	2.4499	2.5868	2.2737
B	1.4858	4.0618	2.5339
C	2.334	6.4432	3.6739
B	1.7637	5.1635	1.1901
H	4.9264	2.3994	2.654
B	3.3262	2.7765	0.722
Na	4.6423	3.304	-1.8976
B	2.894	4.4018	0.0501
H	5.4028	4.0123	0.2392
H	3.7825	6.5935	0.9038
B	7.0043	9.2473	-0.9003
B	8.1431	10.6258	-0.7216
B	8.5753	9.0005	-0.0498
H	6.0665	9.39	-0.2389
H	8.5636	8.7879	0.993
H	3.7987	3.0389	5.0013
H	3.3189	4.5082	5.2113
C	1.8348	3.1529	5.506
H	2.1242	1.6009	2.6388
B	1.6394	3.4173	0.9063
H	0.5268	4.0426	3.0756
H	1.6571	6.111	4.2835
H	3.127	6.6391	4.1967
C	1.8281	7.7439	3.0515
H	0.9865	5.8634	0.8457
H	3.6256	1.8541	0.0861
Cl	5.7017	5.4676	-3.1981
H	2.9051	4.6143	-0.9923
Dy	6.1349	8.0573	-3.1506
B	7.2955	10.2918	-2.2823
B	7.9738	7.8155	-1.2479
B	9.0199	10.8156	-2.274
B	9.8299	9.985	-0.9062
H	7.8437	11.5482	-0.0859
B	9.7061	8.239	-1.1904

H	1.5439	2.3373	5.0916
H	1.1399	3.811	5.4385
H	2.0322	2.9884	6.4301
H	0.7856	2.9696	0.3759
H	2.5043	8.105	2.472
H	1.6306	8.3754	3.7458
H	1.0339	7.5673	2.542
C	8.4215	9.5353	-3.2819
C	8.7923	8.0847	-2.6622
H	6.5428	11.0029	-2.6539
H	7.6867	6.8088	-0.9037
H	9.3445	11.8013	-2.6382
B	9.9834	9.3405	-2.5337
H	10.6836	10.4326	-0.376
H	10.4822	7.5388	-0.8451
C	8.3884	9.7431	-4.806
C	9.1357	6.9593	-3.6743
H	10.9423	9.3596	-3.0756
H	7.6706	10.3632	-5.0009
H	8.1505	8.8939	-5.211
C	9.6346	10.2492	-5.5056
H	9.8123	7.2912	-4.2831
H	8.3424	6.763	-4.1964
C	9.6412	5.6583	-3.0511
H	9.9253	11.0649	-5.0914
H	10.3294	9.5912	-5.4383
H	9.4371	10.4138	-6.4299
H	8.965	5.2972	-2.4718
H	9.8386	5.0268	-3.7456
H	10.4354	5.8348	-2.5418

Table S38 Geometry coordinates of fragment 1 for 6Dy in population analysis calculations. Related to Figure 3.

Na	4.6423	3.3040	-1.8976
B	7.0043	9.2473	-0.9003
B	8.1431	10.6258	-0.7216
B	8.5753	9.0005	-0.0498
H	6.0665	9.3900	-0.2389
H	8.5636	8.7879	0.9930
Cl	5.7017	5.4676	-3.1981
Dy	6.1349	8.0573	-3.1506
B	7.2955	10.2918	-2.2823
B	7.9738	7.8155	-1.2479
B	9.0199	10.8156	-2.2740
B	9.8299	9.9850	-0.9062
H	7.8437	11.5482	-0.0859
B	9.7061	8.2390	-1.1904
C	8.4215	9.5353	-3.2819
C	8.7923	8.0847	-2.6622
H	6.5428	11.0029	-2.6539
H	7.6867	6.8088	-0.9037

H	9.3445	11.8013	-2.6382
B	9.9834	9.3405	-2.5337
H	10.6836	10.4326	-0.3760
H	10.4822	7.5388	-0.8451
C	8.3884	9.7431	-4.8060
C	9.1357	6.9593	-3.6743
H	10.9423	9.3596	-3.0756
H	7.6706	10.3632	-5.0009
H	8.1505	8.8939	-5.2110
C	9.6346	10.2492	-5.5056
H	9.8123	7.2912	-4.2831
H	8.3424	6.7630	-4.1964
C	9.6412	5.6583	-3.0511
H	9.9253	11.0649	-5.0914
H	10.3294	9.5912	-5.4383
H	9.4371	10.4138	-6.4299
H	8.9650	5.2972	-2.4718
H	9.8386	5.0268	-3.7456
H	10.4354	5.8348	-2.5418

Table S39 Geometry coordinates of fragment 2 for 6Dy in population analysis calculations. Related to Figure 3.

Dy	5.3342	5.3451	3.1506
Cl	5.7674	7.9348	3.198
C	3.0475	3.8672	3.2816
C	2.6768	5.3177	2.662
B	4.1741	3.1108	2.2816
B	4.4649	4.1551	0.9002
B	3.4958	5.5871	1.2472
Na	6.8276	10.0984	1.8975
C	3.0813	3.6593	4.8055
B	2.4499	2.5868	2.2737
B	1.4858	4.0618	2.5339
C	2.334	6.4432	3.6739
B	1.7637	5.1635	1.1901
H	4.9264	2.3994	2.654
B	3.3262	2.7765	0.722
B	2.894	4.4018	0.0501
H	5.4028	4.0123	0.2392
H	3.7825	6.5935	0.9038
H	3.7987	3.0389	5.0013
H	3.3189	4.5082	5.2113
C	1.8348	3.1529	5.506
H	2.1242	1.6009	2.6388
B	1.6394	3.4173	0.9063
H	0.5268	4.0426	3.0756
H	1.6571	6.111	4.2835
H	3.127	6.6391	4.1967
C	1.8281	7.7439	3.0515
H	0.9865	5.8634	0.8457
H	3.6256	1.8541	0.0861
H	2.9051	4.6143	-0.9923
H	1.5439	2.3373	5.0916

H	1.1399	3.811	5.4385
H	2.0322	2.9884	6.4301
H	0.7856	2.9696	0.3759
H	2.5043	8.105	2.472
H	1.6306	8.3754	3.7458
H	1.0339	7.5673	2.542
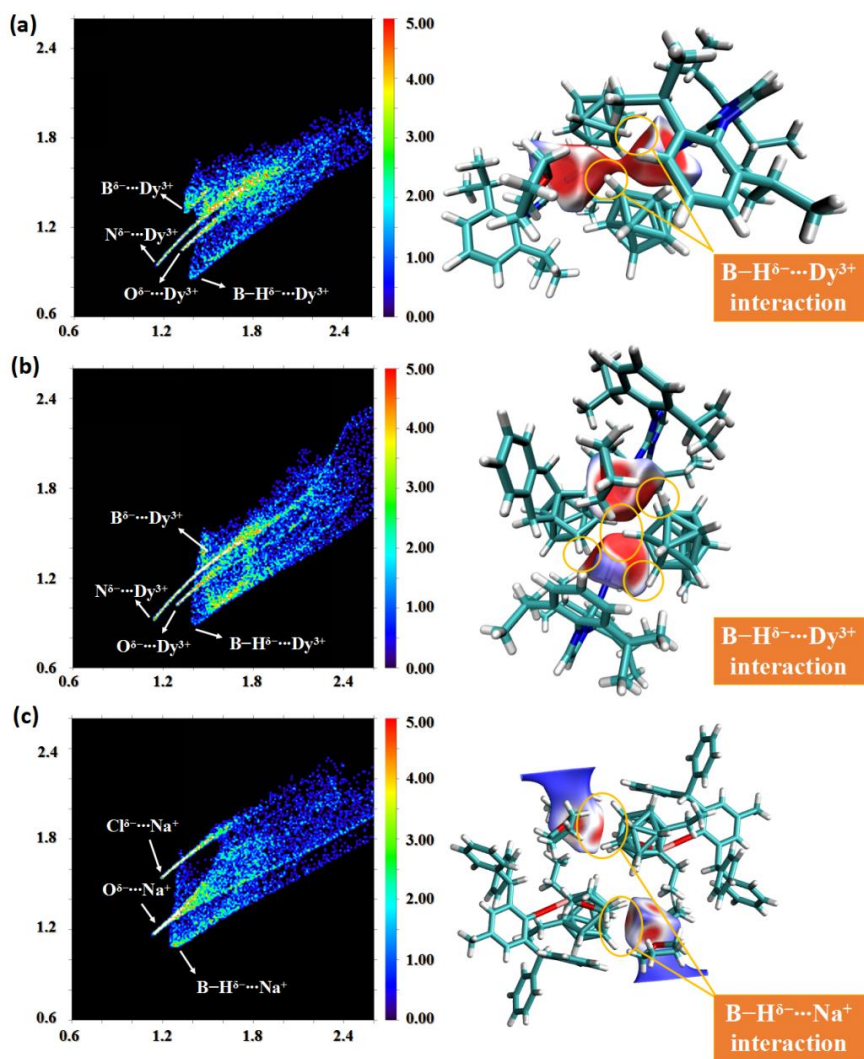
Figure S78 Fingerprint plot (left) and color-mapped isosurface graph of Hirshfeld surface(right) for 2Dy (a), 4Dy (b) and 6Dy (c) respectively. Related to Figure 4.

Table S40 Total electron density at bond critical points (BCPs) (a.u.)[a] Related to Figure 4.

	1	2	3	4	5	ρ_{avg}
2Dy	0.03469	0.02538	0.02521	0.03478	/	0.0300
4Dy	0.03207	0.03541	0.03528	0.01337	0.03214	0.0297
6Dy	0.01048	0.01002	0.01003	0.01050	/	0.0103

[a] Noted: Due to the dense B-H distribution on the surface of the carborane ligand, the BCP is affected by surrounding interactions, which makes the location of BCP not happen to appear on the B$-$H$^{\delta-}$ and M^{n+} lines, but slightly deviates or merges in one place, leading to the fact that the number of BCPs is less than actual amount of B$-$H$^{\delta-}\cdots$M^{n+} in single crystal structure.